INSTITUTO SUPERIOR DE ENGENHARIA DO PORTO
MESTRADO EM ENGENHARIA MECÂNICA




Feasibility study of combining laser cutting with cold forming in a production line

PEDRO FILIPE DA MOTA PRETO
novembro de 2020

POLITÉCNICO
DO PORTO

Instituto Superior de Engenharia do Porto

FEASIBILITY STUDY OF COMBINING LASER CUTTING WITH COLD FORMING IN A PRODUCTION LINE

Pedro Filipe da Mota Preto

2020

ISEP – School of Engineering, Polytechnic of Porto
Mechanical Engineering Department

POLITÉCNICO
DO PORTO

POLITÉCNICO
DO PORTO

Instituto Superior de Engenharia do Porto

FEASIBILITY STUDY OF COMBINING LASER CUTTING AND COLD FORMING IN A PRODUCTION LINE

Pedro Filipe da Mota Preto
1150846

Dissertation presented to ISEP – School of Engineering to fulfill the requirements necessary to obtain a Master's degree in Mechanical Engineering, carried out under the guidance of the Adjunct Professor Francisco José Gomes da Silva and co-supervision of Adjunct Professor Arnaldo Manuel Guedes Pinto.

2020
ISEP – School of Engineering, Polytechnic of Porto
Department of Mechanical Engineering

POLITÉCNICO
DO PORTO

POLITÉCNICO
DO PORTO

JURY

President
Manuel Jorge Dores de Castro, PhD
Associate Professor, ISEP – School of Engineering, Polytechnic of Porto
Supervisor
Francisco José Gomes da Silva, PhD
Associate Professor, ISEP – School of Engineering, Polytechnic of Porto
Co-Supervisor
Arnaldo Manuel Guedes Pinto, PhD
Auxiliar Professor, ISEP – School of Engineering, Polytechnic of Porto
Examiner
Abílio Manuel Pinho de Jesus, PhD
Associate Professor, Faculty of Engineering, University of Porto

ACKNOWLEDGMENTS

To my supervisor, Professor Francisco José Gomes da Silva and co-supervisor, Professor Arnaldo Manuel Guedes Pinto, a special thanks for all the advice and encouragement you have offered me throughout this year and for being a reference of professionalism and love for his profession.

A word of affection and a personal thanks to the Philips team in Drachten and to Ing. Dave Geertsma for the willingness to teach and help me whenever I needed it, for the guidance and for making me feel at home, despite the pandemic situation.

To Trumpf for the opportunity and all technical and human means that allowed the possibility to perform the laser cutting tests.

To my friends, Eduardo Amaral and André Silva, thank you for these years of friendship, support, and good moments at ISEP.

To the external relations office, thank you for the guidance in this process and for the opportunity to challenge myself to get out of my comfort zone.

To my girlfriend Daniela for all the support and motivation throughout my whole university path and specially during this thesis.

A special thanks to my family for the continued effort and support in my decisions.

KEYWORDS

Laser cutting quality, laser cutting parameters, Process repeatability.

ABSTRACT

Cold forming is a manufacturing process that allows high production rates while obtaining a very good accuracy. However, when starting the production of a new part, sometimes it is unavoidable to have some changes in the geometry of the component or even production errors, leading to high losses of time and money in punching equipment.

Laser technology has been improving over the past decades and, as such, it is nowadays used in several different areas. In the industry, laser is essentially used in the cutting process of different materials due to its high versatility and its high cut quality, when compared to similar manufacturing processes. For this reason, this study aims to test the feasibility of combining laser cutting with cold forming in a production line, in order to produce prototypes or small volumes of production, to reduce initial costs and times related to starting the production of a new component.

The following work was developed at Philips Consumer Lifestyle aiming to test the feasibility to produce the Ultron Guard with the combination of laser cutting with cold forming. In a first phase, the laser cut samples were carried out by Trumpf using different laser cutting parameters.

Laser cutting parameters and important aspects observed during the realization of the tests were documented and studied. Posteriorly, the analysis of the samples was performed at Philips where a set of procedures was made in order to analyze the accuracy of the samples, analyze the microhardness, the microstructure and the burr dimensions, to verify if laser cutting achieves the required accuracy and quality, and how the parameters influence the cut quality in order to reach the best cut quality.

PALAVRAS CHAVE

Qualidade do corte a laser, Parâmetros do corte a laser, Repetibilidade do processo.

RESUMO

A conformação a frio é um processo de fabrico que permite elevadas taxas de produção, enquanto obtém uma precisão muito boa. No entanto, no início de produção de um novo componente, às vezes é inevitável ter de realizar algumas mudanças na geometria do componente, ou até erros de produção, conduzindo a elevadas perdas de tempo e de dinheiro em ferramentas de puncionamento.

A tecnologia de laser tem vindo a ser aprimorada nas últimas décadas e, como tal, atualmente é usada em diversas áreas. No setor industrial, o laser é essencialmente usado no processo de corte de diferentes materiais, devido à sua elevada versatilidade e qualidade de corte, comparativamente a processos de fabrico similares. Por esse motivo, o presente estudo procura testar a viabilidade de combinar o corte a laser com conformação a frio numa linha de produção, com o objetivo de diminuir os custos e tempos iniciais associados ao início de produção de um novo componente.

O seguinte relatório foi desenvolvido na Philips Consumer Lifestyle, com a principal finalidade de testar a viabilidade de produzir o Ultron Guard através da combinação do corte de laser com conformação a frio. Numa fase inicial, as amostras cortadas a laser foram produzidas pela Trumpf usando diferentes parâmetros de corte a laser.

Os parâmetros de corte a laser e aspetos relevantes observados durante a realização dos testes foram relatados e analisados. Posteriormente, as análises das amostras foram realizadas na Philips, onde através de um conjunto de procedimentos foi analisada a dimensão das amostras, a microestrutura, a microdureza e, por fim, a dimensão da rebarba para verificar não só se o corte a laser obtém a precisão e a qualidade necessárias, como também compreender a influência dos parâmetros na qualidade de corte a fim de atingir melhor qualidade.

LIST OF SYMBOLS AND ABBREVIATIONS

List of abbreviations

3D	Three-dimensional
AISI	American Iron and Steel Institute
CAD	Computer-Aided Design
CW	Continuous Wave
HAZ	Heat Affected Zone
SEM	Scanning Electron Microscopy

List of Units

bar	Pressure unit
GPa	Giga Pascal
min	Minute
mm	Millimeter
MPa	Mega Pascal
N	Newton
s	Second
W	Watt
°C	Degree Celsius
HV	Vickers hardness

List of Symbols

C	Chemical symbol for Carbon
Cr	Chemical symbol for Chromium
Mn	Chemical symbol for Manganese
Mo	Chemical symbol for Molybdenum
N	Chemical symbol for Nitrogen
Ni	Chemical symbol for Nickel
Si	Chemical symbol for Silicon
%	Percentage

FIGURES INDEX

TABLES INDEX

INDEX

INTRODUCTION

1 INTRODUCTION

1.1 Contextualization

Cold forming is used to produce several different products, due to the high production rates and low production costs, allowing to produce high volumes and tight tolerances. However, when starting the production of a new part, sometimes it is unavoidable to have some changes in the part geometry or even production errors, leading to high losses of time and money in punching equipment.

Laser technology has been improving over the past decades and, as such, it is nowadays used in several different areas. In the industry, laser is essentially used in the cutting process of different materials due to its high versatility and its high cut quality, when compared to similar manufacturing processes. For this reason, it was opted to study the laser cutting feasibility in order to produce prototypes or small volumes of production combined with cold forming, aiming to reduce initial costs and times related to starting the production of a new component, since it does not require the wait of tools, such as punching dies, usually necessary in cold forming process, allowing to speed up the development time of a prototype track.

The intention of this laser process is to combine it with punching in a production line. For this reason, there are several finishing requirements needed to accomplish. In order for the final production line to work properly, it is necessary that, not only the cutting accuracy of laser is equal or better as the one produced by punching, but also to keep the process repeatability equal or better, allowing the working geometry to be always within the tolerances and correctly positioned in every stage of production.

This implementation will also allow the possibility to produce new geometries and work with different materials. Besides these advantages, this implementation will reduce initial times since it does not require the wait of parts, something that is necessary in cold forming process, allowing to speed up the development time of a prototype track. This also allows the production of low volumes, up to 100 000 units, something that was not viable only using cold forming. On the other hand, laser cutting also has some disadvantages which are also going to be studied and mentioned throughout the report.

Among any other projects, a new type of trimmer is being developed at Philips in Drachten, one of the components being the part chosen to carry out this investigation. The principal mechanism of the trimmer is constituted by the cutter and the guard. Both components have teeth that allow the entrance of the hair and, due to the relative

movement between the two pieces, the hair is cut. The cut is helped by the existence of cutting angles on the cutter teeth and cutting radius on the guard teeth (Figure 1).

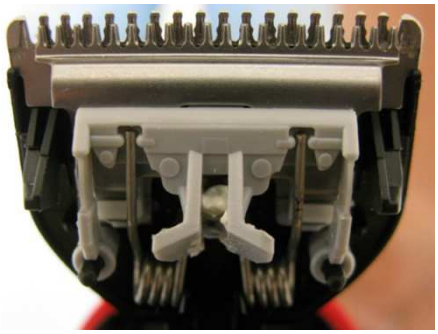

Figure 1 - Trimmer example (Bhatt, 2012)

However, it is necessary to prove that the component is feasible by this process, being the stamping of the teeth the operation that presents the biggest risk. For this reason, for the prototyping, it is relevant to make several thousand products with different outer geometries with laser cutting and to test the ability to stamp the teeth.

The Ultron guard was chosen for this research for two main reasons. The first one is the geometry that, even though it is relatively simple, presents some complex features to laser cut that allow to verify the possibility of using this to prototype other components with even more complex geometries. The other one is the fact that the Ultron guard will be made from AISI 304, of 0.4 mm thickness, which should be one of the harder materials to laser cut that is currently used at Philips in Drachten.

1.2 Purpose and main goals

The purpose of this work is to test the feasibility of producing the Ultron Guard by laser cutting combined with cold forming in a production line, as well as trying to improve the laser cut quality and speed in order to achieve a cut quality similar to the produced by punching, decreasing as well the production times.

In general, this research reflects on the following goals:

- Prototype a positioning and fixing mechanism of the metal strip for the laser machine;
- Test different laser cutting parameters;
- Analyze the laser accuracy and repeatability;
- Analyze and compare the cut surface produced by the different parameters and by punching;
- Analyze and compare the heat affected zone dimension and microhardness with the different parameters;
- Analyze and compare the burr produced by the different parameters.

1.3 Host company

The present work in this dissertation was performed in an industrial environment at Philips Consumer Lifestyle B.V., located at Dracthen, Netherlands, under the guidance of the Engineer Dave Geertsma.

The internship had a total duration of 6 months, starting at 02/03/2020 until the 28/08/2020 with a schedule of 8 hours during the workdays. It must be highlighted that attending to the worldwide situation experienced in this period, the majority of the work was performed from home, which led to some limitations in the development of the work as it will be possible to see further ahead.

Contextualization of the company

Philips first steps where made in Eindhoven, the Netherlands, in 1891 when Frederik Philips and his son Gerard Philips founded Philips & Co. They started the company to meet the growing demand for light bulbs created by the commercialization of electricity. Anton Philips joined the company in 1895. Nowadays, Royal Philips Electronics NV has the head office located in Amsterdam.

Philips is a consumer-centric and market-oriented organization. They develop meaningful products that improve people's health and wellbeing and contribute to a healthy and comfortable life for consumers, as shows their sentence of compromise "Sense and Simplicity".

Philips belongs to the top 50 of global brands and has leading positions on many markets in the fields of health, consumer lifestyle and lighting. By health, Philips does not just mean the medical aspects of health: staying fit, healthy food and a healthy lifestyle are very important for the brand. Philips has over 50,000 registered patents, 36,000 registered trade marketing and 63,000 design rights which illustrates the company's innovative nature.

Philips employs more than 119,000 people worldwide. With health and wellbeing as the company's main points, Philips supplies the professional and consumer markets with products from three overlapping sectors.

Philips Drachten is part of the Consumer Lifestyle (CL) sector. With more than 2000 employees from 35 different nationalities, Philips CL Drachten is one of CL's largest development and production centers in Europe. Philips CL Drachten develops many innovative products that make life more comfortable for the global market. These products include coffeemakers, vacuum cleaners and hot air fryers. Philips CL Drachten has also been the development and production center for Philips shavers since 1950. Here, the most sophisticated Philips electric shavers are being manufactured.

1.4 Dissertation structure

The present dissertation is divided into four chapters.

In the first chapter, an introduction to the thematic under analysis is made in order to frame the work done, clarifying the objectives, the methodology used and the institution where the entire dissertation was developed.

In the second chapter is made a theoretical framework addressing the subjects that are related to the performed project and are also essential for its understanding. Firstly, it is presented the laser mechanism and the cut quality produced by this process, aiming to see the differences between the two processes as well as potential advantages and disadvantages. After, an approach regarding the forming mechanism and taking a closer look to the cut quality produced by this process.

In the third chapter is presented the used methodologies for the development of the practical part of the performed work. In this chapter it is explained the used methods when performing the accomplished laser tests, the laboratorial work, and the measurement of the dimensions of the samples.

The fourth chapter presents the obtained results, as well as the interpretation of the same and the created prototypes, aiming to improve the laser cutting process.

The fifth and last chapter presents the obtained conclusions of the performed works, as well as the limitations and suggestions for future research.

LITERATURE WORK

2 LITERATURE WORK

2.1 Laser

Laser stands for “Light Amplification by Stimulated Emission of Radiation” (Amorim, 2016). Laser cutting is a thermal based process that does not require any contact and it is also highly automated while still ensuring high dimensional accuracy and surface finishing, being for that reason well suited for a large variety of manufacturing industries to produce components in a relatively large amount of components (Kumar & Jayaprakash, 2017).

The process of laser cutting involves the heating, melting and evaporation of material in a well-defined pattern and small area, capable of cutting almost all types of material (Patel, Varsi, & Marathe, 2016; Amaral *et al.*, 2019). It was first introduced in industry in the mid-1970s and since then its applications have not stopped growing and improving, becoming one of the most reliable advanced manufacturing technologies, being nowadays used in several fields such as medicine, beauty, manufacturing industry, weapon system and others (Liu, Duan, & Peng, 2014).

2.2 Laser beam

A laser is a type of light, but in order to have its own properties, it has to differ from the others, which occurs in the light creation, while, for example the sun light is irradiated in every direction, with different wavelength and out of phase, the laser beam has specific properties (Amorim, 2016), such as:

- **Monochromatic:** The light emitted by a laser is a light with a single wavelength (Amorim, 2016);
- **Coherent**: All waves have identical frequency and are (aligned) in phase (Abbas, 2014);
- **Directional:** All waves are almost parallel and for that reason they have a really low diverge (Hashemzadeh, 2014). This has a major importance because it allows to create a compact laser beam with enough power intensity to process the materials. The laser beam can be applied this way with a very small diameter in order to increase a lot the power density that is applied in the workpiece (Amorim, 2016) .

2.3 Laser principal/System

Even though there are several different lasers, nowadays lasers still have the same principals as the first developed one to generate the laser beam. The laser beam is generated by an atomic excitation that occurs inside a glass tube where an active medium is contained, this medium can be solid, liquid or plasma.

The chemical species of the active medium is what determinates the optical output wavelength, because different materials will have different energy levels, resulting in released photons with different energy (Majumdar & Manna, 2003; Li, 2018). In order to understand properly the laser working principal, it is also required to have a previous knowledge of atomic physics.

As it is possible to see in the Figure 2, an atom is constituted by a positive charge nucleus of protons and neutrons that is surrounded by a negative charged cloud of electrons. These electrons are orbiting the nucleus in orbits being that each orbit corresponds to a specific energy level of the electron.

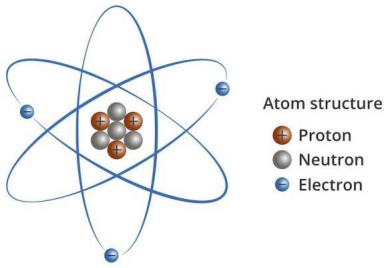

Figure 2 - Atom structure (Sharp, 2019)

When an atom is supplied with energy, the electrons look for a new position in order to maintain the energy equilibrium. If the specific amount of energy is supplied, the electrons will change to a higher energy level orbit, where they stay for a really small amount of time until they return to the ground-state level, releasing the absorbed energy in the form of photons (Amorim, 2016).

During the laser generation process, the medium is excited to the amplifying state by a pumping source that can be flash lamps, lasers, electrons. This energy is then absorbed by the medium source atoms, moving the electrons from a low-energy orbit to a high-energy orbit (Hashemzadeh, 2014). The excited electron in the higher energy state naturally returns to the ground state, emitting the energy difference between the two levels as photon of energy. This phenomenon is known as stimulated emission of radiation, happening coherently with the stimulating radiation, resulting in an identical wavelength, phase and polarization (Majumdar & Manna, 2003). This photon is not laser light yet, the emitted photon may interact with a non-excited atom and possibly get absorbed by it, also exciting the atom to a higher level. This event is called “population inversion”, and is created by the pumping source.

Other photons moving along the optic axis are going to interact with a large number of already excited atoms, disturbing the electrons in the higher state level, making them return to the lower energy level, releasing another photon, in phase, with the same energy and identical with the original one. This phenomenon is called stimulated emission and means that when one already excited atom is stimulated by a photon, results in the stimulating photon plus the released photon.

To create the laser light is necessary to have a larger percentage of excited atoms than atoms in the ground level (Hashemzadeh, 2014). In order to increase the chance of this occurrence, the photons are repeatedly reflected through the excited medium by the mirrors with a percentage of these photons exiting through the partially reflective mirror, building up the laser beam (Abbas, 2014). After the laser beam is produced, it is guided to the focusing lens where it will be focused to actuate in the workpiece. A schematic representation of a Nd-YAG laser machine is represented in the Figure 3.

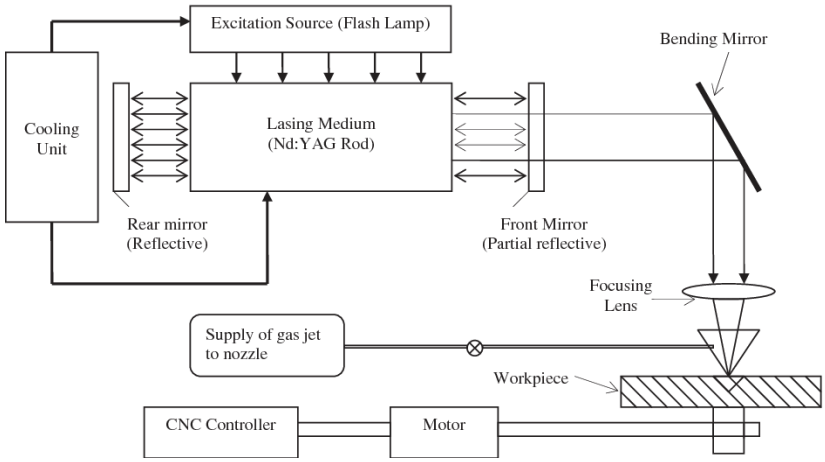

Figure 3 - Schematic representation of a Nd-YAG laser machine (Selvan, Rammohan, & Sachidananda, 2015)

2.4 Laser cutting advantages and disadvantages

As typical to any other manufacturing process, laser cutting also presents its own advantages and disadvantages, as it is possible to understand below.

Advantages:

- Able to work with a wide range of different materials;
- Since laser cutting is a thermal based non-contact process, there is no tool wear, meaning that the workpiece only needs to be lightly clamped in order to prevent the piece from moving during the operation (Powell & Kaplan, 2004; Kumar & Jayaprakash, 2017);
- Capable of producing high complexity geometries (Lazov & Narica, 2015);
- High flexibility and changeovers (Lazov & Narica, 2015);
- High material flexibility (Kellens et al., 2014);

- Easily automated with computer numerical control (CNC) and robotic processing, allowing a high productivity (Muhammad, 2012);
- Small heat affected zone (HAZ), when compared to other thermal cutting processes like flame and plasma (Muhammad, 2012);
- Quiet process, allowing to reduce the noise level in the workplace (Muhammad, 2012);
- Capable of producing highly complex contours (Abbas, 2014).

Disadvantages:

- High power consumption (Patel, Varsi, & Marathe, 2016);
- Can be expensive, depending on the volume of productions while comparing to other methods (Patel, Varsi, & Marathe, 2016);
- Rate of production depends on the type and thickness of the material (Patel, Varsi, & Marathe, 2016);
- HAZ can potentially affect the microstructure;
- Poorly adjusted lasers can cause bad finishing and even burr and burned surfaces (Patel, Varsi, & Marathe, 2016);
- Difficulty when cutting metals with high reflectivity such as copper, brass and sometimes aluminium (Patel, Varsi, & Marathe, 2016).

2.5 SWOT analysis about laser cutting process

In order to analyse the potential problems and benefits linked to the laser cutting process, it was performed a SWOT analysis with the collaboration of some colleagues of Philips team, as it is possible to see in the Figure 4.

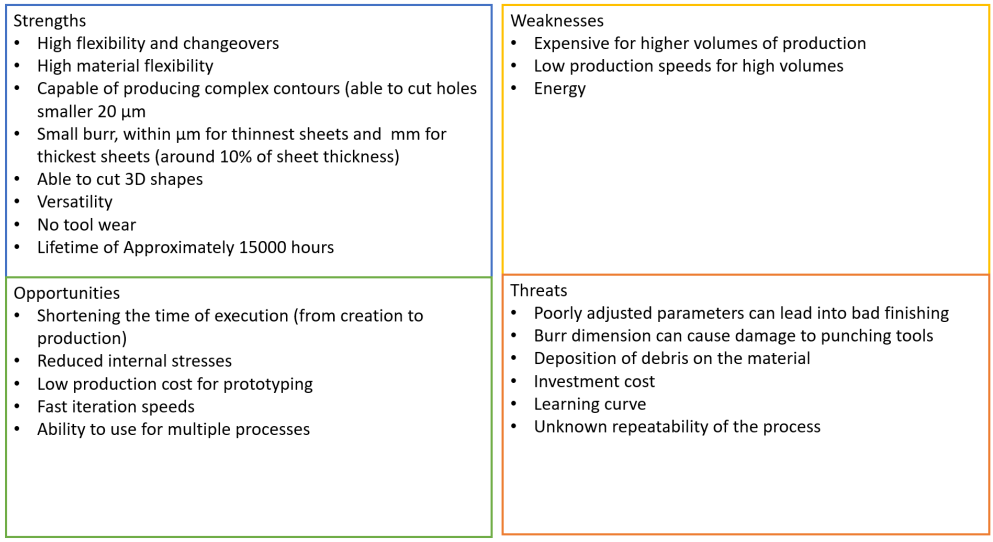

Figure 4 - Laser cutting SWOT analysis about laser cutting process

2.6 Laser cutting quality

The quality of a laser cutting process can be evaluated by different characteristics (Figure 5) in the cut material, such as referred in the next subchapters.

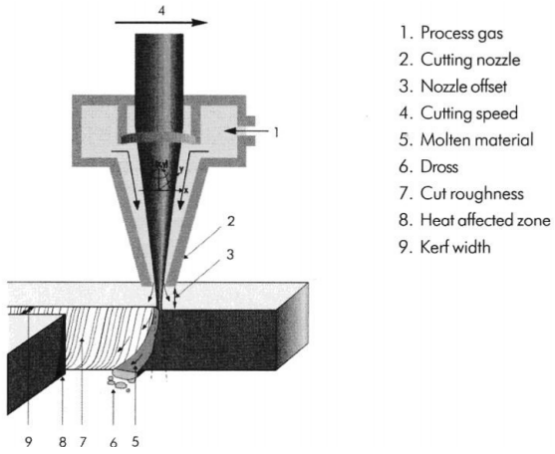

Figure 5 - Laser cut surface characteristics (Wandera, 2006)

2.6.1 Kerf width

Distance between the edges of the groove produced by the laser. This distance is usually measured on the top and bottom part of the processed material, since normally the cut is not parallel, meaning that the distance changes along the material thickness (Kumar & Jayaprakash, 2017).

This phenomenon can occur due to several factors, such as the beam loss of intensity, beam defocusing and gas pressure loss. This implies then that the laser power, cutting speed and assist gas jet are the parameters with the biggest influence in this characteristic (Muhammad, 2012).

2.6.2 Dross

Solidification of molten material in the shape of drops, clinging on the bottom edges of the cut material. This formation is influenced by surface tension and viscosity of the molten material. The high values of this characteristic make the molten material resist from flowing fluently from the cutting zone, increasing the chance of dross formation. To reduce this dross formation, assist gas jet is used in order to expel the molten material, minimizing the dross adherence, even though this does not completely delete the dross formation (Conrado, 2014).

The effect of the assist gas jet also depends on gas pressure and gas type, being that inert gas jet increases the dross formation when compared to a reactive gas, since the surface tension on pure metals is higher than oxidised metals. Other parameters can also be adjusted in order to reduce the dross formation, such as the appropriate focus and cutting speed (Muhammad, 2012).

2.6.3 Heat affected zone (HAZ)

Due to the fact that laser cutting is a thermal based process that involves a huge amount of energy absorbed and conducted by the workpiece, it is evident that a lot of that excessive heat is conducted to the imminence of the cutting zone. The excessive heat is going to affect this zone, transforming the microstructure an affecting the workpiece properties in these zones.

The HAZ can be measured perpendicularly to the cutting direction, where it is possible to observe the microstructure and/or hardness variation from the beginning of the cut edge to the base material (Muhammad, 2012). The HAZ area reduces with the increase of the cutting speed, since the laser passes less heat by cutting length unit of the workpiece, reducing the amount of energy and temperature absorbed and conducted by the workpiece (Wardhana *et al.*, 2019). The HAZ also varies from the top to the bottom of the kerf, being higher on the top side (Hashemzadeh, 2014).

2.6.4 Recast

It is a layer that is formed by the re-deposition of molten material on the cut edges (Muhammad, 2012). This layer (Figure 6) is generally harder than the base material and it is also usually very stressed, meaning that it is more prone to have crack formations (Lv, Wang, & Ji, 2006). According to those authors, the formation of this layer is highly dependent on some laser cutting parameters such as pulse energy, assist gas and cutting speed, where the increase of pulse energy resulted in an increase of energy delivered to the process, leading to bigger recast layers. The increase of the cutting speed leads to a smaller recast layer, since the reduction of energy density on the cut area is expected. The recast layer also tends to reduce with the increase of assist gas pressure. According to Kleine, Whitney and Watkins (2002), the use of ultra-short laser pulses (pulse durations of 10^{-12} - 10^{-15} s) also tends to reduce the recast layer.

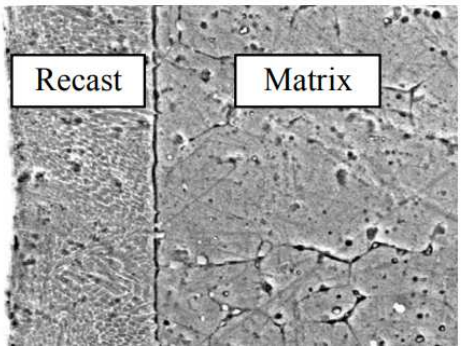

Figure 6 - Recast layer (Lv, Wang, & Ji, 2006)

2.6.5 Cut surface roughness

The surface roughness is the texture and quality of the cut surface, in the form of irregularities of the surface profile and it can affect the component tolerances, wear behavior, fatigue life and tensile strength (Wandera, 2006).

There are two usual standard measurements of surface roughness that can be applied in laser cutting (Pocorni *et al.*, 2013). The first and most common one is the average roughness (Ra) (Muhammad, 2012). This average roughness translates the arithmetic average deviation of the assessed profile in a certain length. The other one is the R_z, which is the maximum peak throughout the analyzed surface (Pocorni *et al.*, 2013). The cut surface roughness is influenced by several parameters such as the assist gas jet pressure, nozzle shape, cutting speed and laser power, but it is often related to the natural striations from the non-steady nature of laser cutting (Abbas, 2014).

2.6.6 Striations

During the laser cutting of mild steel oxygen, the ignition phase occurs under a high power laser beam, focused together with the coaxial oxygen jet, and causes the steel sheet to oxidize exothermically when the high power laser touches the cutting front.

The highly energetic burning front quickly moves away from the center of the laser beam and once the laser beam is left behind, the burning front cools and extinguishes. The moving laser then repeats the process on the next area, generating a pattern of striations along the cut edge.

Generally, the distance between striations increases with the cutting speed and normally, the faster the cutting speed, the less is the heat penetration and the better is the cut quality. When cutting with inert gas, where there is no exothermic reaction, the striations are associated with inefficient removal of the molten material. The quality of the cutting surface in nitrogen cutting is enhanced using higher gas pressures compared to the gas pressures used in cutting oxygen. The laser cut surfaces show two different striation patterns, one with a finer structure adjacent to the upper surface and one with a coarser pattern adjacent to the lower surface of the workpiece (Wandera, 2006).

2.7 Cutting parameters

There are several different parameters to have into account before a laser cut is performed, in order to have a good cut edge finishing and a short process time, as well as a good relation between both. These parameters can be split into **laser system parameters**, that cannot be adjusted by the operator and the **process parameters**, which can be adjusted by the operator. These choices depend on the material type and thickness of the workpiece (Abbas, 2014).

2.7.1 Laser system parameters

2.7.1.1 Power and intensity

The amount of energy emitted per second in the form of laser light is the laser power, while the intensity of the laser beam is the power transferred in the area where the beam is concentrated.

A higher laser intensity is obtained by focusing the laser beam to a small spot, being this desirable for cutting applications, since the heating of the material in that area occurs faster, which reduces the time for the heat to dissipate to the rest of the workpiece. This also allows to use higher cutting speeds and tends to produce a better cut quality. The optimization of these parameters is very important since using excessive power results in a higher kerf, a thicker recast layer and a dross increase, while using lower laser power can result in incomplete cuts (Wandera, 2006).

2.7.1.2 Wavelength

It is a particular characteristic of each laser since it depends on the energy levels of the atoms in laser medium (Figure 7). In a laser cutting process, the laser beam must completely penetrate the workpiece and the wavelength of the laser has a major impact on this, having a decisive influence on the material's surface absorptivity (Hashemzadeh, 2014).

The reflectivity of metallic materials to a laser beam is a function that depends on the laser wavelength, being that, typically metals have a higher reflectivity to longer wavelengths, meaning less capacity of absorption. Even though metals have a high reflectivity to CO_2 laser beam at room temperature, they become better absorbers with the increase of temperature (Wandera, 2006).

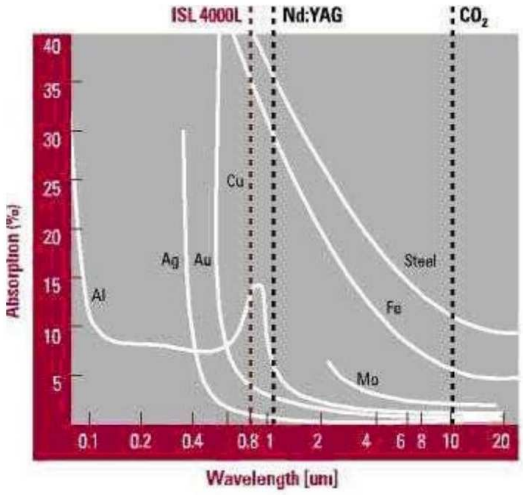

Figure 7 - Absorption phenomena of typical metals over a range of different laser (Bell Laser, 2020)

For that reason, when comparing the two most common commercial lasers, CO_2 and Nd:YAG lasers, the last one has some advantages due to the wavelength of 1.06 µm, which is ten times smaller than the CO_2 wavelength:

- **Nd:YAG laser beam** can be focused in a smaller spot, translating in a finer and more detailed cut;
- **Nd:YAG laser beam** is easier to be absorbed, being for this reason more suited to work on metals with higher reflectivity.

Unlike CO_2 lasers, the beam of a Nd:YAG laser can travel through glass, enabling the possibility of using high quality lenses to focus to a small spot. This also allows the use of optical fibres to carry the beam from significant distances to the workpiece. It can also be seen as an disadvantage, since it cannot cut some organic materials that are transparent to this light (Powell & Kaplan, 2004).

2.7.1.3 Beam quality

The laser beam quality is characterized by its mode, which is the energy distribution through the beam cross section (Berkmanns, & Faerber, 2008). A uniform energy distribution is essential because it allows the beam to be focused in a smaller spot, increasing this way the beam intensity which also translates into faster cutting speeds and better cut quality (Conrado, 2014).

Laser beam mode can be referred to a gaussian intensity distribution and, theoretically, the term with the lowest order (TEM_{00}) refers to a gaussian intensity about a central peak. This gives a very high intensity when comparing to other modes, where the beam is focused on a small spot size. The TEM_{00} also confers the biggest depth of focus, thus giving the best performance when cutting thicker materials. However, in practice, lasers usually deliver a higher order mode, conferring a larger focus spot size than the TEM_{00} (Bell Laser, 2020).

2.7.2 Process parameters

2.7.2.1 Continuous wave (CW) or pulsed laser power

Laser cut can be executed in continuous wave or pulsed, which is determined in function of the workpiece material or on the wanted process (Conrado, 2014; Silva, 2008). The cutting speed is determined by the average power intensity, the higher the average power the higher the cutting speed can be, meaning that a high power cw laser can achieve higher cutting speeds than the pulsed laser (Hashemzadeh, 2014).

However, the penetration in the workpiece is determined by the peak pulse power in pulsed cutting and by the average power in continuous wave. When cutting a fine component, a more precise cut is intended, and the pulse operation is preferred since the high power in the short pulses ensures an effective heating, as well as an effective removal of the molten material from the kerf zone, reducing the dross formation and

the low average power reduces the heat conduction, keeping the workpiece cool, being for this reason also more suited for micro cutting of thin section materials and materials with higher thermal conductivity (Berkmanns & Faerber, 2008).
The duration of the pulse is typically between 100 µs and 1 ms, with a pulse frequency varying from 1 Hz and 100 Hz, depending on the thermal dissipation capacity of the active medium during the operation (Gerck & Lima, 1997).

2.7.2.2 Focal length of the lens

Converging lenses are usually used to focus the beam on a small spot. The focal length of the lens is an important parameter of the optical component, since the smaller the focal length, the smaller the beam diameter at the focal point and the smaller the cut width are obtained (Conrado, 2014).

The focal length of lens is the distance from the position of the focal lens to the focal spot (Figure 8). It determines the shape of the focused beam onto the workpiece depth (Boc, 2020; Patidar & Rana, 2018), determining the focused spot size and also the focus depth, which defines the thickness that can be cut (Wandera, 2006).

The minimum spot size is still depending on the wavelength, beam mode, the diameter of the unfocused beam at the lens and the focal length of the lens. The focal position must be controlled in order to ensure the best cutting performance (Bell Laser, 2020).

When cutting material thinner than 4 mm, a short focal length is recommended since the smaller focused spot gives a narrow kerf and a smoother cut edge. When cutting thicker materials, a longer focal length is preferred, and the depth of the focus should be around half of the material thickness. The use of longer focal length lens also increases the working distance, which minimizes the risk of contamination of the lens (Wandera, 2006).

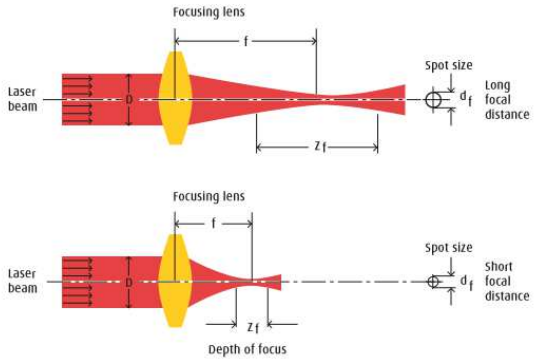

Figure 8 - Focal length of the lens (Berkmanns & Faerber, 2008)

2.7.2.3 Focal position relative to the workpiece

The correct focal position must be ensured to provide the optimum cutting performance. This may require some alterations when working with different materials or thicknesses.

According to Hashemzadeh (2014), the focal position can be placed somewhere between the upper surface and lower surface and its position affects the cut quality, cutting speed and the kerf width (Figure 9).

When cutting with oxygen, for thin sheets, the maximum cutting speed is achieved when the focal position is positioned on the upper surface, and when cutting thick sheets the maximum cutting speed is obtained when the focal position is located about one third of the plate thickness below the upper surface. However, when cutting with inert gas, the optimum focal position is typically closer to the lower surface, because it creates a larger kerf that allows a larger part of the gas to penetrate the kerf and eject the molten material. If the focal position is too high relative to the upper surface, or too below from the lower surface, the power density is not enough to produce the cut (Wandera, 2006).

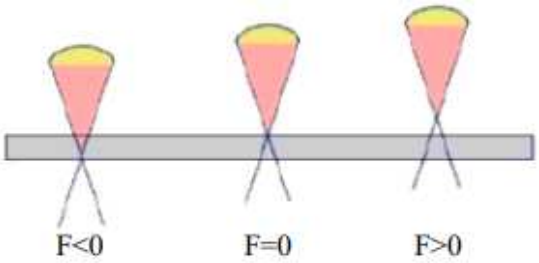

Figure 9 - Focal position relative to the workpiece (Conrado, 2014)

2.7.2.4 Cutting speed

Cutting speed is defined according to the power intensity of the laser beam and the material thickness. It also must be balanced in order to have an appropriate share in the ratio between the operation time and the cut quality (Bell Laser, 2020).

The energy supplied to the cutting zone can be divided into the energy used to generate the cut and the energy that is lost in the cut zone. With the increase of the cutting speed, the energy lost in the cut zone is decreased, increasing this way the efficiency of the cutting process. However, using too high cutting speeds tend to induce the appearance of striations, dross formation and even the incomplete cut of the workpiece.

Lower speeds used when cutting thicker materials, leads to an increase of the lost energy in the cut zone, causing an increase of the HAZ, consequently a lower efficiency and a decrease of the cut quality.

Cutting speed of a material is, in general, inversely proportional to its thickness and the speed must be reduced when cutting a sharp corner in order to avoid burning (Conrado, 2014; Silva, 2008). Cutting speed must also be balanced with the gas flow rate and the laser beam intensity.

2.7.2.5 Gas type and gas pressure

The assist gas has a major impact on the cutting result, having different important functions in the process (Figure 10). The workpiece material and the intended results determine the gas type to be used (Conrado, 2014).

The two most common gas types used are oxygen and nitrogen, each one having its own advantages and disadvantages, an inert gas such as nitrogen expels the molten material without allowing the drips to solidify on the underside, avoiding dross formations, while a reactive gas such as oxygen takes part in an exothermic reaction with the material, where additional heat is supplied in the cutting process, allowing higher cutting speeds. However, the use of oxygen also develops oxidation, affecting the surface quality.

Oxygen is normally used to cut mild steel and low-alloyed steels. Nitrogen gas requires higher gas pressure in order to remove the molten material from the kerf cut and it is the preferred gas to cut materials like stainless steel, high-alloyed steels, aluminium, and nickel alloys. The high gas pressure acts as an extra mechanical force to blow the molten material from the cut kerf. When using high pressure nitrogen to cut stainless steel, it produces a bright and oxide free cut edge. However, the cutting speeds are lower than the oxygen assisted process.

The main problem associated with inert gas cutting is the dross formation in the underside of the kerf, which can be reduced with the optimization of other processing parameters like nozzle diameter, focal position and gas pressure (Bell Laser, 2020).

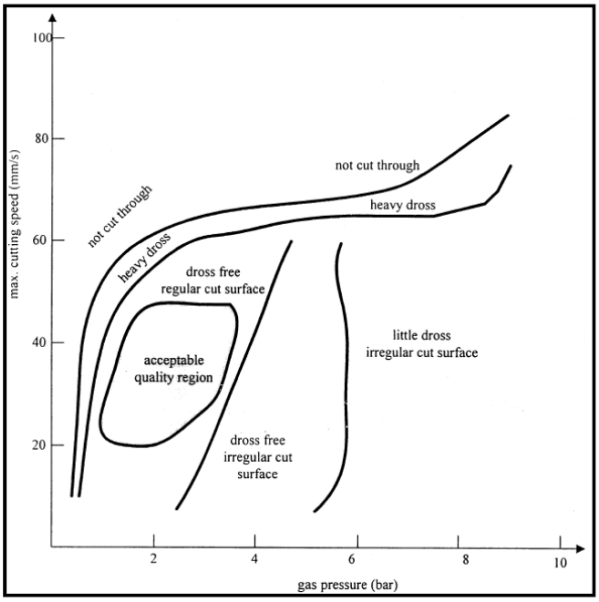

Figure 10 - The acceptable-quality cutting region of 3 mm mild steel oxygen-assisted laser cutting (Muhammad, 2012)

2.7.3 Laser cutting methods

2.7.3.1 Fusion cutting

The mechanism of laser fusion cutting consists on the heating, above the fusion point of the material, transforming it into a molten state, where it is then expelled by the high pressured assist gas to the bottom part of the workpiece.

The gas used to expel the molten material is applied coaxially and are usually inert (i.e. argon, helium and nitrogen), protecting also the cutting point from the surrounding air, avoiding sideways burning and oxidations, and minimizing the dross formation on the bottom edges of the kerf. The cooling effect of the gas is negligible due to the really small area involved in the process.

This type of process is normally used to cut materials with high reflectivity, such as stainless steel, aluminium and brass (Faro, 2006; Kheloufi & Amara, 2014; Ferreira, 2017).

2.7.3.2 Reactive fusion cutting

The reactive fusion cutting mechanism is similar to the fusion cutting. The difference is that instead of using an inert assist gas, a reactive gas is used, typically oxygen or mixtures containing oxygen. The use of oxygen causes exothermic reactions, leading to a temperature increase. The increase of energy added by the exothermic reaction depends on the workpiece material, where this increase is around 60% for a non-alloy steel and can reach 90% when cutting titanium. This additional energy on the process allows a higher cutting speed that can be twice the speed compared to process without an exothermic reaction (Faro, 2006).

However, this reaction causes different effects on the cut surface, depending on the workpiece material. On a non-alloy steel, the most visible effect is the formation of a thin oxide layer on the cut surface. This also brings an advantage since the oxide reduces the dross formation because it improves the molten material flow. This dross formation does not happen when cutting stainless steel or aluminium since the oxide is formed by high fusion point compounds, that solidify fast and increase the dross formation.

2.7.3.3 Vaporisation cutting

In vaporisation cutting, the material is removed mainly in the form of vapor. The energy provided by the laser has to be high enough, so that the material reaches its vaporisation temperature in a very short interaction of time, being for this reason easier achieved with a pulsed laser (Muhammad, 2012).

In the beginning, the laser beam actuation causes a temperature increase of the surface. As the temperature continues increasing, the reflectivity of the material decreases,

increasing the absorptivity and leading to fast increase of the temperatures until the boiling point, generating vapor. The vapor leaves the surface at a high speed, also dragging some particles, creating a cylindrical cavity named keyhole. The appearance of the keyhole causes abrupt increase of the absorptivity, due to the multiple reflections that allows the hole to deepen quickly (Faro, 2006).

Another important step when laser cutting is the piercing operation, especially when dealing with small features. The mechanism of metal laser piercing can be explained in four major steps, being these the surface heating, surface melting, vaporisation and molten material ejection (Hashemzadeh, 2014):

- **Surface heating:** In the beginning, the laser beam is focused on the metal surface, starting the interaction between the electrons and the metal surface. The excited electron collides with lattice photons and other electrons converting the energy to heat in a very thin surface layer of the metal sheet.
- **Surface melting:** Being the laser intensity high enough and the interaction time between the laser beam and the metal surface sufficient, a thin layer of the surface begins to melt. The laser beam intensities are normally so high that the interaction time of the molten layer is too short to result in a significant heat conduction to the material.
- **Vaporisation:** The continued interaction between the laser beam and the molten layer typically results in such an increase of temperatures that the temperature of the material gets higher than the vaporisation temperature, causing the vaporisation of the material.
- **Melt ejection:** During the vaporisation, two types of melt material ejection occur. The first one is the ejection of the molten layer that is ejected by the induced recoil pressures caused by the vaporisation and, secondly, the ejection caused by probable existence of nucleation mechanisms that may cause the violent boiling of the material.

In Table 1 are described some studies performed analysing the influence of some laser cutting parameters on the cut quality.

Table 1 - Studies made with stainless steel

Author	Description
(Stelzer *et al.*, 2013)	The goal of this study was to analyse the influence of the cutting speed on the cut quality of an AISI 304 with different thicknesses, between 1 and 10 mm. The experiments were conducted using two different types of laser, fibre laser and CO_2 laser, both using a laser power of 3 kW and an inert assist gas. When cutting the thinnest sheet (1 mm), the smaller kerf width was obtained with the fibre laser. However, as

	expected, the kerf width increased with the sheet thickness. Nevertheless, when analysing the kerf width throughout the sheet thickness, the CO_2 laser obtained more consistent results. Regarding the average surface roughness, the highest values were detected closer to the bottom region of the cut edge and when comparing it on both types of laser, similar roughness was obtained for thinnest sheets, up to 4 mm thickness, and for thicker sheets the CO_2 laser obtained significantly better roughness.
(Ghany & Newishy, 2005)	This research was conducted in order to evaluate the optimum laser parameters when cutting austenitic stainless steel sheet with 1.2 mm thickness, using a Nd:YAG laser beam in pulsed and CW mode, and nitrogen or oxygen as assist gas. For the pulsed laser mode, dross free and sharp edge surface was achieved with the following parameters: frequency between 200 and 250 Hz, laser power of 210 to 250 W, cutting speed between 1-2 m/min, focal position of -0.5 to -1 mm and nitrogen gas pressure of 9 to 11 bar. For the CW mode, most of the used parameters were the same, now the speed being between 6 to 8 m/min and the power ranging between 900 and 1100 W. The increase of cutting speed during the pulse mode led to an insufficient overlapping of the pulse, causing an incomplete cut. The increase of frequency also generated a lower roughness since the pulse overlapping was bigger. However, in the CW mode, the increase of the cutting speed (until 8 m/min, where a bigger increase induced vibrations and instability in the equipment) with equivalent increase of power, generated a better cut quality, with smoother, bright surface and smaller kerf width. Regarding to the assist gas, when using nitrogen with a lower pressure than 9 bar led to dross formation, and higher-pressure values produced better quality and clean surfaces. However, pressures above 11 bar did not significantly improved the cut surface. Using oxygen as assist gas, resulted in a poor surface quality with the presence of oxidation, as well as a wider kerf. Changes on the oxygen pressure revealed big variations since 4 bar was the pressure that showed best results, with no dross, reducing the pressure led to incomplete cutting and increasing the pressure led to big dross formations.
(Junior, Ventrella, & Gallego, 2016)	The study focused on the influence of parameters such as peak power, pulse duration and the existence or not of a protective atmosphere on the size, geometry and depth on micro holes, when cutting a 1 mm thick AISI 316L metal sheet

	with a pulsed Nd:YAG laser. During the tests, the peak power varied from 1 kW to 7 kW, the pulse duration was 1 ms and 2 ms, without assist gas and using Argon as assist gas. The cutting of the total thickness was only achieved at a high enough power level, and after that, the diameter of the exit hole kept increasing with the process energy. It was also observed that the exit hole kept losing the circular geometry with the increase of process energy, and this was more evident in processes without assist gas. Related to the pulse duration, if the process energy has been maintained, the pulsed with a bigger duration caused less effect on the surface. The effect was even smaller when using assist gas.
(Amaral *et al.*, 2019)	This work intended to study the influence of process parameters, such as laser power, cutting speed and assist gas pressure on the cut surface when laser cutting AISI 316L sheet of 2 mm thick, with CO_2 and fibre laser. The analysed samples did not show any evidence of microstructure change on the cut surface because the applied laser intensity did not interact enough time to increase the temperature enough to result in a microstructure change. Related to the dross and roughness analysis, the study obtained very small dross dimensions for both laser types, however, it was also reported an increase of dross and roughness with the decrease of laser power, cutting speed or assist gas pressure.
(Patel & Sanghavi, 2014)	The study analysed a 3 mm AISI 304 metal sheet cut surface roughness, when cutting with a CO_2 laser. The research was done varying three process parameters: the cutting speed, gas pressure and input power. Using the ANOVA tool, the authors concluded that the parameter with the biggest impact on the surface roughness was the power, having a contribution of more than 50%, followed by the errors induced by human or machines, with a contribution of more than 30%. Gas pressure and cutting speed had a relatively small contribution, being 12.27% and 0.06%, respectively.

Table 2 - Studies performed analyzing the influence of cutting parameters on the HAZ

Author	Description
(Miraoui, Boujelbene, & Zaied, 2016)	This study is focused on the thermal effect of CO_2 high-power laser cutting. The authors have investigated the influence of three laser cutting parameters such as laser power, cutting speed and laser beam diameter when cutting an 8 mm S235 steel sheet and analysed the heat affected zone width and HAZ microhardness. The results showed that HAZ width increases with laser power and it decreases with cutting speed. It was also observed that laser power has the biggest impact followed by cutting speed, while the laser beam diameter has a negligible effect. The parameters have similar influence on the HAZ microhardness as on the HAZ width, increasing with laser power and decreasing with cutting speed. However, the laser beam diameter has a significant effect, decreasing the HAZ microhardness with the increase of the diameter.
(Sheng & Joshi, 1995)	The research analysed the effect of laser power and cutting speed on the HAZ dimension when cutting AISI 304 stainless steel with 3.2 mm thickness with a CW CO_2 laser. The results showed an increase of the HAZ dimension with the increase of laser power and it decreases with cutting speed, due to the decrease of heat that any point in the material receives caused by the faster movement of the laser beam.
(Rajaram, Sheikh Ahmad, & Cheraghi, 2003)	This study was performed on AISI 4130 steel using a CO_2 laser in order to analyse the influence of cutting speed and laser power on the cut quality. The results showed that generally HAZ increases with the increase of laser power and decreases with the increase of cutting speeds. This was explained by the ability of the material to conduct the heat, since with the increase of cutting speeds the interaction time decreases, resulting in less heat conducted and, hence, a smaller HAZ. However, when using higher laser power, the results showed a decrease of the HAZ at slower cutting speeds but, at higher cutting speeds, the HAZ also increased when compared to lower laser power.
(Madić & Radovanović, 2003)	The study analysed the HAZ dimension and the effects induced by laser cutting parameters such as cutting speed, laser power, assist gas pressure and focal position on it. The tests were performed on a 3 mm thickness AISI 304 stainless steel sheet using a CW CO_2 laser machine assisted by nitrogen. The experiments showed that increasing the laser power results in an increase in the HAZ width until a certain power range, due to the increase of absorbed thermal energy by the material.

	However, after that power range, the HAZ width started decreasing, probably due to the interaction effect of the laser power width with other cutting parameters. This trend was also observed by other researchers (CO_2 Laser cut of 4130 Steel). Regarding the cutting speed, it was observed that its increase causes the decrease of HAZ width, because it reduces the interaction time between the laser beam and the material. Gas pressure increase translated on the decrease of HAZ width presumably because the efficient cooling effects of the assist gas. Lastly, it was observed that a lower focal position induced a smaller HAZ width, because when the focal position is close to the lower surface of the sheet, the kerf width becomes wider, allowing the assist gas to eject the molten material more effectively, minimizing the heat penetration into the material.
(Miraoui, Boujelbene, & Bayraktar, 2013)	The study performed on a 5 mm thickness AISI 304L metal sheet analysed the influence of laser power and cutting speed on microhardness. The experiments were performed with a CO_2 laser using a laser power range from 3 kW to 5 kW and a cutting speed range from 640 mm/min to 4000 mm/min. When analysing the microhardness, in accordance with other studies, it was observed that it increases as laser power increases, and decreases as cutting speed increases.

2.8 Forming

Differently from what happens in other manufacturing processes, in the forming processes, the change in the geometry of the components is done in the solid state and achieved through tools and procedures that allow and promote the flow of the material in the plastic regime. The characteristics of the forming processes make them very efficient in terms of using the material and reducing waste (Gomes *et al.*, 2017; Silva *et al.*, 2018).

The forming in metallic materials consists in the creation of a permanent deformation in the material. For this to occur, it is necessary to apply external forces of such an intensity that the point at which the material can return to its original shape is exceeded.

If the shear stress limit of the material is exceeded, then the atoms move into the field of attraction of the adjacent atoms and a new permanent state of equilibrium is reached occurring the plastic deformation (Tschaetsch, 2005). To reach this state, it is always necessary to reach a certain level of stress that depends on the characteristic of each material. In the Figure 11, it is possible to observe the typical behavior of metals in tensile tests (Moreira, 2018).

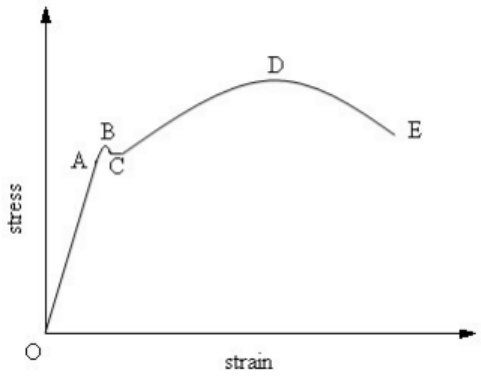

Figure 11 - Typical stress-strain of a ductile metal (Moreira, 2018)

According to the Figure 11, in a first phase, up to point A, there is a proportionality relationship between the applied stress and the strain of the material. During this phase, if the force is no longer applied, the material will return to its original shape. This phase is called the elastic phase. However, if the applied force continues to increase and point B, the elastic stress limit, is reached, a part of the deformation applied to the material will be permanent.

Continuing increasing the applied force, there is no longer proportionality between the stress exerted on the material and its deformation. In C, there is the yield point. This is a short and transient phase between elastic and plastic deformation.

After this phase, it is again necessary to increase the applied stress to continue to deform the material until point D, and the respective ultimate tensile strength is reached. This is the highest stress that the material will withstand and, from this point the material will start to decrease its section. Continuing the material will end up breaking at the breaking stress point (point E).

When a cut is performed in forming, the workpiece goes through all the phases previously described (Moreira, 2018).

These can be classified into two distinct groups, being bulk deformation processes, which integrate processes such as forging, extrusion and rolling, and sheet metalworking processes, which include shearing and bending processes (Cordeiro, 2016). In the Figure 12, it is possible to observe the main forming processes.

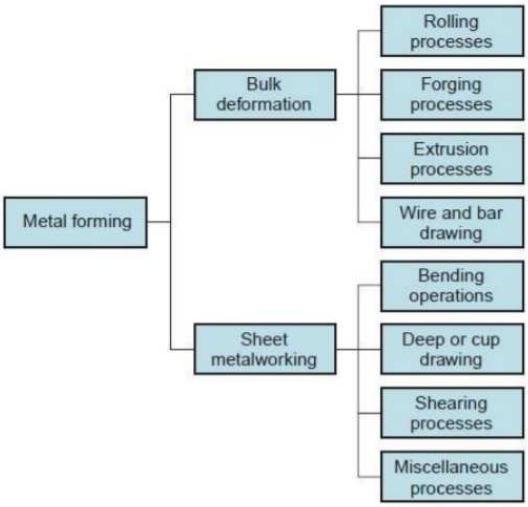

Figure 12 - Classification of metal forming processes (Arunachalam, 2018)

The bulk deformation processes can be performed at cold (near room temperatures) or at higher temperatures. At cold temperature, it is possible to obtain components with superior mechanical strengths and hardness, however the ductility and toughness of the components decreases. With this, the appearance and growth of cracks in the components is increased, making it a more suitable process to produce relatively simple geometries.

Comparatively, hot forming processes allow larger deformation rates and less steps of deformation, but due to the contraction during the cooling process, do not allow to obtain high dimensional accuracy. The hot bulk deformation processes, allows components with greater ductility, being thus used for parts with more complex geometries and larger dimensions, reducing fracture problems. The reduction of the load needed to deform these materials due to the high temperature allows the use of equipment with less force and power but one of the main disadvantages is the high energy consumption that is necessary for heating the components to be deformed (Cordeiro, 2016).

The cold forming process of metals is a manufacturing process that is characterized by the ability to produce parts with good production rates with almost total use of the raw material, meaning small amounts of scrap material.

2.8.1 Cutting operation

Cutting operations can also be performed with the forming process. These processes are operations that remove excess material in a given component to obtain a final product. This can be described as the separation of an outline from a plate or band using tools (die and punch) moved by a press. Highlight that within this type of process there is the conventional tool cut and the fine cut (precision), being the latter developed to avoid further machining, which could be necessary using the conventional method (Cordeiro, 2016).

Cutting is one of the most used processes for cutting sheet metal, being that the maximum thickness of which generally varies between 6 and 8 mm. This process does not alter the mechanical properties of the parts produced, being carried out mostly at cold temperatures (Rodrigues & Martins, 2010).

A cutting tool consists of a cutting punch with a contour equal to the intended, and a die, with the same contour, but with an offset which represents the cutting clearance.

As for the mechanics of conventional tool cutting, it can be explained into three distinct phases. In a first phase the crushing of the metal sheet takes place which begins with the descent of the press where the punch is. After this, the metal sheet gets stuck between the punch and the die and, from this moment on, the material is forced to enter the die creating elastic deformations in both sides of the metal sheet. In the second phase the cut occurs. Following the process, the material will be under a very high shear stress creating a pure cutting surface. The third and last stage is rupture, where, after a certain moment of the press descent movement, the plate breaks, which will allow the material to be separated (Cordeiro, 2016).

These three different phases will also generate three distinct zones on the cutting surface represented in the Figure 13, where it is also possible to see a normal cut surface morphology created by punching.

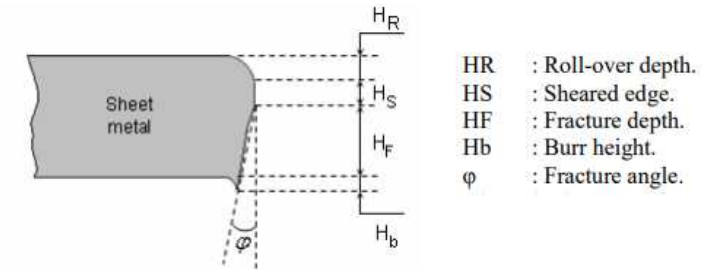

Figure 13 – Geometry of the cutting edge (Makich *et al.*, 2008)

The clearance between the punch and the die must be suitable for the metal sheet, being problematic if too large or too small. As it is possible to see in Figure 14, the greater the number of cuts a tool performs, the wear of the tools increases, leading to higher burr. The produced burr is a local plastic deformation near the contour of the workpiece where, in the zone actuated by the punch, as a result of the clearance between punch and die (Cordeiro, 2016).

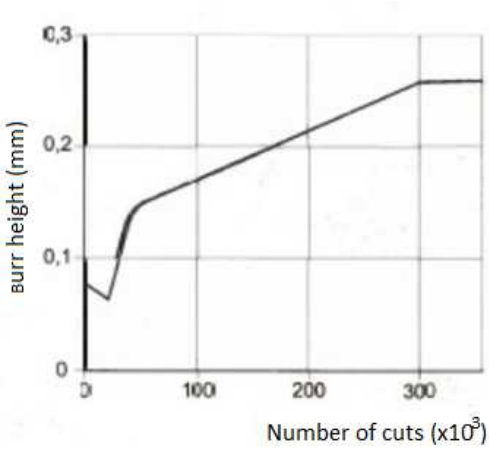

Figure 14 - Evolution of burr height with number of cuts. Adapted from Cordeiro (2016)

Forming can also be divided into different groups, depending on how the loads are used. This classification divides forming into five large groups, being these forming under compressive conditions, forming under compressive and tensile conditions, forming under tensile conditions, forming by bending and forming under shearing conditions, as it is possible to see in Figure 15 (Encerrabodes, 2018).

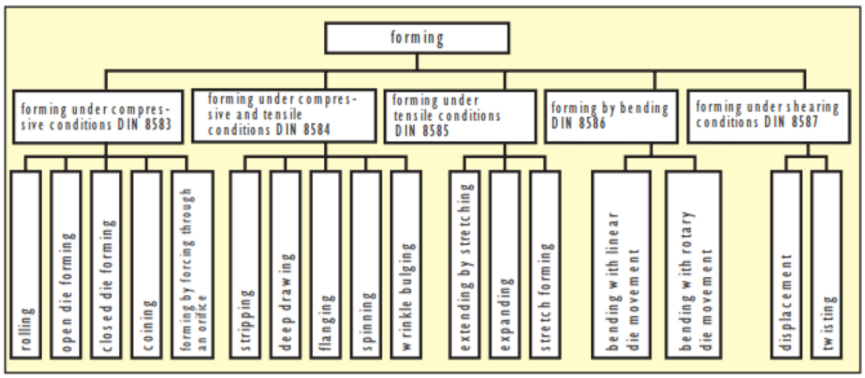

Figure 15 – Forming Classification (Encerrabodes, 2018)

MATERIALS AND METHODS

3 MATERIALS AND METHODS

3.1 Materials

The Ultron Guard will be made of a 0.4 mm thickness AISI 301 metal sheet which is a material already used to produce several different parts, however there are different options of this material with different properties. For the laser cutting tests, it was opted to choose the material with the highest tensile strength available within Philips, being the AISI 301 with a tensile strength between 1700 and 1900 MPa the material selected because it is, in theory, the hardest one to work with, and thus, it will also be possible to laser cut the other types of AISI 301.

Due to confidentiality reasons and given to the fact that the laser cutting tests were performed by Trumpf corporation, it was necessary to perform some geometry changes in the Ultron Guard as it is possible to see in Figure 16. This new prototype geometry was created in NX 10 and in order to test the possibility to produce smaller features with laser cutting, it was also added two small holes one with a 0.4 mm diameter and the other one with 0.2 mm diameter, and a slot with a 0.15 mm radius. All these smaller features are not possible to produce by conventional punching since the thickness of the metal sheet is bigger than the holes diameter.

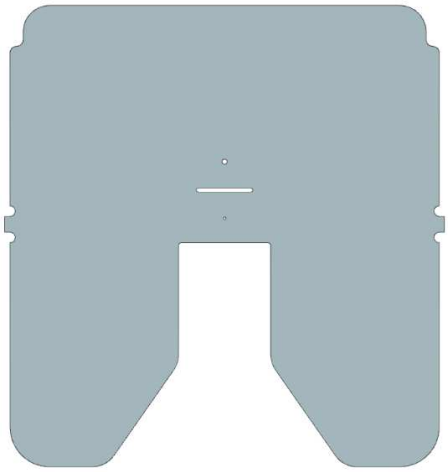

Figure 16 - Study case part

The main characteristics of the used material for the tests are specified in the Table 3.

Table 3 - Metal sheet properties

Material			Sheet thickness (mm)		Sheet width (mm)	
AISI 301			0.4		45	
Chemical composition (Mass fraction alloying elements in percentage)						
C	**Si**	**Mn**	**Cr**	**Ni**	**Mo**	**N**
0.10	1.20	1.20	16.70	6.60	0.70	0.07
Physical properties						
Density at 20°C (g/cm³)			**Thermal conductivity at 20°C (W/(mK))**			
7.91			14.7			
Mechanical properties						
Tensile strength (MPa)		**Elastic modulus (GPa)**		**Vickers hardness**		
1700-1900		185		600± 30		

3.2 Used means

The used laser machine was the Trulaser Cell 3000 and the laser devise was the TruFiber 500. The main characteristics of the used laser cutting equipment are specified in Table 4.

Table 4 - Laser equipment characteristics

Brand	Laser device	Laser type
Trumpf	TruFiber 500	Fiber
Adjustable power range (W)	**Wavelength nm**	**Beam quality (M^2)**
15-500	1075 ± 7	1.2 ± 0.1
Brand	**Laser machine**	
Trumpf	TruLaser Cell 3000	
Axis travel range (X / Y / Z) in mm	**Max. axis speed simultaneous (m/min)**	**Positioning accuracy (X / Y / Z) in mm**	**Max. axis acceleration simultaneous (m/s^2)**
800 / 600 / 400	85	0.015	17

3.3 Laser cutting tests

The laser cutting tests were performed by Trumpf together with an application report that, for confidentiality reasons, does not have public access. However, some parts of this report are based on the results achieved in that report and it even utilizes some information present on it.

The laser cutting tests were performed by Trumpf and, for that reason, it was opted to start the first tests (test 1) using the suggested laser cutting parameters by Trumpf. After this, the next performed tests intended to compare were on how the change of some parameters affects the cut quality, thus the selected laser parameters to change were the parameters that had the highest influence in the cut quality according to the literature, being chosen to change the laser power (W), cutting speed (mm/min), assist gas pressure (bar) and pulse duration (ms).

To observe how each selected laser cutting parameter affects the cut quality, it was opted to change them individually by increasing 20% and decreasing 20% from the suggested values. For each test, they were performed three samples in order to reach the intended level of confidence, intending to test the repeatability of the process. Due to the big differences regarding the geometric dimensions between the outer contour and the small inner features, the used parameters had to be different for these geometries.

Given the fact that the suggested laser peak power for the outer contour was 500 W and that the maximum laser power of the Trufiber 500 is also 500 W, it was not possible to increase the laser power in the outer contour. In addition, the pulse duration parameter was not directly programable in the Laser Technology Table and, for this reason, it was not possible to perform the tests changing the pulse duration. In order to prevent oxidation during the laser cutting operation, it was opted to use nitrogen (N_2) as assit gas with a 1.7 mm diameter nozzle.

The focal position was the same during all the contour and it was used a focal position of 0, meaning that the focal point was placed on the upper surface of the metal sheet. It needs to be highlighted that throughout the report, when mentioning the upper surface, it concerns the surface that was facing up during the laser cutting process and when mentioning lower surface, it concerns the surface that was facing down during the laser cutting process. This focal position translated in a distance of the laser nozzle to the metal sheet of 0.35 mm. The beam caustic shape in the focal point for the used zoom is visible in Figure 17, where it is possible to see that the beam diameter in the focal point is approximately 40 µm. It is also possible to observe that when positioning the focal point on the top surface when cutting a 0.4 mm thickness sheet, the theoretical kerf width is also approximately 40 µm.

The parameters used in the different tests are specified in Table 5, where the parameters that changed in each test are in bold.

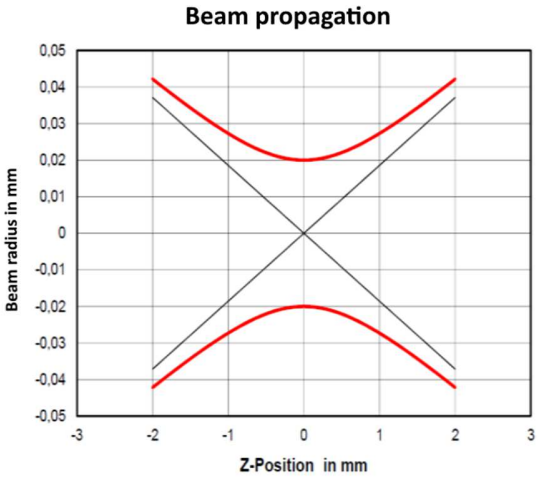

Figure 17 - Beam caustic shape Trumpf 2020

The piercing operation to start the cutting operation used some different parameters, more specifically the focal position that was changed to -2 mm, the assist gas pressure used was the same pressure of 18 bar for the whole geometry, and a nozzle distance to the metal sheet of 4 mm was selected. The piercing operation time was 0.1 s.

Table 5 - Used laser cutting test parameters

	Geometry	Peak power (w)	Cutting speed (m/ min)	Gas pressure (bar)	Pulse frequency (Hz)	Performed analysis
Test 1	Small holes	80	Max. 0,3 Min 0,06	Max. 24 Min. 22	500	SEM, HAZ
	Outer contour	500	20	15	20000	
Test 2	Small holes	**96**	Max. 0,3 Min 0,06	Max. 24 Min. 22	500	SEM, HAZ
	Outer contour	500	20	15	20000	
Test 3	Small holes	**64**	Max. 0,3 Min 0,06	Max. 24 Min. 22	500	HAZ, Microhardness
	Outer contour	**400**	20	15	20000	
Test 4	Small holes	80	**Max. 0,36** **Min 0,07**	Max. 24 Min. 22	500	SEM

	Outer contour	500	**24**	15	20000	
Test 5	Small holes	80	**Max. 0,24 Min 0,05**	Max. 24 Min. 22	500	
	Outer contour	500	**16**	15	20000	
Test 6	Small holes	80	Max. 0,3 Min 0,06	**24**	500	SEM
	Outer contour	500	20	**18**	20000	
Test 7	Small holes	80	Max. 0,3 Min 0,06	**Max. 19 Min. 18**	500	
	Outer contour	500	20	**12**	20000	

3.4 SmartScope analysis

To analyze the samples' dimensions, it started by using a Smartscope CNC 250 that creates a 3D cloud points model of the samples. The Smartscope is placed in a controlled temperature and humidity room, in order to prevent the samples from expanding or contracting during the analysis and thus eliminating another factor from affecting the final results. The description of this process is described in Table 6.

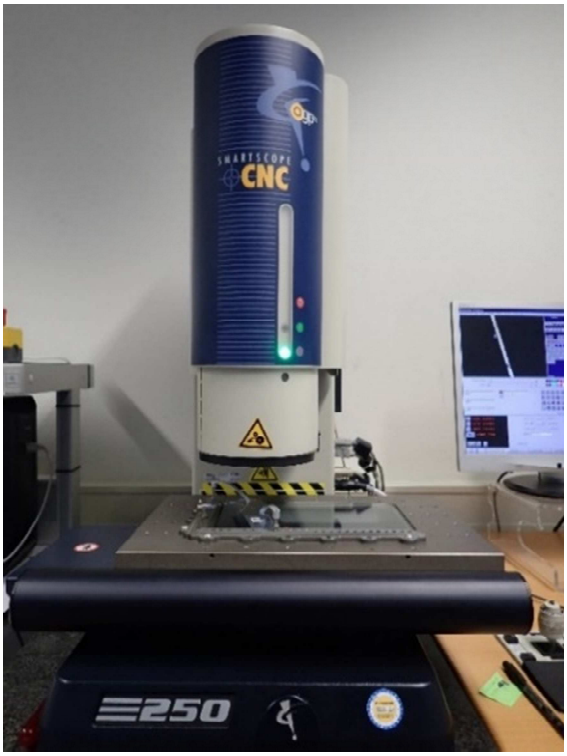

Figure 18 - Smartscope CNC 250

Table 6 - Samples analysis procedure using the SmartScope

Procedure	Representation
Before starting the analysis of every sample, each one was previously cleaned using compressed air, in order to avoid the presence of any dust particles that could potentially affect the results. The cleaning of the samples could be improved by using an ultrasonic bath in acetone. However, in order to not influence the future tests and to not do an excessive cleaning that could also remove some burrs or molten material attached during the laser cutting process, it was opted not to go for this route. In order to have the minimal variations on the analysis of the samples, it was opted to analyze all the samples with the lower surface of the samples turned up, since theoretically, it was the surface with the poorer cut quality, as it was observed. With the positioning of the samples with the lower surface facing up,	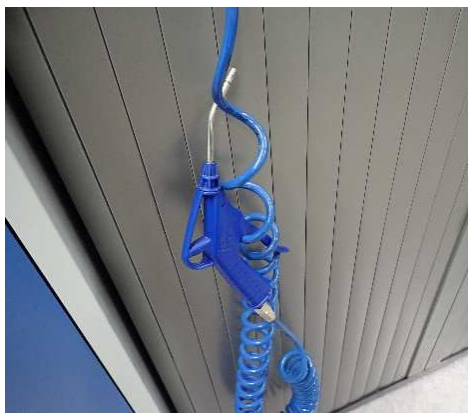

there is a smaller risk of the backlight of the Smartscope blending with some molten material attached in that surface, that could potentially result in an incorrect measurement of the samples.

One important step in this analysis is the correct clamping of the samples on the benchtop of the machine, given the fact that the benchtop moves on two axis (X and Y) and a faster acceleration of it can induce a slight displacement of the sample on the benchtop and, thus, produce an error on the sample analysis. Two different approaches were done: in the first one, the sample was clamped against the benchtop glass, however, due to the limitation of the clamping mechanism, it was not possible to achieve a totally flat sample, hence during the analysis of the sample in the Smartscope it was required to do several zoom compensations throughout the analysis of the sample, since the backlight of the Smartscope would start to blend with the sample edge. This was improved with placing an acrylic piece underneath the sample. This chosen piece was narrower than the samples to avoid the presence of some visible burr on the pilot holes between the sample and the acrylic piece, aiming to have the samples as flat as possible. It was also used another clamper in the middle of the sample in order to have a flatter sample. However, it was not possible to obtain a totally flat sample, especially on the inner contour, since this part was not clamped itself and the whole metal sheet had a slight curvature probably caused by the fact that it was provided from a roll. The use of this acrylic piece also had some downsides, since it was not a completely homogeneous piece,

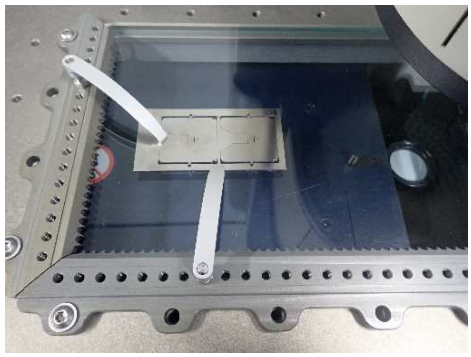

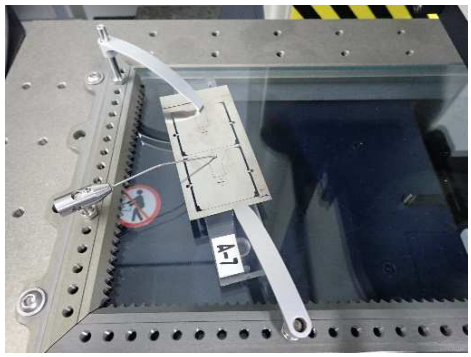

due to the presence of some holes, as it will be possible to see ahead.

After the sample has been cleaned and properly clamped, it was time to start analyzing the sample using the Smartscope. For this, a first manual zoom adjustment on an edge of the sample is done manually, using the Smartscope controllers and after a finer zoom adjustment has been done using the software function. Having the correct zoom, it was proceeded to the back light adjustment in order to achieve a light value on the software of approximately 50% since a too high or too low light would result in an incorrect measurement of the sample. After the previous steps have been done, it was time to select the edge to analyze. This was performed by selecting two points, both closer to the edge intended to analyze. These points consist of a start point and an end point where the end determines the direction of the automatic analysis. After this, the software detects the limits between the back light, represented in the figure as white, and the samples are represented in the figure as black. After detecting this limit, the software generates a series of points throughout the analyzed area. After this, the software automatically moves the benchtop throughout the edge until it reaches an obstacle or until it comes back to the starting point. During the analysis of some samples, the Smartscope started doing some loops around some edges, because it would encounter one type of this obstacles and could not return to the starting point. With this series of points, the software generates the 3D model of the analyzed piece.

During the analysis of several samples, there were found problematic areas to analyze due

to the presence of small particles of molten material between the kerf, as it is possible to see in the figure. For this reason, some of the 3D models created by the Smartscope have some small zones without points. Therefore, in the measurement of these samples it was avoided to use these zones to measure.	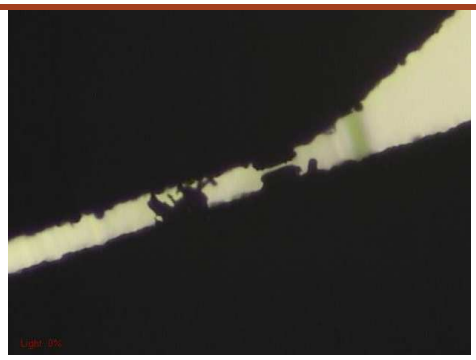
Another limitation during this analysis was due to the used of clamping mechanism, which was caused by the location of the middle clamper, that created in some samples a dark zone where it was not possible to analyze with the Smartscope, as it is possible to observe in the figure. However, the use of this clamper in this location was essential in order to provide a sample as flat as possible for this analysis.	

3.5 Polyworks analysis

Having the 3D model of the samples produced in the Smartcope, it was followed by the measurement of those models. This measurement was performed with the PolyWorks software with the procedure being described in Table 7.

Table 7 - Sample analysis procedure in Polyworks

Procedure	Representation
The 3D model created by the Smartscope is imported to Polyworks as points' cloud and it can either be selected as a surface or as a boundary object. In order to make the measurement of the samples easier and faster, it was opted to align the samples on the same position every time. For this, it was imported a CAD file of the Ultron Guard prototype, where only the pilot	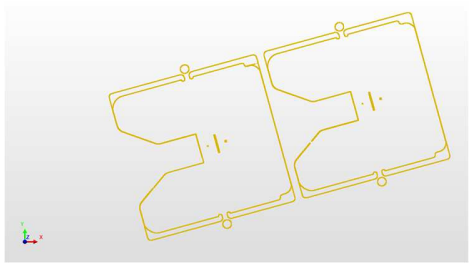

holes would be used in order to perform the alignment of the 3D model samples.

To minimize measurements deviations between certain edges or even between samples, it was performed a scaling of the points along the Z axis since the Smartscope changes the Z coordinate every time a focus was performed, as it is possible to observe in the picture. After this scaling along the Z axis, the points of the 3D model samples were all almost in the same XY plane.

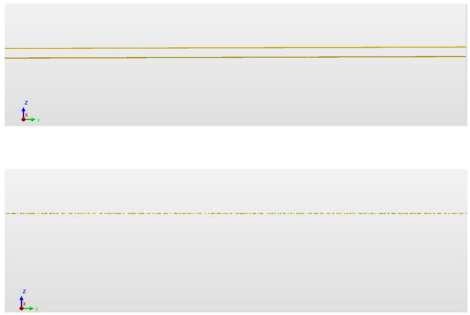

Having the two components inserted in Polyworks, a first rough alignment was performed manually, selecting one point in every pilot hole circle of the CAD model, and in the corresponding pilot holes of the 3D model of the sample, totaling 8 points.

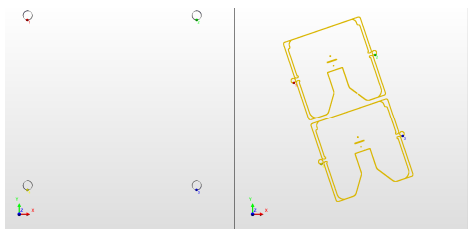

To achieve a better alignment of the 3D model sample, a finer alignment was performed by creating circles on the location of the pilot holes with a diameter slightly bigger than the pilot holes. With this, it was then possible to select all the points within that circles and after using the software function “Best-Fit Data to reference Objects”, the 3D model of the sample was automatically aligned in a way that those selected points would fit the best around the pilot holes of the CAD object.

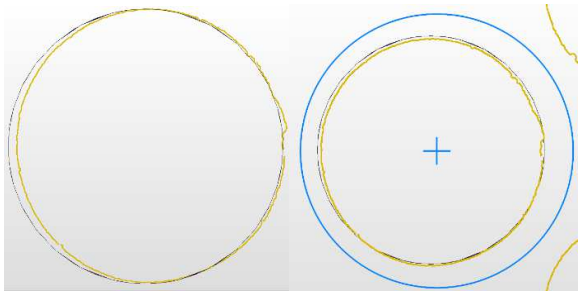

In order to measure the desired dimensions, it was created a rectangle surrounding the points of an intended edge to measure as it is possible to see in the first picture. After this, the points within the rectangle were selected and, using these points, it was created a line that best fitted in these points.

The same strategy was done to create lines on every edge intended to measure.

A similar strategy was done in order to measure circles’ diameter but, instead of a rectangle surrounding the pretended points,

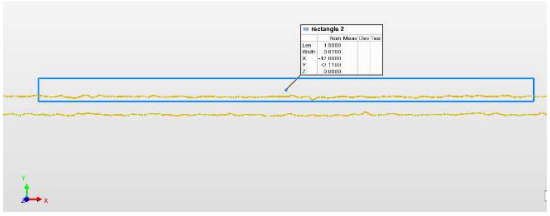

it was opted to use a circle, which is the case of the biggest circle on the second picture, and instead of creating a line that fit those points, it was created a circle as well, which is the case of the smaller circle on the second picture. With this, it was then possible to measure the distances between the intended lines or circles.

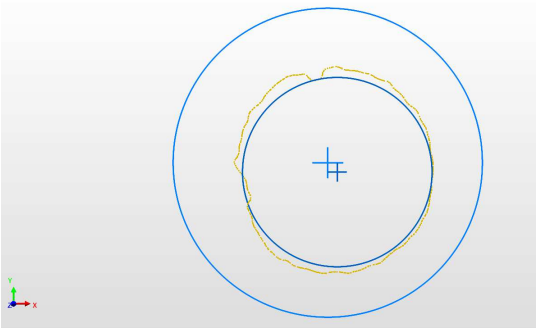

After analyzing more carefully how the software performs the measurement between two distances, it was observed that this measurement was done by calculating the distance of a perpendicular line to the first selected line to the middle of the second selected line, as it is possible to see in the picture.

In order to observe if this type of measurement had a significative impact on the measured distances, it was performed another type of measurement where it was created an average point of the selected points within the rectangles instead of the line and, after, it was measured the distances between the points. These different types of measurements were performed in different distances to ensure that there was no inconsistency between the results.

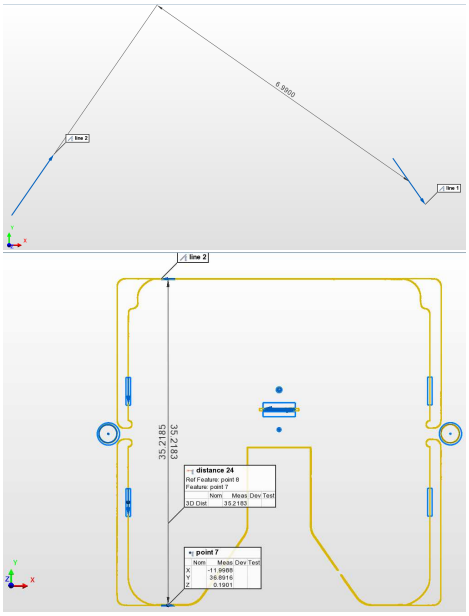

With the previous alignments done, it was possible to ensure that all the 3D models of the samples would be positioned really close between each other, whereby the location of the rectangles and circles created to select the used points to perform the measurements would be accurate enough to include all those points. Due to this, it was possible to create a macro script to perform all the previous steps automatically. In the analysis of every sample 3D model, it was ensured the correct positioning of those rectangles and circles in

order to make sure that all the measurements were correct.
At the end of every sample analysis, it was created a PDF report Microsoft Excel® report to later calculate the average dimensions of the tests.

Regarding the measuring of the holes' diameter, it was observed that the used method could be inducing a small variation on the dimensions due to a usual problem close to the starting point of the laser operation. In order to test this, it was opted to do a new measurement of these holes, this time doing a manual selection of the intended points to analyze, discarding the points that belonged to that problematic area close to the starting/ending point (Figure 19) and compare it to the other method (Figure 20). When comparing both methods, it is possible to see that the dimensions' variation was really small, whereby it was opted to use only the automatic points selection.

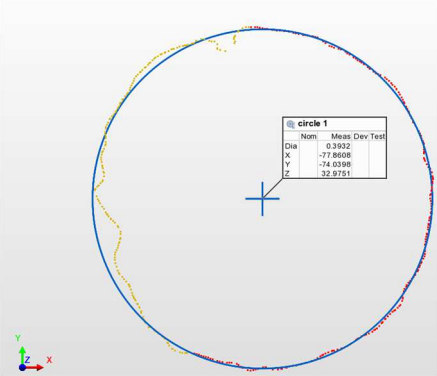

Figure 19 - Circle diameter measurement using manual selection of points

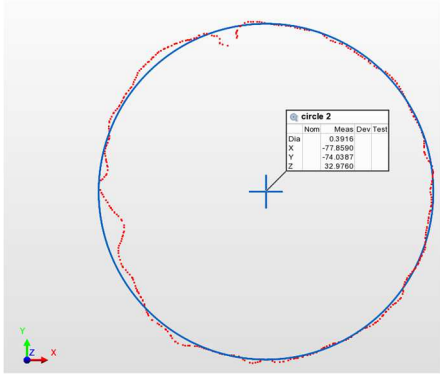

Figure 20 - Circle diameter measurement using automatic selection of points

3.5.1 Microstructure analysis

The analysis of the microhardness and microstructure was performed in order to analyze how different laser cutting parameters and different cutting geometries influence the heat affected zone (HAZ). For this reason, it was opted to etch the samples using a cross section that went across the outer geometry and the smaller inner features, as it is possible to see in Figure 21.

The analysis of the microstructure was made in three different samples, being these the samples performed in the test carried out with the suggested laser cutting parameters, the test with the highest laser power and with the lowest laser power, since according to the literature these are the parameters that have the biggest influence in the HAZ.

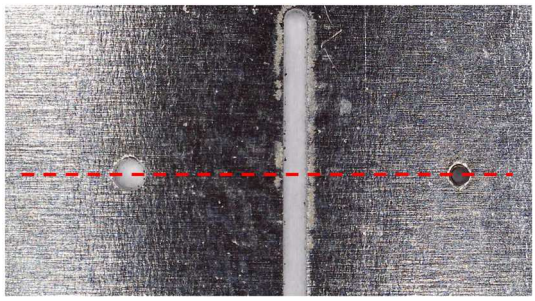

Figure 21 - Cross section location

The preparation procedure of the samples in order to analyze the microstructure and microhardness started by etching the samples close to the intended zone, avoiding cutting too deep into the intended holes to analyze. After the samples were embedded in epoxy (Figure 23) to later carefully grind them until the cross section was in the correct location (Figure 22).

This was followed by a polishing process of different steps in order to achieve a surface free of scratches for the microstructure analysis. The polishing procedure started with a fine grinding using a 6 µm grit, followed by 3 µm and a 1 µm grit. The final polishing step was done using a 0.25 µm grit.

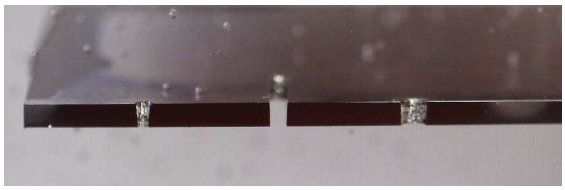

Figure 22 - Detail embedded cross section

Figure 23 - Embedded sample

The etching of the samples was performed using Lichtenegger and Blöch color etching solution, where austenite turns brown. The observation of the microstructure was performed on the microscope. In order to have a better idea of the dimensions of the HAZ, it was analyzed the microstructure of the samples using SEM, where it was possible to distinguish the base metal with the presence of deformation marks induced in the rolling process of the metal sheet from the HAZ where these marks were not visible.

However, since there was not a significant difference in the microstructure between the samples analyzed on the microscope, only the sample performed with the suggested parameters and the sample performed with the higher laser power were analyzed on the SEM.

RESULTS

4 RESULTS

4.1 Laser cutting tests analysis

In the tests, the fixation of the metal sheet in the TruLaser Cell 3000 working area was done using magnets and a jig underneath the metal sheet, as it is possible to see in Figure 24 and Figure 25.

The jig geometry was an offset of the Ultron Guard prototype with 1.5 mm clearance to the cutting edge but, in some areas, this clearance was smaller, reaching only 0.2 mm in some zones (Figure 24). This resulted in the accumulation of splatter that was improved in the second fixation method, which only used magnets to fix the metal sheet without jig and, for this reason, the tests were performed using this second method.

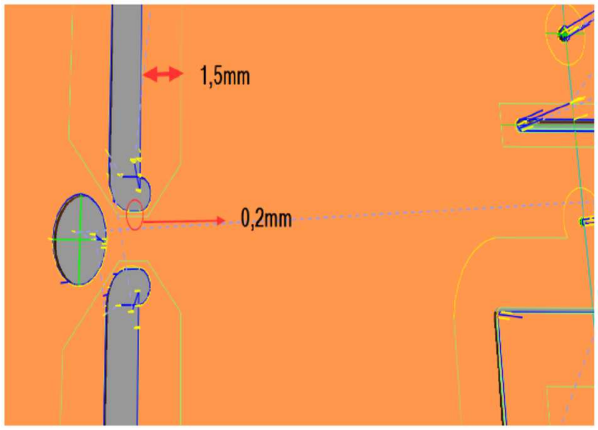

Figure 24 - Jig clearance

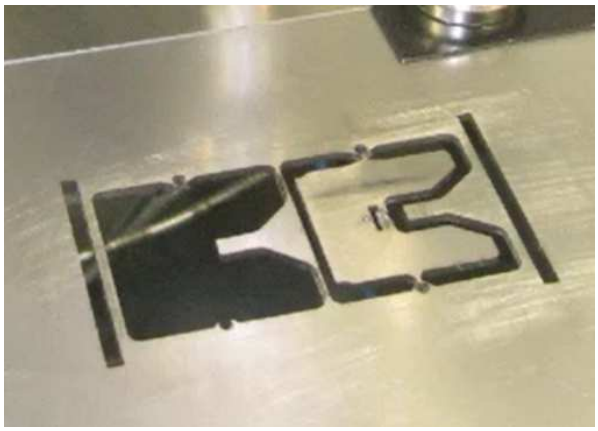

Figure 25 - Used jig

4.1.1 Laser path

Due to the geometry of the prototype, the cut of the geometry was produced in different steps as it is possible to see in Figure 26, where each zone marked with a different color represents one different step. In this figure, the pilot holes and smaller inner features are not marked since they automatically require independent laser paths. This type of path created some defects that will be addressed ahead.

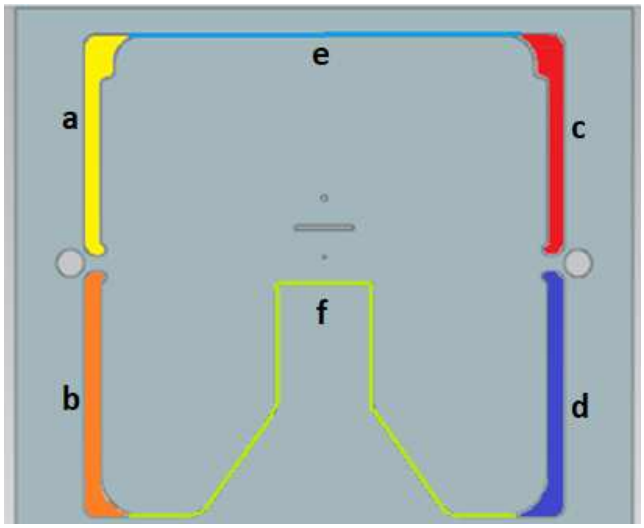

Figure 26 - Different laser path steps

4.1.2 Laser cutting tests

The performance of the tests was monitored online and also throughout a video, where it was possible to see some relevant aspects and, when analyzing the video of the laser cutting operation of a sample without the jig, it was possible to see a problem. In Figure 27 and Figure 28, it is possible to see how the fixation of the metal sheet was made.

This problem is caused by the bending of the metal sheet under the assist gas pressure effect. In Figure 27, it is possible to see the metal sheet before being under the effect of the assist gas pressure, and in Figure 28 it is possible to see the metal sheet under the influence of the assist gas pressure. Observing the marked area in both figures, it is possible to see the presence of a shadow between the metal sheet and the metal plate in Figure 28, caused by the bending effect of the metal sheet. The flexion of the metal sheet during the laser cutting operation translates into a different focal position than the initially determined, meaning that the cut will be performed in less effective zone and will also translate into a wider kerf than the expected. This question will be later approached.

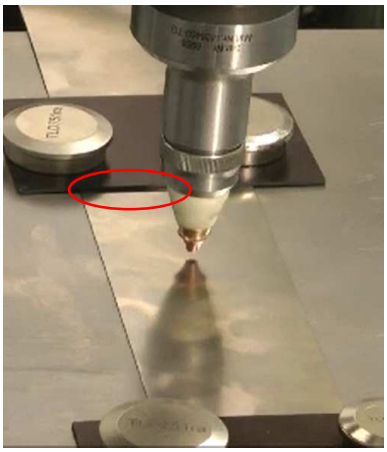

Figure 27 - Metal sheet before assist gas pressure influence

Figure 28 - Metal sheet after assist gas pressure influence

4.1.3 Naked eye observation

The observation of the samples at the naked eye allowed to see a significative difference between the upper and lower surface of the samples during the laser cutting process. As it is possible to observe in Figure 29, the upper side of the samples presents a very clean surface, as well as smooth cut edges. It was also possible to see a slightly different curvature between the inner contour and the rest of the metal sheet, but this was probably caused by different stress levels induced during the storage of the metal sheet in a roll. When analyzing the lower surface, as it is possible to see in Figure 30, it is visible some oxidation on the cut edges, as well as some burr attached on the pilot holes. The cut quality looks pretty good without any visible burrs, except for the one on the pilot holes.

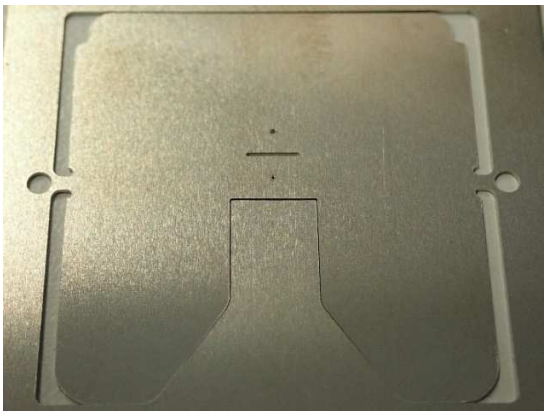

Figure 29 - Sample 2 of the test 6 (upper surface)

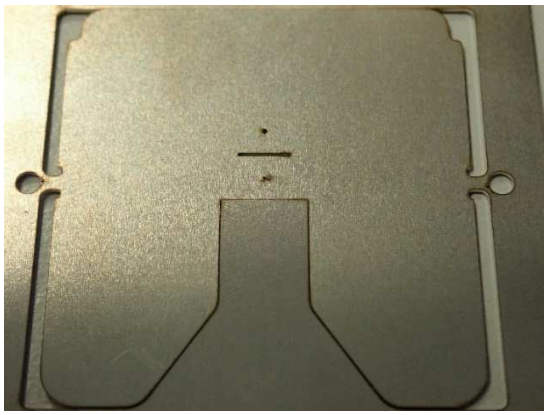

Figure 30 - Sample 2 of the test 6 (lower surface)

4.2 Samples dimensions

To make the analysis of the dimensions and of some observed problems, it is easier if the geometry is divided into two different parts, being one the general outer contour (Figure 31) and the other the pilot holes and the inner slot and corresponding holes (Figure 32).

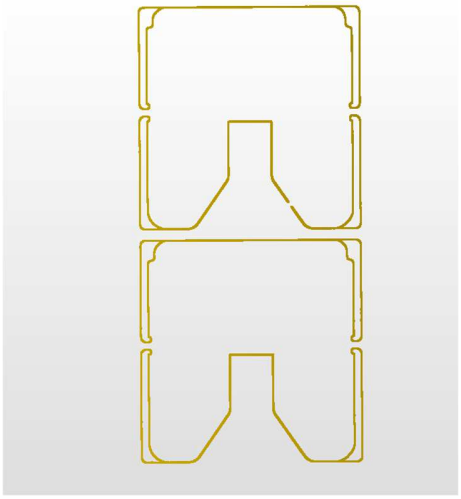

Figure 31 - Geometry outer contour

Figure 32 - Geometry pilot holes and inner features

In Figure 33 it is possible to see the location of the dimensions of the pilot holes and inner features analyzed in the following two tables. In Table 8 are specified the nominal dimension values and the average dimensions obtained from the three samples of each test.

In Table 9 it possible to see the average deviations of each dimension in relation to the nominal values. These average deviations were calculated using the absolute value of each deviation obtained from the three samples of each test, in order to reach a more correct value, since some deviations were positive and other ones were negative, something that would lead to an average deviation value smaller than the real one. To have a better idea of the dimensions that were not within the required tolerance of 20 µm, these dimensions were marked as it is possible to see in Table 9.

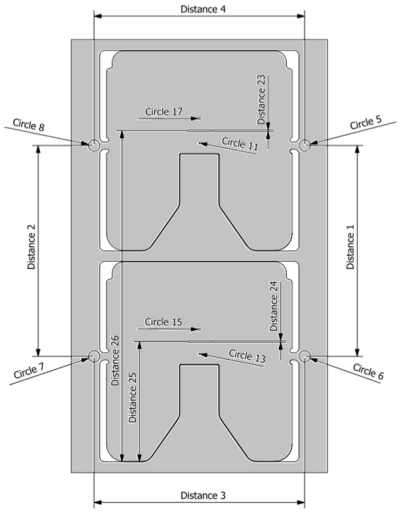

Figure 33 - Pilot holes and inner slot and holes distances and circles

Table 8 - Pilot holes and inner slot and holes average dimensions

Average dimension (mm)									
Object Name	**Control**	**Nominal dimension**	**Test 1**	**Test 2**	**Test 3**	**Test 4**	**Test 5**	**Test 6**	**Test 7**
circle 5	Diameter	2.0000	1.9791	1.9784	1.9801	1.9801	1.9792	1.9793	1.9807
circle 5	X	18.5000	18.4994	18.4962	18.4945	18.4945	18.5009	18.4994	18.4967
circle 5	Y	55.4000	55.3975	55.3964	55.3913	55.3913	55.3960	55.3972	55.4004
circle 6	Diameter	2.0000	1.9785	1.9785	1.9801	1.9801	1.9787	1.9788	1.9784
circle 6	X	18.5000	18.4864	18.4879	18.4912	18.4912	18.4887	18.4871	18.4845
circle 6	Y	18.5000	18.4160	18.4134	18.4108	18.4108	18.4157	18.4144	18.4142
distance 1	3D Distance	37.0000	36.9815	36.9830	36.9805	36.9805	36.9803	36.9827	36.9862
circle 7	Diameter	2.0000	1.9665	1.9670	1.9698	1.9698	1.9696	1.9681	1.9728
circle 7	X	18.5000	18.5000	18.4998	18.4964	18.4964	18.5007	18.5010	18.5012
circle 7	Y	18.5000	18.4015	18.4020	18.4082	18.4082	18.4023	18.3993	18.3987
circle 8	Diameter	2.0000	1.9691	1.9681	1.9702	1.9702	1.9696	1.9693	1.9709
circle 8	X	18.5000	18.4854	18.4909	18.4936	18.4936	18.4873	18.4918	18.4855
circle 8	Y	55.4000	55.3869	55.3878	55.3894	55.3894	55.3846	55.3874	55.3888
distance 2	3D Distance	37.0000	36.9853	36.9858	36.9811	36.9811	36.9823	36.9881	36.9901
distance 3	3D Distance	37.0000	36.9864	36.9876	36.9877	36.9877	36.9895	36.9881	36.9857
distance 4	3D Distance	37.0000	36.9849	36.9871	36.9881	36.9881	36.9882	36.9912	36.9823
circle 11	Diameter	0.2000	0.1686	0.1675	0.1665	0.1665	0.1677	0.1663	0.1714

circle 11	X	0.0000	0.0187	0.0154	0.0283	0.0283	0.0171	0.0117	0.0153
circle 11	Y	55.8500	55.8401	55.8328	55.8356	55.8356	55.8362	55.8385	55.8390
circle 13	Diameter	0.2000	0.1678	0.1743	0.1614	0.1614	0.1698	0.1680	0.1702
circle 13	X	0.0000	0.0103	0.0099	0.0114	0.0114	0.0083	0.0086	0.0051
circle 13	Y	18.8500	18.8480	18.8462	18.8478	18.8478	18.8483	18.8407	18.8436
circle 15	Diameter	0.4000	0.3902	0.3951	0.3910	0.3910	0.3904	0.3908	0.3914
circle 15	X	0.0000	0.0055	0.0027	0.0084	0.0084	0.0032	0.0033	0.0026
circle 15	Y	23.1500	23.1587	23.1579	23.1584	23.1584	23.1566	23.1525	23.1554
circle 17	Diameter	0.4000	0.3917	0.3965	0.3909	0.3909	0.3880	0.3918	0.3900
circle 17	X	0.0000	0.0163	0.0095	0.0169	0.0169	0.0155	0.0110	0.0119
circle 17	Y	60.1500	60.1427	60.1412	60.1513	60.1513	60.1375	60.1407	60.1449
distance 23	3D Distance	0.3000	0.2678	0.2693	0.2729	0.2729	0.2683	0.2683	0.2677
distance 24	3D Distance	0.3000	0.2683	0.2696	0.2725	0.2725	0.2670	0.2675	0.2674
distance 25	3D Distance	21.1000	21.1533	21.1310	21.1060	21.1060	21.1296	21.1253	21.0862
distance 26	3D Distance	58.1000	58.1238	58.0927	58.1020	58.1020	58.1083	58.1145	58.0767

Table 9 - Pilot holes and inner slot and holes average deviations

Average deviation (mm)								
Object Name	**Control**	**Test 1**	**Test 2**	**Test 3**	**Test 4**	**Test 5**	**Test 6**	**Test 7**
circle 5	Diameter	0.0209	0.0216	0.0199	0.0210	0.0208	0.0207	0.0193
circle 5	X	0.0023	0.0046	0.0059	0.0035	0.0029	0.0013	0.0033
circle 5	Y	0.0035	0.0037	0.0087	0.0036	0.0051	0.0034	0.0023
circle 6	Diameter	0.0215	0.0215	0.0199	0.0201	0.0213	0.0212	0.0216
circle 6	X	0.0136	0.0121	0.0088	0.0122	0.0113	0.0129	0.0155
circle 6	Y	0.0160	0.0134	0.0131	0.0189	0.0157	0.0144	0.0142
distance 1	3D Distance	0.0185	0.0170	0.0195	0.0224	0.0197	0.0173	0.0138
circle 7	Diameter	0.0335	0.0330	0.0302	0.0304	0.0304	0.0319	0.0272
circle 7	X	0.0025	0.0014	0.0037	0.0022	0.0010	0.0022	0.0019
circle 7	Y	0.0055	0.0028	0.0082	0.0021	0.0053	0.0025	0.0033
circle 8	Diameter	0.0309	0.0319	0.0298	0.0301	0.0304	0.0307	0.0291
circle 8	X	0.0146	0.0091	0.0071	0.0131	0.0127	0.0082	0.0145
circle 8	Y	0.0131	0.0122	0.0106	0.0157	0.0154	0.0126	0.0112
distance 2	3D Distance	0.0147	0.0142	0.0189	0.0174	0.0177	0.0119	0.0099
distance 3	3D Distance	0.0136	0.0124	0.0123	0.0131	0.0105	0.0119	0.0143
distance 4	3D Distance	0.0151	0.0129	0.0119	0.0115	0.0118	0.0088	0.0177
circle 11	Diameter	0.0314	0.0325	0.0335	0.0338	0.0323	0.0337	0.0286
circle 11	X	0.0187	0.0154	0.0283	0.0169	0.0171	0.0117	0.0153
circle 11	Y	0.0099	0.0172	0.0144	0.0146	0.0138	0.0115	0.0110
circle 13	Diameter	0.0322	0.0257	0.0386	0.0310	0.0302	0.0320	0.0298

circle 13	X	0.0103	0.0099	0.0114	0.0115	0.0083	0.0086	0.0051
circle 13	Y	0.0020	0.0051	0.0055	0.0014	0.0017	0.0093	0.0064
circle 15	Diameter	0.0098	0.0049	0.0090	0.0098	0.0096	0.0092	0.0086
circle 15	X	0.0055	0.0027	0.0084	0.0038	0.0032	0.0033	0.0026
circle 15	Y	0.0087	0.0079	0.0084	0.0088	0.0066	0.0025	0.0054
circle 17	Diameter	0.0083	0.0035	0.0092	0.0099	0.0120	0.0082	0.0100
circle 17	X	0.0163	0.0095	0.0169	0.0140	0.0155	0.0110	0.0119
circle 17	Y	0.0073	0.0088	0.0155	0.0102	0.0125	0.0093	0.0051
distance 23	3D Distance	0.0322	0.0307	0.0271	0.0319	0.0317	0.0317	0.0323
distance 24	3D Distance	0.0317	0.0304	0.0275	0.0323	0.0330	0.0325	0.0326
distance 25	3D Distance	0.0533	0.0310	0.0282	0.0186	0.0296	0.0253	0.0372
distance 26	3D Distance	0.0344	0.0185	0.0061	0.0100	0.0125	0.0198	0.0411

Analyzing the pilot holes dimensions, it is possible to state that, even though the majority of the dimensions are not within the required tolerances, the dimensions for the same pilot holes are really close between the tests, varying only a maximum of 3 µm. However, it is possible to see an approximately 10 µm variation between the pilot holes between sides.

This phenomenon was probably related to a slight deviation of the metal sheet in the support to one of the sides, causing that side to suffer more bending or due to a constant deviation of the axis motion system. It was also possible to observe a rougher area close to the starting/ending point marked on Figure 34, that was possibly caused by a piercing position too close to the circle edge that lead to an accumulation of molten material on the lower surface, as it is possible to see in Figure 35, whereby lead to a heat transference between the molten material and the metal sheet, increasing the temperature of the base metal temperature in that area, and/or also due to a not proper approach curvature from the piercing point to the circle edge, that lead to a high temperature increment of the material in that zone.

When still observing the pilot holes geometry obtained on Polyworks, it was also possible to observe a slight ovalization of the same, where the geometry of the hole was tighter along the X axis and had the correct dimensions along the Y axis, as it is also possible to see in Figure 34 and Figure 34, when comparing that circle with theoretical circle of the CAD file, this lead to the dimensions of the pilot holes being smaller than expected. In Figure 36, it is possible to see that the upper surface presents a clean cut edge with no oxidation nor visible signs of heat affected zone. Furthermore, it is seen a slight deviation on the circle contour close to the starting/ending point area.

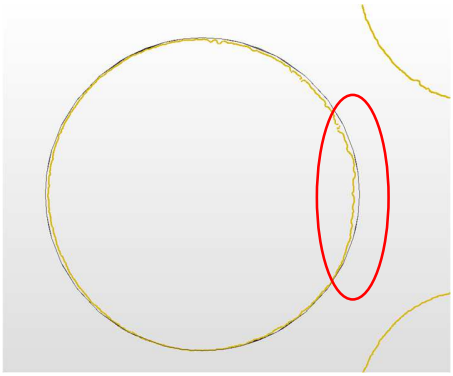

Figure 34 - Pilot hole 7 of test 1 sample 1

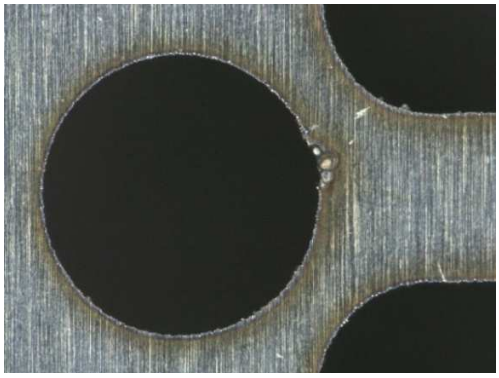

Figure 35 - Microscopic picture of the lower surface of the pilot hole 8 of the sample 1 of the test 4 (100x enlarged)

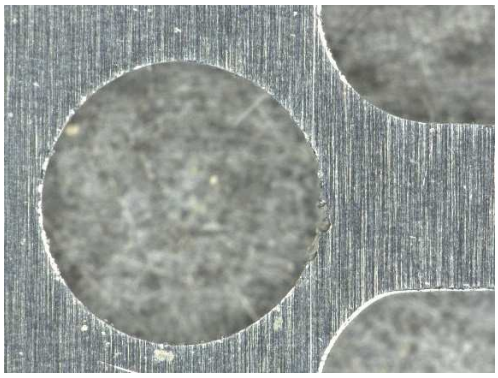

Figure 36 - Microscopic picture of the upper surface of the pilot hole 8 of the sample 1 of the test 1 (100x enlarged)

When analyzing the inner holes dimensions, more specifically the holes with 0.4 mm diameter, it is possible to see that the samples performed with the higher laser power (test 2) achieved a considerable improvement, having about half the deviation achieved in the other tests.

In resemblance to the pilot holes, it was observed the ovalization of the holes, as it is possible to observe in Figure 37 and Figure 38, and a rougher area close to the starting/ending point also probably due to the same causes.

In these holes, there was also a preponderance of molten material attached along the hole contour, as it is possible to see in Figure 38. This may be caused by a combination of a less effective gas effect to eject the molten material with a less effective laser beam, due to a different focal point caused by the flexion of the metal sheet. In some of these holes, it was also visible large amounts of molten material close to the starting/ending point area, possibly caused by the proximity of the piercing point that lead to the first initial molten, that is harder to expel, to be attached in that zone, as it is possible to observe in Figure 39. In some samples, it was visible some splatter around the hole, as it is possible to see in Figure 40.

Observing Figure 41, it is possible to see a much smoother cut edge with a small zone of oxidation near the starting/ending point area, where it is also visible a small amount of molten material on the cut edge.

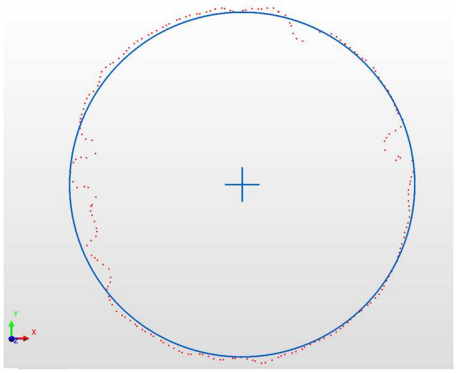

Figure 37 - 0.4 mm hole (sample 2, test 1)

Figure 38 - Microscopic picture of the 0.4 mm hole (sample 2, test 1) (200x magnification)

Figure 39 - Microscopic picture of the 0.4 mm hole (sample 2, test 1) (200x magnification)

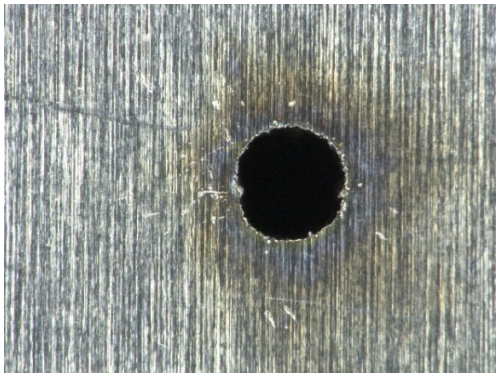

Figure 40 - Microscopic picture of the 0.4 mm hole (sample 1, test 1) (200x magnification)

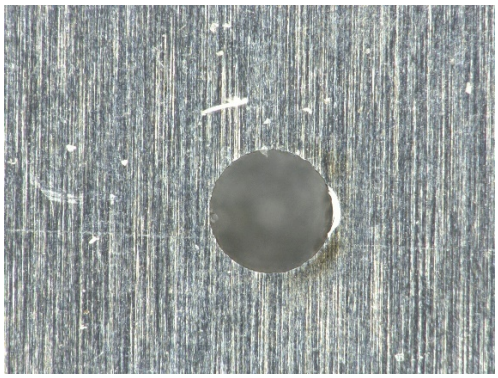

Figure 41 - Microscopic picture of the 0.4 mm hole (sample 1, test 1) (200x magnification)

Besides that, it was even observed one incomplete hole as it is possible to see in Figure 42, which for that reason, all the dimensions related to that hole were not used to calculate the average dimensions and deviations.

In this figure, it is possible to observe the laser course, where in the middle of the piercing point it is visible a significant amount of molten material. It is also visible an increase on temperature close to the starting/ending point demonstrated by the color of the surface oxidation. Lastly, in this hole it is visible that the incomplete cut could be avoided by changing the ending point to a later position, where the cut was already previously affected.

It must be highlighted that this was the only sample where this problem occurred. This may have happened due to the combination of different factors such as the flexion of the metal sheet during the cutting process, due to gas pressure that lead to the change of the focal point and, thus, decreased the effectiveness of the laser beam, or also due to a defective actuation of the clamping mechanism. For this reason, all the measurements related to this circle were not considered when calculating the average dimensions and deviations.

Figure 42 - Microscopic picture of the hole 17 of the sample 2 of the test 3 (200x magnification)

On the smaller holes, with a diameter of 0.2 mm, it was observed similar problems as the ones on the previous holes, but in these ones these problems were more evident. As it is possible to see in Figure 43 and Figure 44, the hole presents a considerable level of ovalization similar with what was already seen on the holes since the holes presented again shrank along the X axis and with normal dimensions along the Y axis, having a big contribution to the measured diameter, which was on average significantly smaller than what was intended.

However, these holes presented a more irregular shape, not only related to the presence of molten material along the cut edge, but also probably due to the laser axis motion system, as it is possible to see in Figure 44.

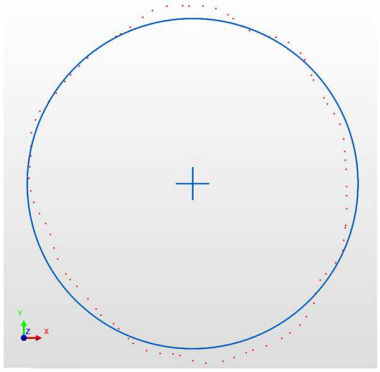

Figure 43 - 0.2 mm hole (sample 1 of the test 4)

Figure 44 - Microscopic picture of the hole 17 (sample 1 of the test 4) (200x magnification)

Another visible difference when analyzing these holes was the bigger quantity of splatter attached on the lower surface, as it is possible to see in Figure 45.

When observing the upper surface, it is observed the presence of molten material all around the cut edge, as it is possible to see in Figure 46. This was caused by the increase of localized heat in that area, leading to an insufficient cooling by the assist gas, as well as insufficient material capacity to conduct that heat. This is once again more pronounced close to the starting/ending area, where the molten material was dragged further away from the cut edge by the assist gas.

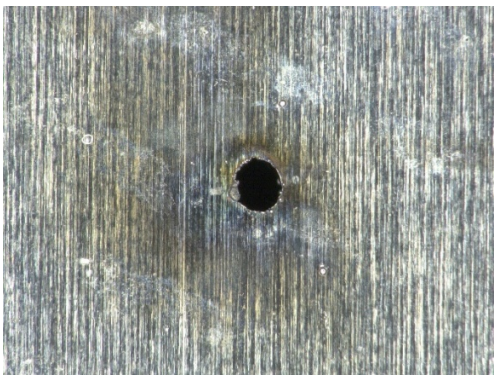

Figure 45 - Microscopic picture of the hole 17 (sample 1 of the test 1) (200x magnification)

Figure 46 - Microscopic picture of the hole 17 (sample 1 of the test 1) (200x magnification)

Regarding the inner slots (Figure 47), the measured dimension was determined by the distance between the parallel edges, where it was observed a dimension significantly inferior to the expected one. However, once again the dimensions remained similar between the different tests.

The observation of the Figure 47 and Figure 48 allow to see that the cut edge was pretty smooth, however in Figure 49 and Figure 50, it is visible small amounts of burr and molten material attached to the cut surface. Analyzing the upper surface, it is observed once again a smooth cut edge, but it is also visible a small deviation of the cut line on the bottom part of the semicircle.

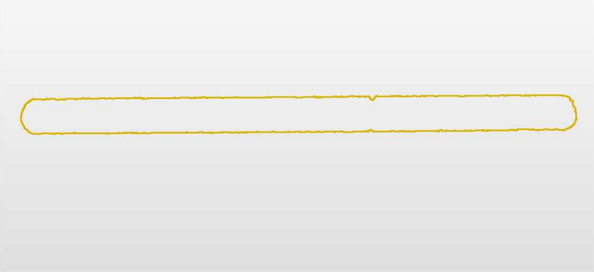

Figure 47 - Inner slot (sample 3 of the test 2)

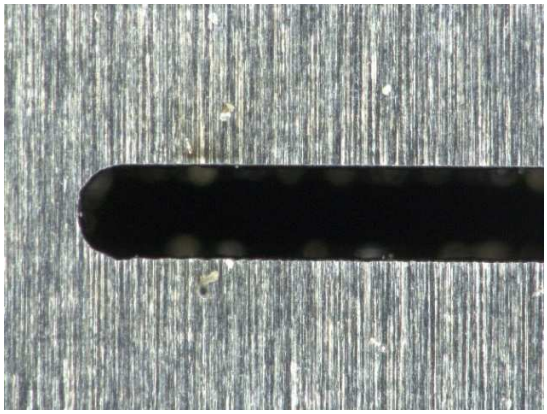

Figure 48 - Microscopic picture of the upper surface of the inner slot of the sample 2 of the test 1 (200x magnification)

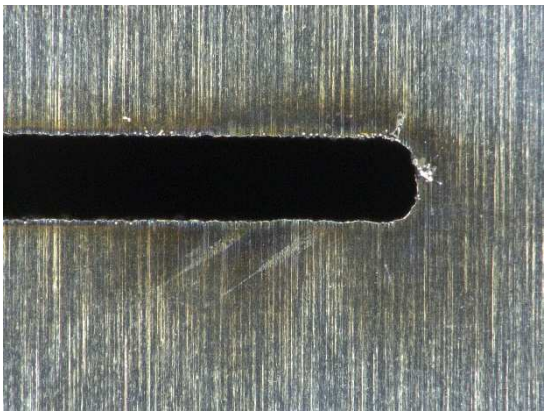

Figure 49 - Microscopic picture of the lower surface of the inner slot (sample 1 of the test 4) (200x magnification)

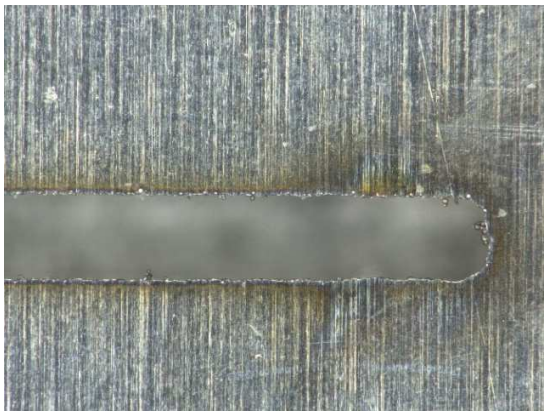

Figure 50 - Microscopic picture of the lower surface of the inner slot (sample 2 of the test 1) (200x magnification)

In Figure 51 it is possible to see the location of the dimensions of the outer contour analyzed in the following two tables. Similar to previously referred, Table 10 specify the nominal dimension values and the average dimensions obtained from the three samples of each test, and in the Table 11 it possible to see the average deviations of each dimension in relation the nominal values.

These average deviations were again calculated using the absolute value of each deviation obtained from the three samples of each test. The dimensions that were not within the required tolerance of 20 µm were marked, as it is possible to see in the Table 11.

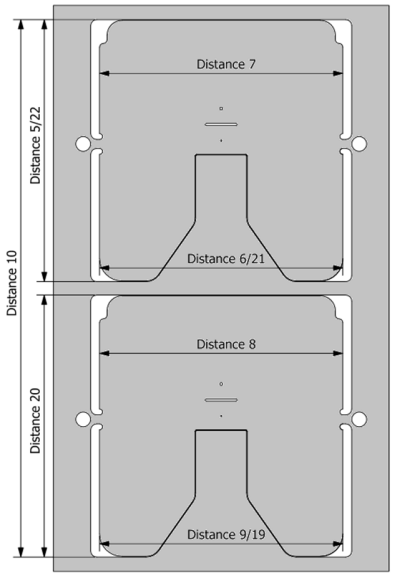

Figure 51 - Outer contour dimensions

Table 10 - Outer contour average dimensions

Average dimension (mm)									
Object Name	**Control**	**Nominal dimension**	**Test 1**	**Test 2**	**Test 3**	**Test 4**	**Test 5**	**Test 6**	**Test 7**
Distance 5	3D Distance	35.2000	35.2198	35.2116	35.2192	35.2192	35.2211	35.2143	35.2105
Distance 6	3D Distance	32.6000	32.5943	32.5958	32.5942	32.5942	32.5984	32.5994	32.6006
Distance 7	3D Distance	32.6000	32.5918	32.5938	32.5901	32.5901	32.5953	32.5972	32.6005
Distance 8	3D Distance	32.6000	32.5978	32.5965	32.5985	32.5985	32.6006	32.6010	32.5956
Distance 9	3D Distance	32.6000	32.5958	32.5951	32.5946	32.5946	32.5970	32.5986	32.5942
Distance 10	3D Distance	72.2000	72.2005	72.1969	72.1980	72.1980	72.2002	72.1968	72.1993
Distance 19	3D Distance	32.6000	32.5960	32.5952	32.5950	32.5950	32.5971	32.5989	32.5943
Distance 20	3D Distance	35.2000	35.1998	35.2034	35.2044	35.2044	35.2021	35.2007	35.1980
Distance 21	3D Distance	32.6000	32.5944	32.5961	32.5943	32.5943	32.5989	32.5994	32.6009
Distance 22	3D Distance	35.2000	35.2194	35.2111	35.2190	35.2190	35.2203	35.2142	35.2100

Table 11 - Outer contour average deviations

Average deviation (mm)								
Object Name	**Control**	**Test 1**	**Test 2**	**Test 3**	**Test 4**	**Test 5**	**Test 6**	**Test 7**
Distance 5	3D Distance	0.0198	0.0116	0.0192	0.0168	0.0211	0.0143	0.0105
Distance 6	3D Distance	0.0057	0.0042	0.0058	0.0020	0.0021	0.0009	0.0017
Distance 7	3D Distance	0.0082	0.0062	0.0099	0.0042	0.0047	0.0028	0.0037
Distance 8	3D Distance	0.0022	0.0035	0.0015	0.0022	0.0020	0.0018	0.0044
Distance 9	3D Distance	0.0042	0.0049	0.0054	0.0016	0.0030	0.0016	0.0058
Distance 10	3D Distance	0.0106	0.0075	0.0041	0.0073	0.0035	0.0045	0.0007
Distance 19	3D Distance	0.0040	0.0048	0.0050	0.0016	0.0029	0.0014	0.0057
Distance 20	3D Distance	0.0008	0.0034	0.0054	0.0028	0.0021	0.0024	0.0025
Distance 21	3D Distance	0.0058	0.0039	0.0057	0.0017	0.0021	0.0009	0.0017
Distance 22	3D Distance	0.0194	0.0111	0.0190	0.0158	0.0203	0.0142	0.0100

Regarding the outer contour, it is possible to see that only two dimensions exceed the tolerances, and again all the dimensions are really close between the whole tests. Analyzing more carefully the samples on Polyworks and on the microscope, it was possible to observe that the majority of the cut edges were smooth (Figure 52), but nevertheless there were still found some regular and some unusual problems.

One usual observed problem in some samples was the presence of burr in some areas, as it is possible to see in Figure 53. It was also observed in some samples the presence of molten material attached on the cut surface, as it is possible to see in Figure 54.

Figure 52 - Microscopic picture of the lower surface of the inner slot (sample 2 of the test 3) (100x magnification)

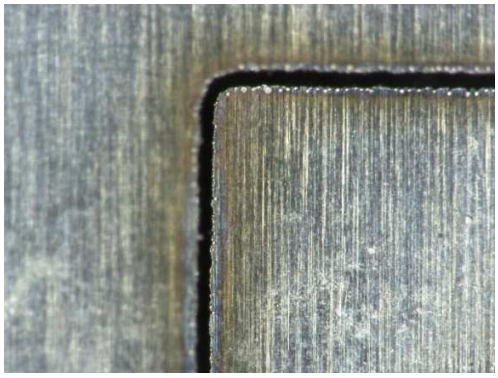

Figure 53 - Microscopic picture of the lower surface of the inner slot (sample 2 of the test 3) (200x magnification)

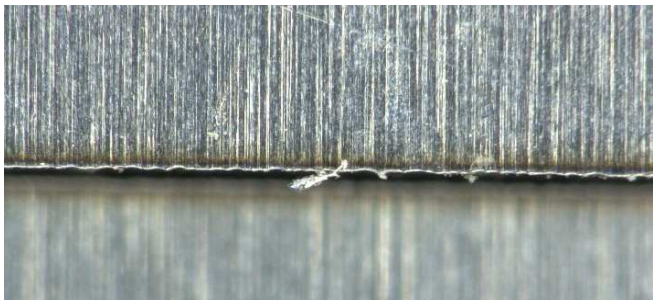

Figure 54 - Microscopic picture of the lower surface of the inner slot (sample 2 of the test 3) (200x magnification)

Regarding the only dimensions that surpass the required tolerances, it is possible to see in the Annex 11 that the sample 1 of the test 5 is the only one sample that is surpassing the required tolerances by a significant amount, whereby it was analyze more carefully the edges used to determine those dimensions on Polyworks (Figure 57) and on the microscope (Figure 55).

As it is possible to observe, the cut edge presents an undulation pattern on the zone used to measure. However, moving along that edge towards the right side, it was possible to see that the undulation was absent (Figure 56), suggesting that this was not caused by a factor related to the laser cutting process, but probably something related to the fixation of the metal sheet during the process, which may have caused the vibration of the metal sheet in that zone. It must be highlighted that distance 5 and 22 are the same, but using different measuring methods.

Figure 55 - Undulation zone on the lower surface (sample 1 of the test 5) (200x magnification)

Figure 56 - Microscopic picture of the lower surface (sample 2 of the test 5) (200x magnification)

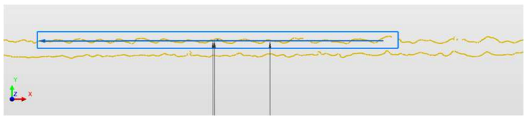

Figure 57 - Detail of edge with undulation

One usual problem observed caused by the path of the laser, as it is possible to see in Figure 58 and Figure 59, where there is a zone where the cut was not continuous, occurs on the zone where the laser crosses from the inner geometry to the outer one to perform the loop. This was observed in most of the zones where this was done.

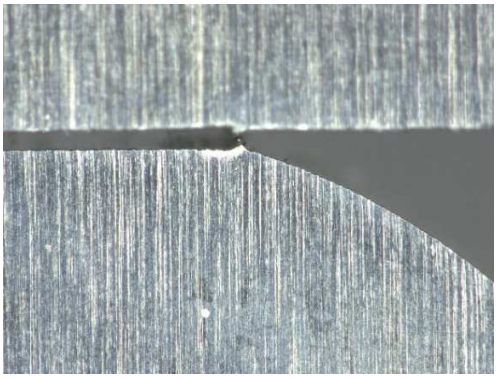

Figure 58 - Microscopic picture of the not continuous cut zone of the upper surface (sample 1 of the test 1) (200x magnification)

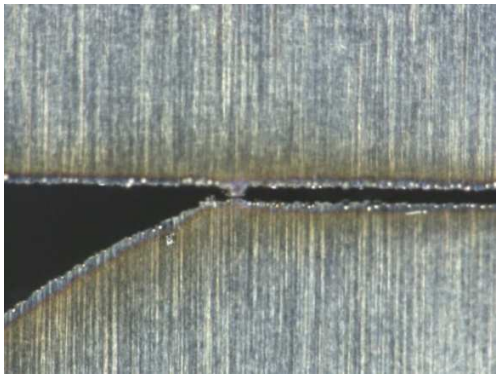

Figure 59 - Microscopic picture of the not continuous cut zone of the lower surface (sample 1 of the test 1) (200x magnification)

Observing the obtained deviations in the Table 9 and in the Table 11, it is possible to see that there is not a significant difference between the different tests or even between the samples of the same tests.

A bigger difference in the dimensions could be expected in the tests performed with a higher and lower cutting speed, due to the higher and lower demand, respectively, required on the axis motion system. However, among these tests there was not a significant difference. It is also possible to state that all dimensions of the outer contour are within the required tolerances. However, when analyzing the pilot holes, inner slot and holes, most of the diameters were not within the required tolerances, with the holes having constant geometry defects.

As already mentioned before, the metal sheet suffered some deflexion during the laser cutting operation, being that for this reason the middle of the metal sheet was further away from the laser nozzle and thus, due to the laser beam caustic shape, it is expected that the closer to the middle the cut is, the wider the kerf is. However, analyzing Figure 60, it is possible to see that this did not happen. Even so, the observed kerf dimensions are still bigger than the expected kerf with around 40 µm, probably caused by the flexion of the metal sheet.

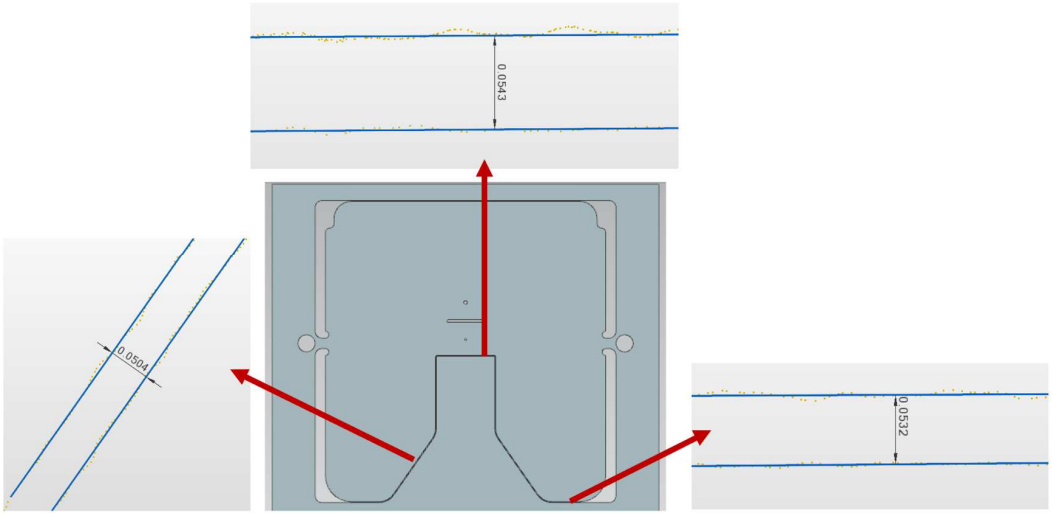

Figure 60 - Test 2 sample 1 kerf dimensions

In order to have a more detailed idea of how the samples geometry produced by laser cutting compares to the original one, it was created a color map showing the deviations between the CAD file and the point cloud.

A similar procedure to the one explained in Table 7 was carried out to perform the color map of the deviations between the point cloud and the geometry of the CAD file. For this, it was inserted a CAD file containing only the cut surfaces, as it is possible to see in Figure 61 and Figure 62.

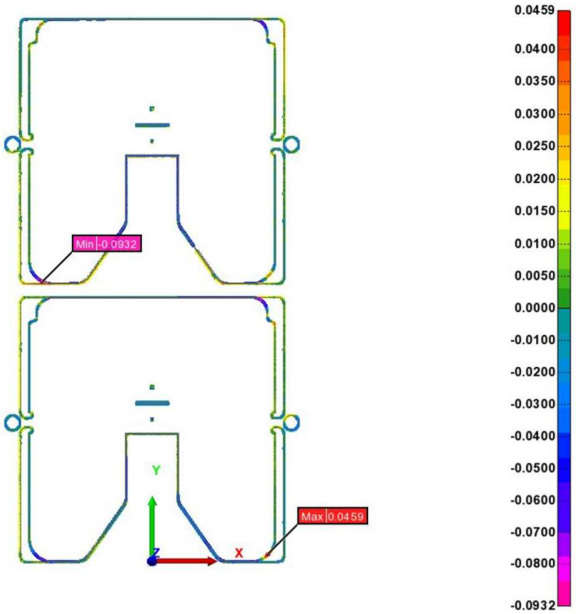

Figure 61 - Color map of the sample 2 of the test 6

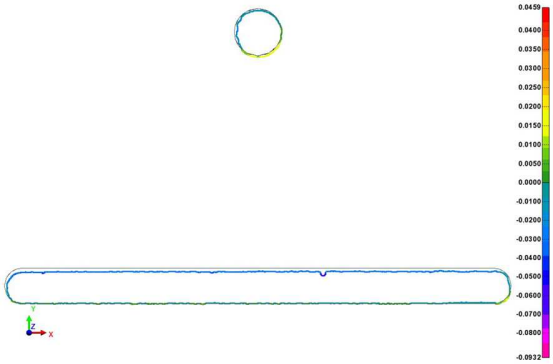

Figure 62 - Test 6 sample 2 inner slot color map

In the Figure 62, it is possible to have a better idea why most of the slots' dimensions observed in Table 9 were not within the required tolerances.

Even though the entire contour presents a smooth and regular edge, it is possible to see that it is necessary to improve the laser path programming, since the lower edge observed in figure is aligned with the original geometry and the upper one is lower than the original geometry, making the slot thinner than intended. In this figure, it is also possible to see how the 0.4 mm diameter from the sample aligns with the original geometry.

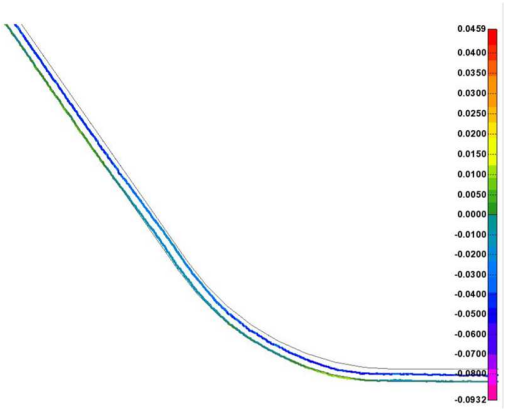

Figure 63 - Test 9 sample 2 angular cut color map

The linearity and accuracy of the angular cut can be observed in Figure 63, where it proved to be very accurate. The deviation of the second line to the original geometry concerns to the difference of the kerf with the distance created on the CAD file, as already mentioned before.

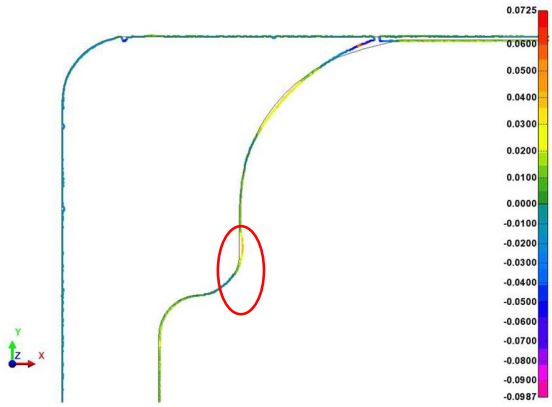

Figure 64 - Test 9 sample 2 color map detail 1

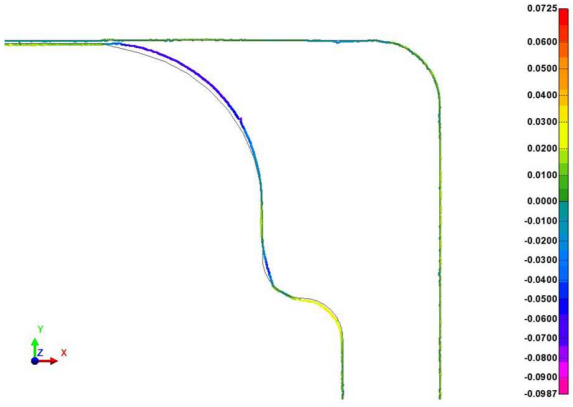

Figure 65 - Test 9 sample 2 color map detail 2

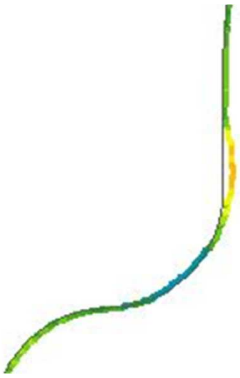

Figure 66 - Test 9 sample 2 color map detail 3

Analyzing Figure 64 and Figure 65, it is possible to see some problems observed in all the samples, the first one being caused by the incorrect choice of the laser path, that made the curve with the largest radius to deviate close to the outer edge, creating a large gap in that zone, as it is possible to see in Figure 65, where these are the zones with the largest deviations. In Figure 64, it is also possible to see in the marked area a zone where the laser deviated inwards. However, on the other side of the samples, as it is possible to see in Figure 66, close to the same zone, the laser did not create a complete curvature, but it followed a straight line instead.

4.3 SEM analysis

The SEM analysis was performed on the test samples that showed a bigger difference among the tests observed on the microscope. In these analyses, pictures were taken from different zones of the samples in order to see how the parameters changes affected the burr formation, heat affected zone and also the cut quality. To have a better comparison among all the laser cut

samples and the punched, all pictures where taken in similar areas and using the same magnification in those areas.

It must be referred that the samples 1 of the test 2 and 1 of the test 4 where not cleaned before the SEM analysis. However, after analyzing these two samples and observing some dirt residues, it was opted to clean the punched sample and the sample x of the test 6 in a 5 minutes ultrasonic bath in acetone.

For this reason, when analyzing the samples of the test 2 and 4, it is possible to see more amounts of dirt and stains on the surface.

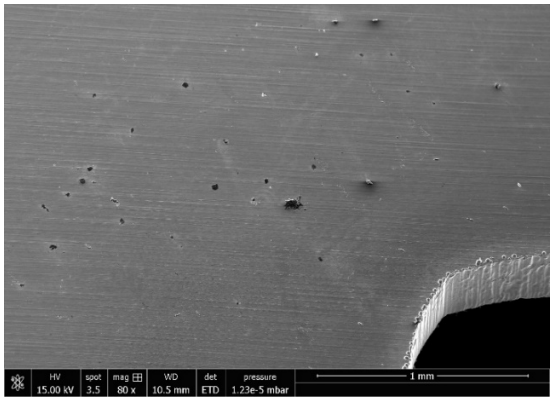

Figure 67 - SEM overview picture of the cut zone of the lower surface of the sample 2 of the test 2

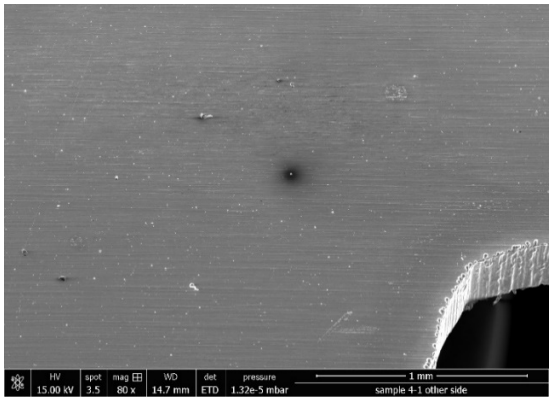

Figure 68 - SEM overview picture of the cut zone of the lower surface of the sample 1 of the test 4

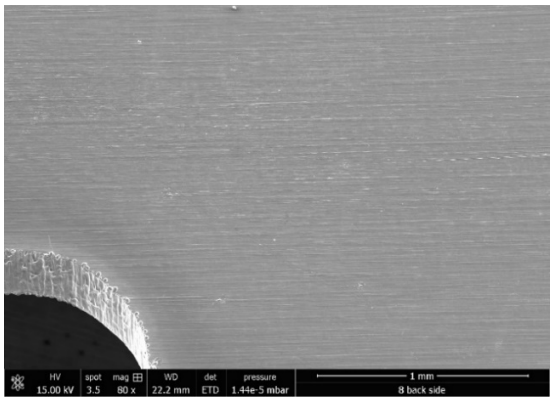

Figure 69 - SEM overview picture of the cut zone of the lower surface of the sample 6 of the test 1

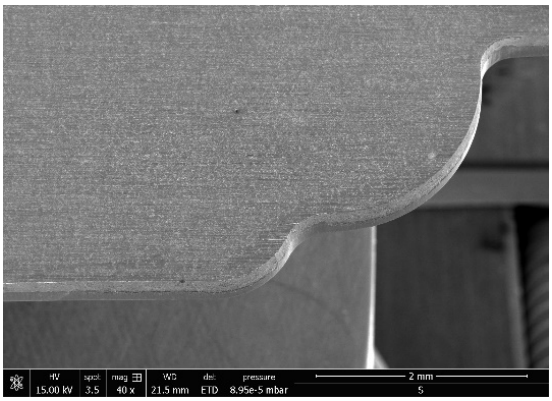

Figure 70 - SEM overview picture of the cut zone of the lower surface of the stamped sample

Taking a closer look to a zone of the bottom surface of the samples, it was possible to observe a significant difference related to the amount of splatter attached to the surface. In Figure 67, it is

possible to see the presence of some splatter with considerable dimension, reaching around 50 µm.

When observing the Figure 68, it is possible to see a big increase of the presence of splatter. However, in this test, most of the splatter had really small dimensions (around 1 µm) and only few reached larger dimensions of approximately 20 µm, being this preferred.

The test 6, seen in Figure 69, did not present any visible splatter. Comparing the tests, the test 4 had a better performance than the test 2, since the smaller dimensions of splatter will not affect as much the distance between the guard and the cutter or the wear caused by the splatter. The test 6 presents the best result of the three analyzed tests, where the increase of the assist gas pressure increased the effectiveness to eject the molten material, resulting in a splatter free surface. In the Figure 70 it is possible to observe a cut surface of a punched sample, in this case the burr is significantly smaller than the produced by laser cut however this was performed by a relatively new punching tool, being that due to the wear, the burr tends to increase.

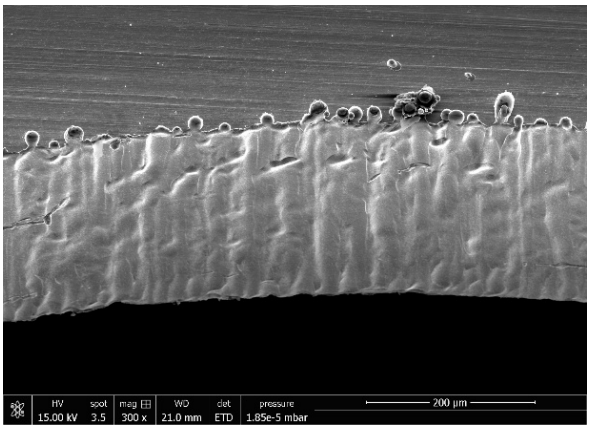

Figure 71 - SEM detail picture of the cut zone of the lower surface (sample 2, test 2)

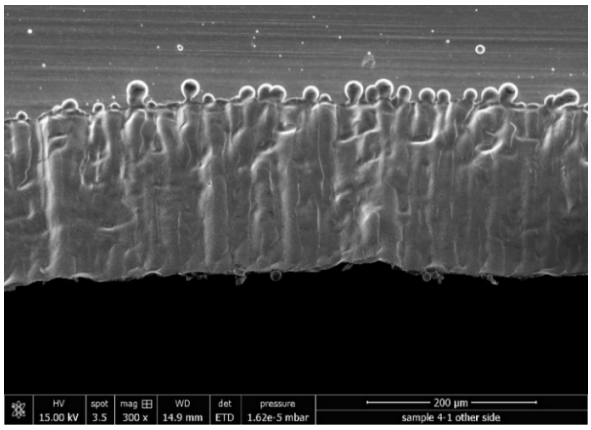

Figure 72 - SEM detail picture of the cut zone of the lower surface (sample 1, test 4)

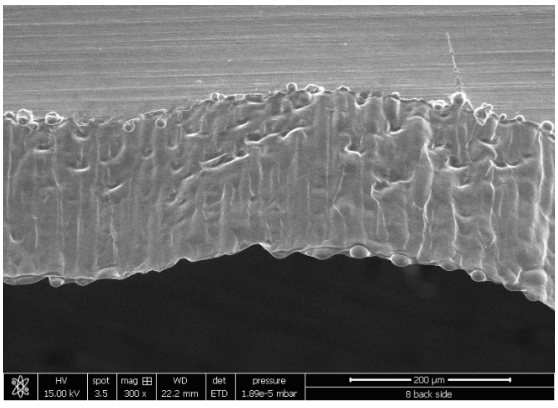

Figure 73 - SEM detail picture of the cut zone of the lower surface (sample 1, test 6)

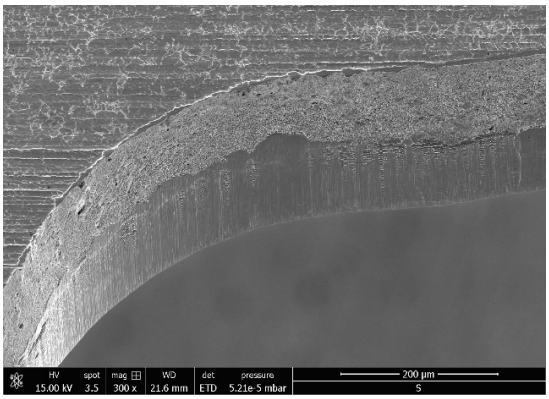

Figure 74 - SEM detail picture of the cut zone of the lower surface of the stamped sample

Analyzing more closely a zone on the bottom surface of a cut edge it is possible to see that Figure 71 presents the smoother cut edge of the three laser cut samples. However, the burr produced in this test was similar to the burr produce in test 4 (Figure 72) reaching around 50 µm.

It is also possible to see in Figure 72 the presence of small particle of molten material close to the upper surface, meaning that the increase of speed lead to an insufficient capacity for the assist gas to eject the molten material. Regarding the burr, the test 6 (Figure 73) achieved the best result of the laser cut samples, where the burr reached dimensions of approximately 20 µm. The stamped sample (Figure 74) had really small burr, however, it was also possible to see some zones with a bigger burr.

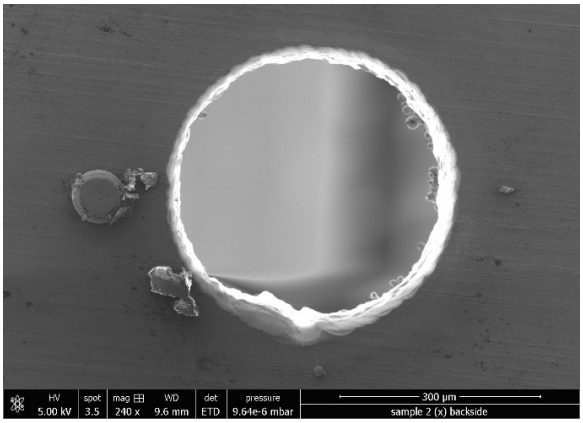

Figure 75 - SEM picture of the 0.4 mm of the upper surface (sample 2, test 2)

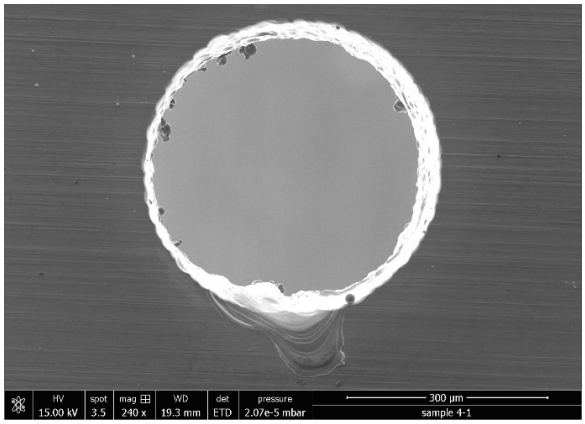

Figure 76 - SEM picture of the 0.4 mm of the upper surface (sample 1, test 4)

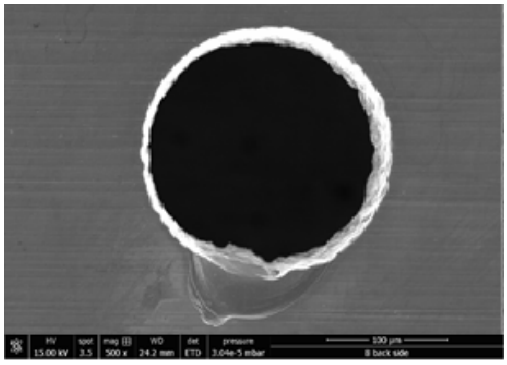

Figure 77 - SEM picture of the 0.4 mm of the upper surface (sample 1, test 6)

Observing the 0.4 mm diameter holes on the top surface, it is possible to see that Figure 75 (test 2) is the only test with the presence of splatter around the hole. The results of the test performed with the highest cutting speed and with the highest assist gas pressure had similar results, not

having the presence of splatter, but both having molten material dragged outside the hole, close to the starting/ending zone, as is it possible to see in the Figure 76 and Figure 77. In all samples, it was also possible to see a usual problem close to the starting/ending zone, where it looks that the cut was not properly finished. This may be caused by a not correct laser path.

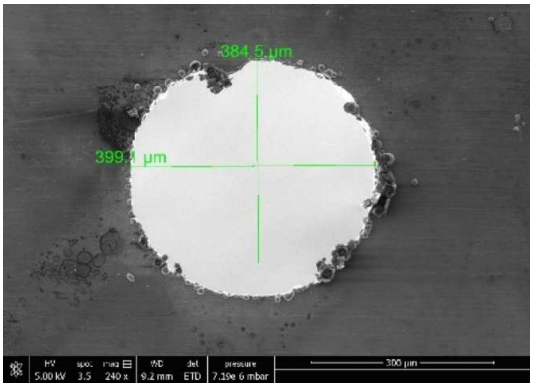

Figure 78 - SEM picture of the 0.4 mm of the lower surface of the sample 2 of the test 2

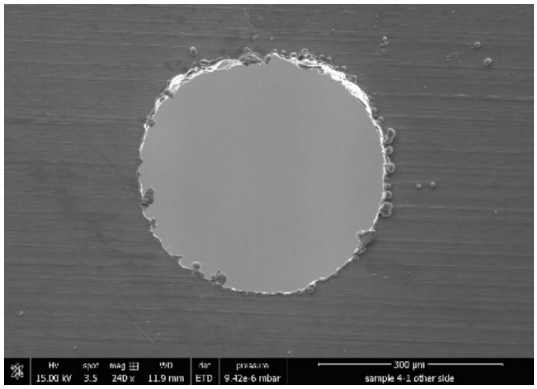

Figure 79 - SEM picture of the 0.4 mm of the lower surface of the sample 1 of the test 4

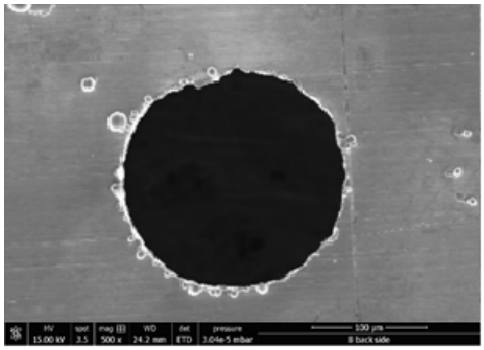

Figure 80 - SEM picture of the 0.4 mm of the lower surface of the sample 1 of the test 6

The analysis of the 0.4 mm diameter holes on the lower surface shows an increase of problems when comparing to the upper surface. All samples had a significant amount of burr, with the test 2 (Figure 78) having the biggest amount of burr and the test 4 (Figure 79) and 6 (Figure 80) having similar amounts of burr. However, it is possible to see that the increase of assist gas pressure in test 6 forced the molten material to go outside the hole, something that was not observed in the other tests, where some of the burr was leaning to the inside of the burr. It was also possible to see in the Figure 80 that the increase of gas pressure lead to an increase of splatter on the lower surface, when comparing to the other tests.

As it is possible to see in the analyzed samples, the variation of some parameters improve some aspects on the cut quality, but also decrease other ones, whereby it is important to find the most appropriate combination of parameters in order to have the intended results.

In the Figure 78, it is also possible to see the dimension of the hole obtained in SEM and, when comparing it to the dimensions obtained by using the smartscope, the dimensions are very similar.

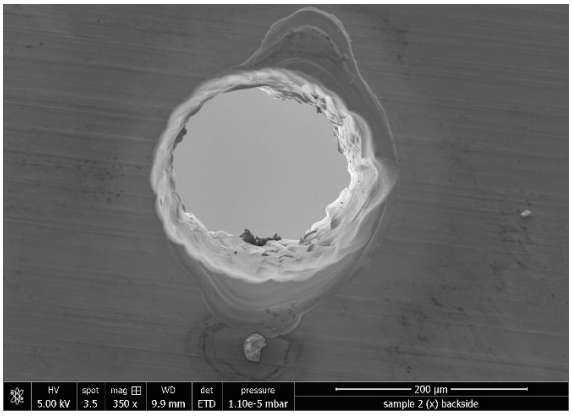

Figure 81 - SEM picture of the 0.2 mm of the upper surface of the sample 2 of the test 2

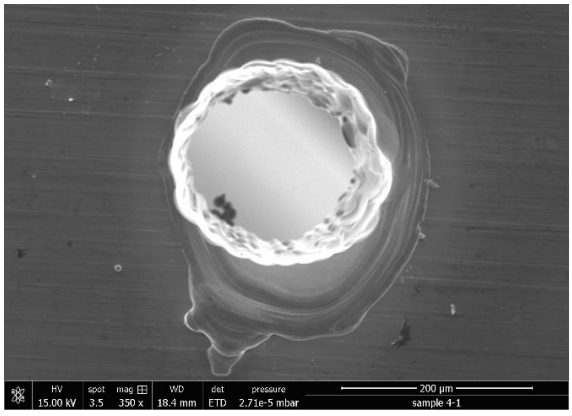

Figure 82 - SEM picture of the 0.2 mm of the upper surface of the sample 1 of the test 4

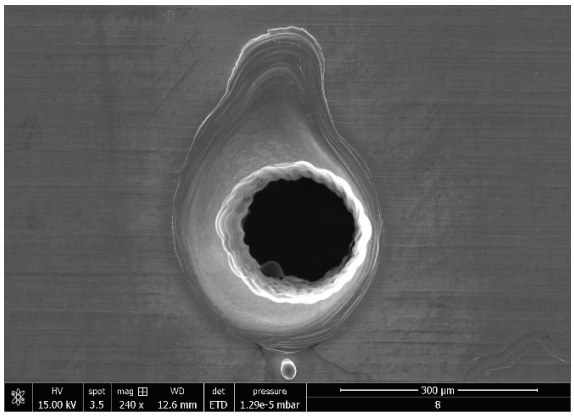

Figure 83 - SEM picture of the 0.2 mm of the upper surface of the sample 1 of the test 6

When analyzing the 0.2 mm diameter holes on the top surface, it is possible to see an expected increase of temperature of the metal sheet in comparison to the 0.4 mm diameter holes, as it is possible to see by the increase of dragged molten material on the surface.

In similarity to the results observed in the 0.4 mm diameter hole, the test performed with the highest laser power (Figure 81) had the less amount of dragged molten material, suggesting that the time required to vaporize the material decreased, thus decreasing the heat conducted to the rest of the metal sheet. It is also possible to see small amount of splatter present on the metal surface in the test 2 and 4 (Figure 82), while in test 6 it was observed only one splatter, as shown in the Figure 83.

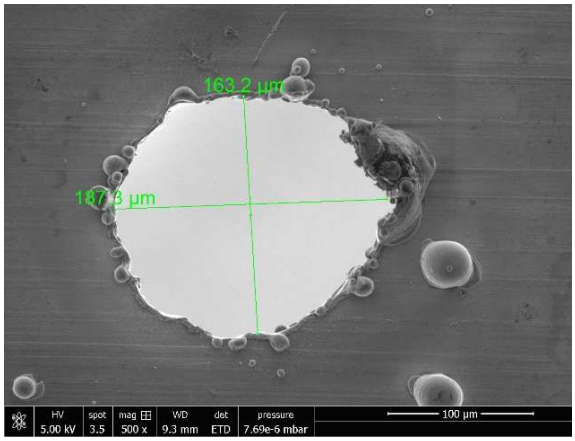

Figure 84 - SEM picture of the 0.2 mm of the lower surface of the sample 2 of the test 2

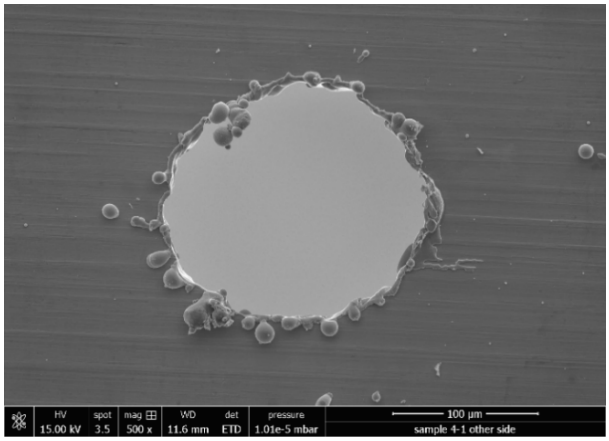

Figure 85 - SEM picture of the 0.2 mm of the lower surface of the sample 1 of the test 4

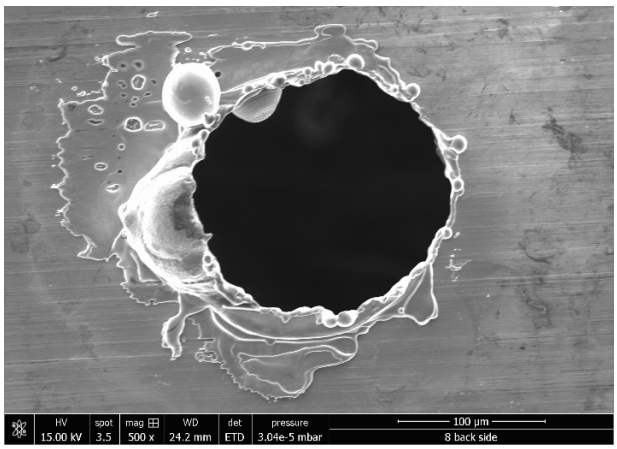

Figure 86 - SEM picture of the 0.2 mm of the lower surface of the sample 1 of the test 6

Observing the 0.2 mm diameter holes on the top surface, it is possible to see big differences between the tests. In the test performed with the highest laser power (Figure 84), it is possible to observe the presence of small amounts of burr (not present all around the hole) with considerable dimensions, but with a big agglomerate of molten material in the area close to the starting/ending zone, and also the presence of some splatter reaching around 40 µm.

The test 4 (Figure 85) presents burr all around the hole and some splatter with small dimensions. The test performed with the highest assist gas pressure resulted in large amounts of molten material, being forced against the lower surface, as it is possible to see in the Figure 84 and, in similarity to test 2, it also presents a bigger agglomeration of molten material close to the starting/ending zone.

4.4 HAZ analysis

It must be highlighted that in the microscopic pictures of the microstructure, the sample surface is facing down and the SEM pictures the upper surface is facing up.

4.4.1 Outer contour

The observed microstructure of outer edge in the Figure 87, in particular the Figure 88 and Figure 90 shows that both samples achieved a similar HAZ dimension, which was expected since this edge was cut using the same parameters in both tests, as mentioned before. The test performed with the lowest laser power (Figure 92) also did not show a significant difference on the HAZ, being similar to the observed in the other tests.

An interesting result observed in these samples was the fact that the HAZ close to the upper surface (Figure 89) was significantly bigger than the observed close to the lower surface (Figure 91), being that in the first zone it reached almost 60 µm, and close to the lower surface it was approximately 30 µm.

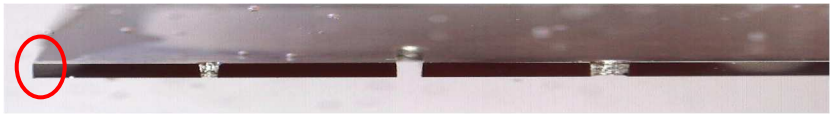

Figure 87 - Outer contour observed zone

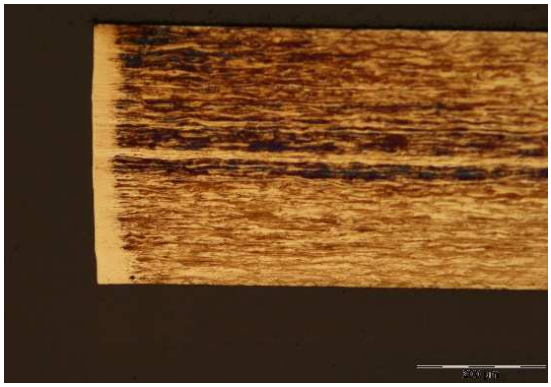

Figure 88 - Test 1 sample 1 outer edge microstructure

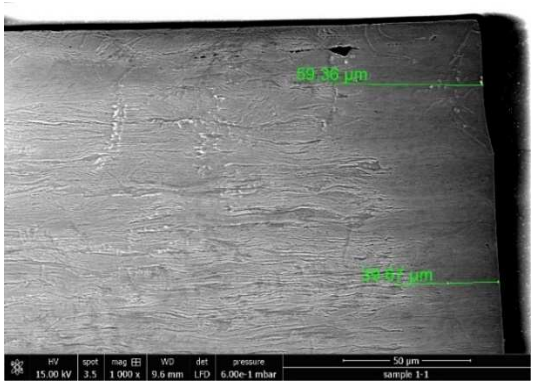

Figure 89 - Test 1 sample 1 outer edge HAZ dimension

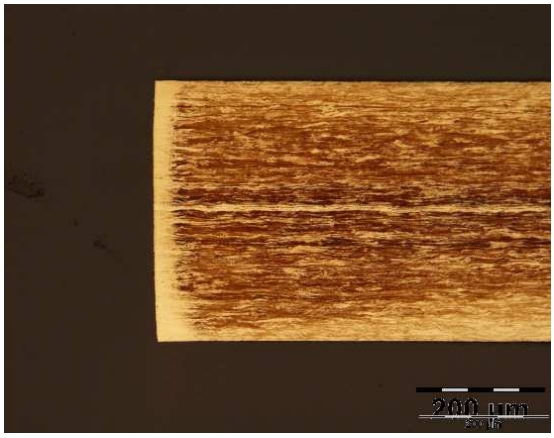

Figure 90 - Test 2 sample 1 outer edge microstructure

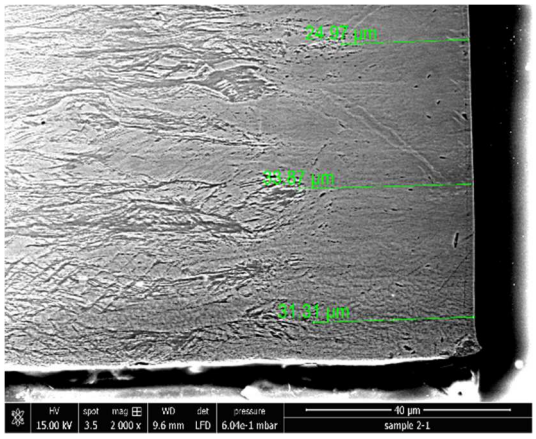

Figure 91 - Test 2 sample 1 outer edge HAZ dimension

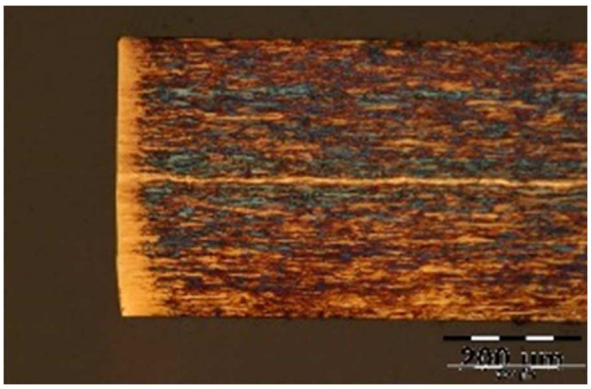

Figure 92 - Test 3 sample 1 - outer edge microstructure

4.4.2 0.2 mm hole

Comparing the Figure 93 with the Figure 95, it is possible to see a big reduction of the HAZ with the increase of laser power. This is also visible in the Figure 94, where the HAZ reached almost 40 µm and in the Figure 96, where the HAZ only reached approximately 21 µm.

In the SEM pictures, it is also possible to see the presence of a recast layer throughout the cuts and the dimension of this molten material reached close to twice the dimension of the test performed with the suggested cutting parameters, reaching approximately 11 µm in this test, and almost 5 µm in the test performed with the higher laser power.

Comparing Figure 95 with Figure 97, it is possible to see an increase of the HAZ in the test performed with the lowest laser power. This corresponds to what was previously mentioned, being that in the test performed with the higher laser power, the vaporization of the material occurs faster, decreasing the interaction time between the laser beam and the metal sheet, thus decreasing the amount of heat conducted to the metal sheet. Another interesting aspect observed in these pictures is the fact that the holes present different dimensions on the upper and lower surface.

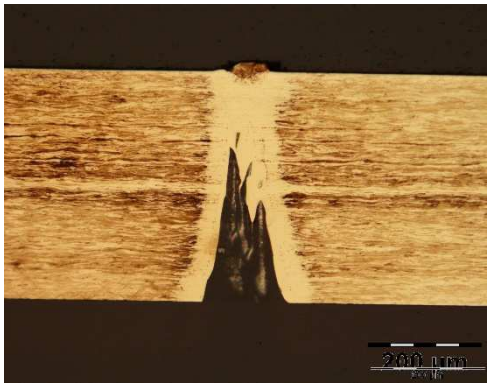

Figure 93 - Test 1 sample 1 - 0.2 mm hole microstructure

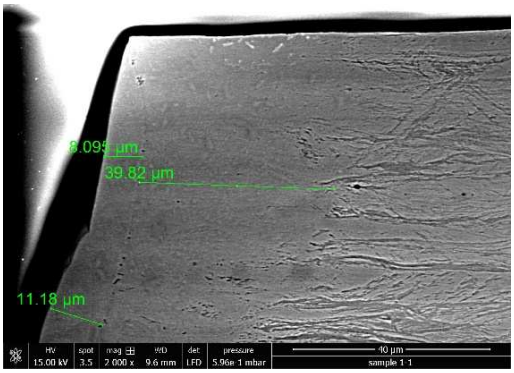

Figure 94 - Test 1 sample 1 - 0.2 mm hole HAZ dimension

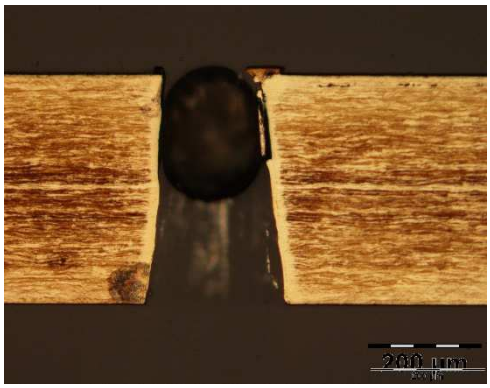

Figure 95 - Test 2 sample 1.- 0.2 mm hole microstructure

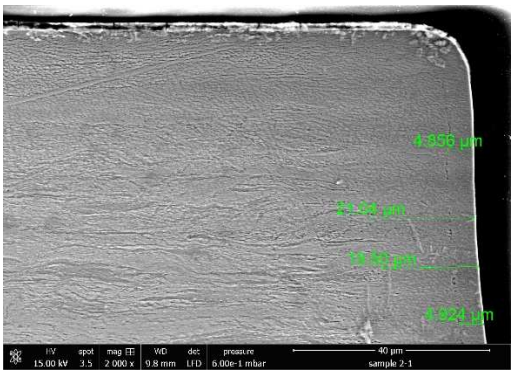

Figure 96 - Test 2 sample 1 - 0.2 mm hole HAZ dimension

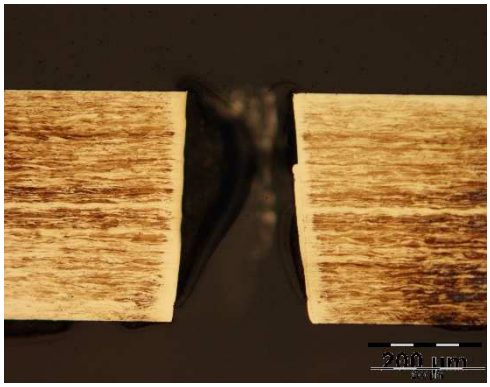

Figure 97 - Test 3 sample 1 - 0.2 mm hole microstructure

4.4.3 Inner slot

Comparing Figure 98 with Figure 100, it is not possible to see significant differences regarding both samples, having a similar HAZ. Taking a closer look, it is possible to see in the Figure 99 that the HAZ in the sample performed with the suggested laser cutting parameters reached around 25 µm and that the sample performed with the highest

laser power (Figure 101) reached approximately 30 µm. However, in this zone, the distinction between the base material and the HAZ is not very clear, and thus, this dimension can be slightly different. The sample performed with the lowest laser power presents a significant difference on the HAZ, as it is possible to see in the Figure 102, where the HAZ has almost twice the dimension when compared to the other two samples.

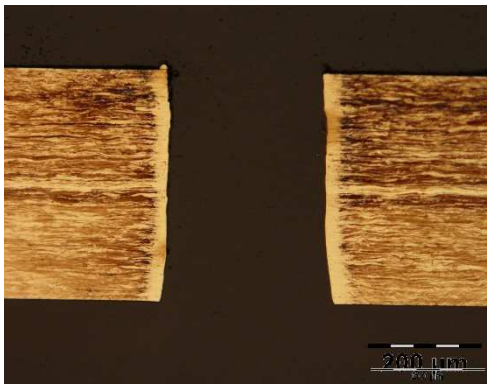

Figure 98 - Test 1 sample 1 slot microstructure

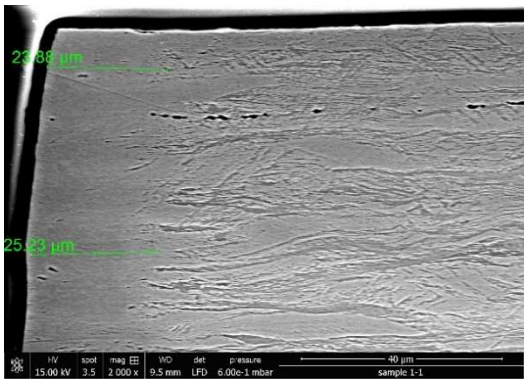

Figure 99 - Test 1 sample 1 slot HAZ dimension

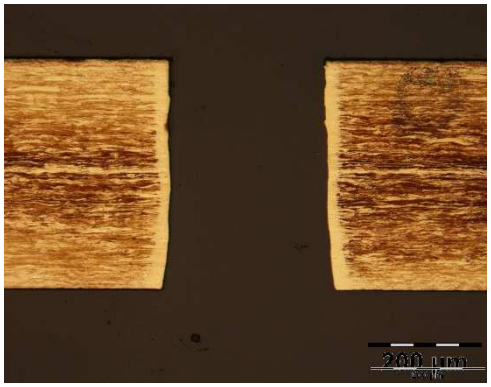

Figure 100 - Test 2 sample 1 slot microstructure

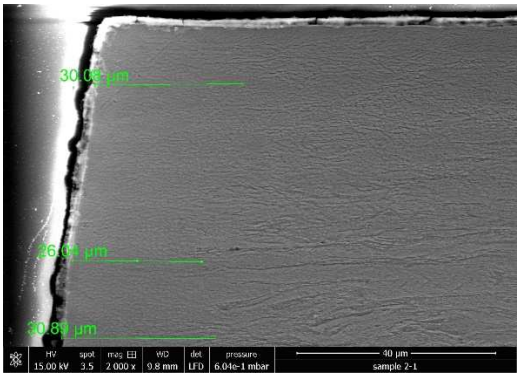

Figure 101 - Test 2 sample 1 slot HAZ dimension

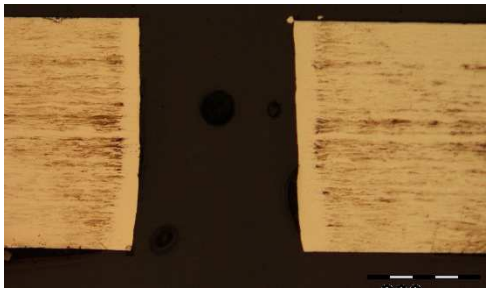

Figure 102 - Test 3 sample 1 slot microstructure

4.4.4 O.4 mm hole

The observation of the 0.4 mm holes performed in the test with the suggested parameters (Figure 103) and test with the highest laser power (Figure 105) shows similar results to the previously observed in the slots of the same tests. Observing the SEM

pictures taken close to the lower surface, it is observed once again that both tests achieved a similar dimension of the HAZ, being that in test 1 (Figure 104) the HAZ reached almost 20 µm and in test 2 (Figure 106) it reached around 19 µm.
It must be referred that the particles observed in Figure 106 are debris that were probably dragged from the polishing process. In similarity to the previous analyzed zones, the HAZ observed in the test performed with the lowest laser power (Figure 107) achieved the highest HAZ when compared to the other analyzed samples
.

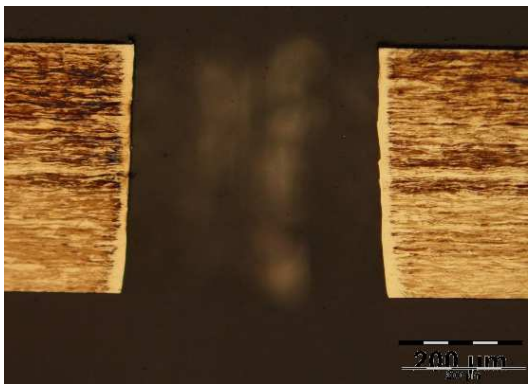

Figure 103 - Test 1 sample 1 - 0.4 mm hole microstructure

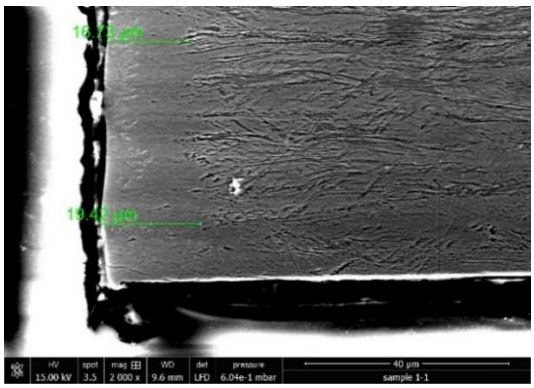

Figure 104 - Test 1 sample 1 - 0.4 mm hole HAZ dimension

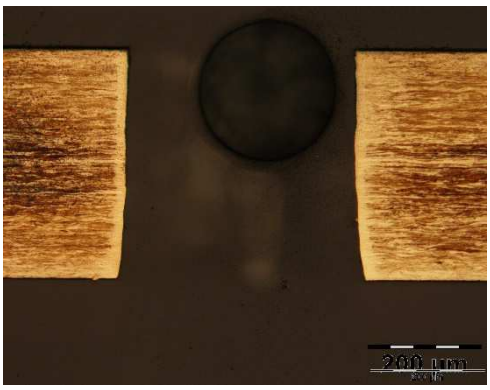

Figure 105 - Test 2 sample 1 - 0.4 mm hole microstructure

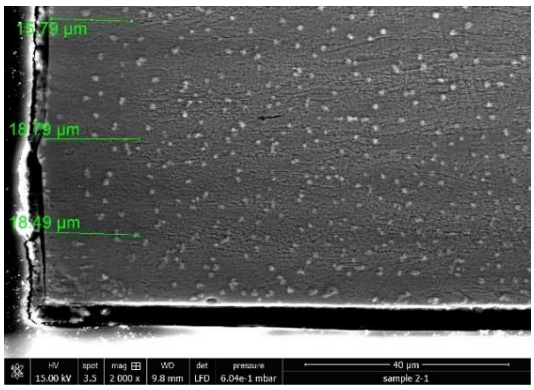

Figure 106 - Test 2 sample 1 - 0.4 mm hole HAZ dimension

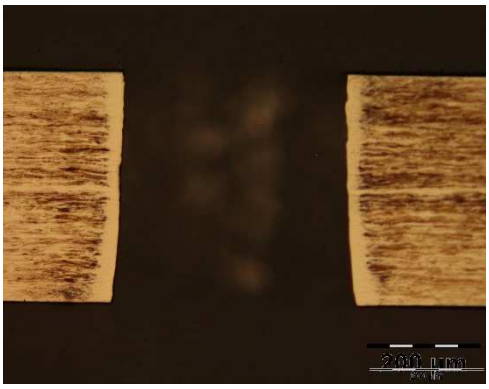

Figure 107 - Test 3 sample 1 - 0.4 mm hole microstructure

4.5 Microhardness analysis

The analysis of the microhardness was performed only in the sample 1 of the test 3, since it was the analysed sample that has presented the biggest HAZ, and because there was not a significant difference in the HAZ of the samples.

Figure 108 - Outer edge microhardness

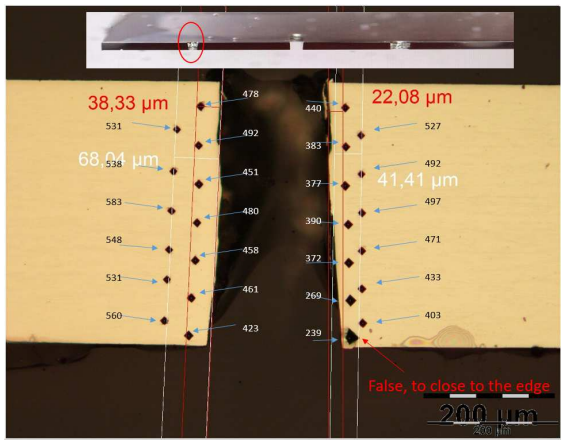

Figure 109 - 0.2 mm diameter hole microhardness

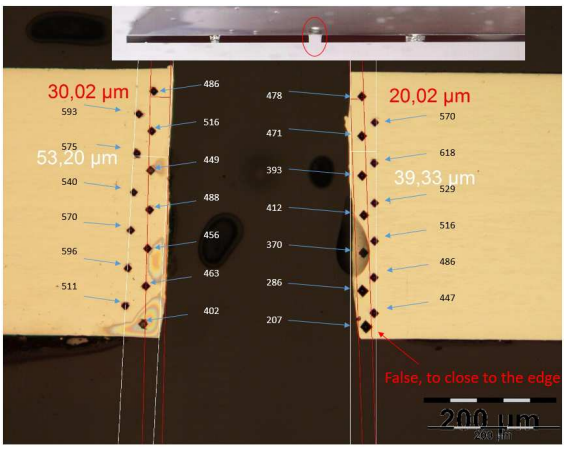

Figure 110 - Inner slot microhardness

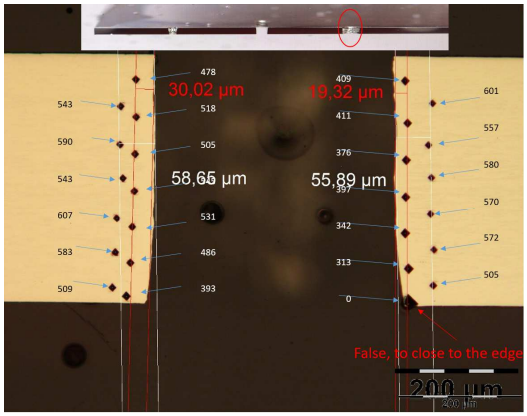

Figure 111 - 0.4 mm diameter hole microhardness

When analyzing the microhardness in indentations performed at close distances in the different analyzed zones, it is possible to see that the microhardness is very similar in all the four analyzed zones.

This means that the cooling times in these zones are also similar, since it was expected to have a faster cooling on the outer contour (Figure 108) and a slower one the smaller the performed hole is (Figure 109). As expected, the indentations performed at a higher distance from the cut edge than the HAZ dimension previously analyzed obtained a microhardness value similar to the base material.

4.6 Prototyping

In order to improve the cut quality and achieve the required repeatability of the laser process, it is required to have a mechanism that positions the metal sheet properly and guarantees that the metal sheet does not move during the process, also improving the flexion problem observed in the laser cutting tests.

To accomplish these requirements, 3 prototypes where made, each one having its advantages and disadvantages. In all the prototypes, the feeding of the metal sheet was performed using the same mechanism, similar to the already used in the cold forming process. To do this, it was opted to use a servo roll feeder with an accuracy of 15 µm.

Also, in all the prototypes, for the positioning of the metal sheet in the laser machine, it was opted to take advantage of the pilot holes used in the cold forming production line, and also position the metal sheet using pilot pins. For this reason, the suggestion for the future is to first punch the pilot holes to have the required tolerances and repeatability on them, only after performing the laser cut.

One of the restrictions while developing these prototypes was caused by the dimensions and the proximity of the laser nozzle to the metal sheet, limiting the location options of not only the pilot pins, but also of some fixation components. For this reason, it was discarded the option to use the pilot holes associated to the zone where the laser would actuate, and it was chosen to use the pilot holes immediately after and before these.

4.6.1 Prototype 1

In this prototype, the metal sheet is fed by the servo roll feeder, entering in an adjustable pilot pins mechanism where the metal sheet is first guided to the zone where the cut is performed (Figure 112). After, the metal sheet goes into another adjustable pilot pins mechanism in order to ensure the correct position of the metal sheet, and to avoid it from wobbling between the laser cut zone as well.

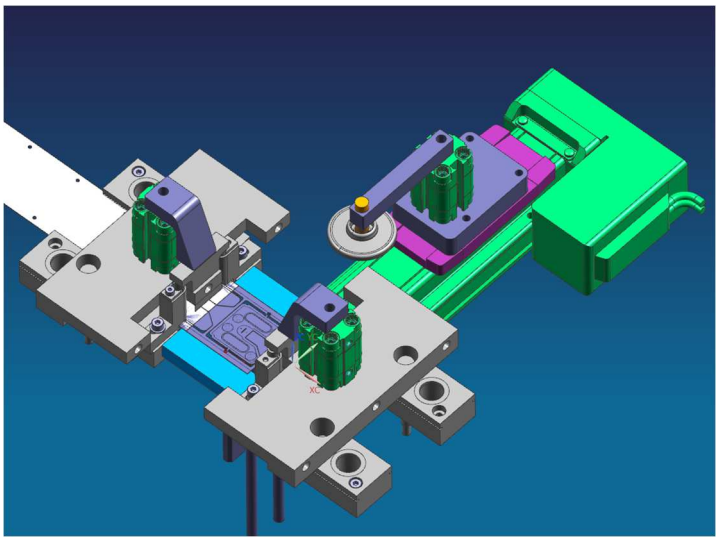

Figure 112 - Prototype 1

Each adjustable pilot pins mechanism is actuated by a pneumatic cylinder with a force of 51 N. Between the two adjustable pilot pin mechanisms, the metal sheet is guided with two guides on the side that also help to prevent the metal sheet from flexing. It must be highlighted that the used adjustable pilot pins mechanism is an already existing mechanism in the company, and thus, it does not require further investment.

When the metal sheet enters the zone where the laser cutting process is going to be performed, the main goal in this zone is to prevent the metal sheet from flexing, to ensure that the laser focal point is acting always in the most effective zone, and also to avoid any vibrations of the metal sheet caused by the assist gas.

The mechanism in charge to achieve this task was limited due not only by the laser path that performs almost a complete loop, only being left two connection areas between the geometry contour to the metal sheet, but also due to the proximity of the laser nozzle to the metal sheet surface. For this reason, it was opted to insert a vacuum system bellow the metal sheet. However, this mechanism should be easily changed to work with other production geometries.

In order to achieve the best vacuum as possible, it was inserted a pneumatic cylinder on a linear actuator that aims to approximate the metal sheet to the vacuum system, sealing the vacuum between the two parts.

The clamping of the metal sheet and the vacuum system is initiated by the linear actuator, which positions the clamper attached to the clamping cylinder on top of the metal sheet, followed by the actuation of the clamping cylinder. After the cylinder clamps the metal sheet against the vacuum cylinder, this process is repeated in reverse order, allowing the laser head to perform the laser cut without any obstacle in its way. Once the laser cutting process is concluded, the cylinders that actuate the pilot pins return to its standing positions, allowing the servo roll feeder to move the metal sheet to its next cutting position, where the process repeats.

Regarding the vacuum system in this prototype, it was opted to use two vacuum cups that will perform a total vacuum force of 9 N on the metal sheet (Figure 113). The metal sheet will be supported in a 3 mm thickness metal part that is basically a 1.5 mm smaller offset of the prototype, except for the area where the inner slot and holes are. The vacuum cups are attached to a metal part, similar to the top one, that is distanced by the top one by some spacers, with the same height of the vacuum cups (Figure 114). The vacuum system is attached by three connectors from the bottom of the system to the laser machine.

One potential problem that can occur with this prototype is the fact that the proximity of the zone where the laser actuates to the vacuum cups can lead to these ones melting from the heating of the metal sheet, disabling the vacuum.

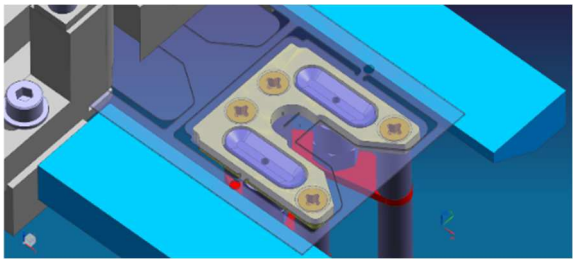

Figure 113 - Prototype 1 vacuum system (1)

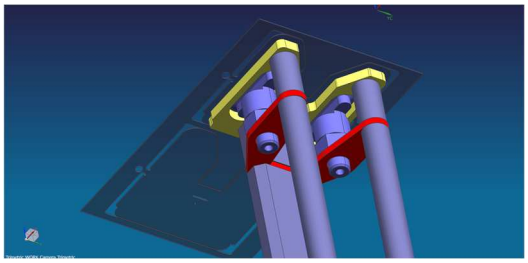

Figure 114 - Prototype 1 vacuum system (2)

4.6.2 Prototype 2

This prototype is similar to the previous one with the only difference being on the fixation system. In this prototype, the fixation of the metal sheet is made by another vacuum system. However, this one is made of three different components that can be produced by laser cutting.

This vacuum system (Figure 115) is made of a top part with a geometry similar to the used in the previous prototype, being the only difference the existence of 12 holes with a diameter of 4.5 mm to produce the vacuum with the metal sheet.

With these values and assuming a vacuum pressure of -0.6 MPa, it was possible, using the equation (1) and assuming a friction coefficient of 0.1 for metal to metal vacuum, calculate the theoretical vacuum force produced on the metal sheet, obtaining a value of 11.45 N.

$$F_{\_TH} = P \times A \times \mu \quad (1)$$

A=190.85 mm^2

F_TH=11.45 N

The middle part of the vacuum system is a spacer that allows the air flow to reach all the holes on the top part, and it also provides rigidity to the system. The bottom part not only closes the system sealing the vacuum, but also connects with the vacuum tube. Even though the three parts that make this vacuum system are relatively easy to produce, the assembly of these parts can have some problems since, due to the restrictions and small dimensions of the parts, it was opted to glue these parts together, something that can result in misaligned or looser parts, which can result in vacuum leaks.

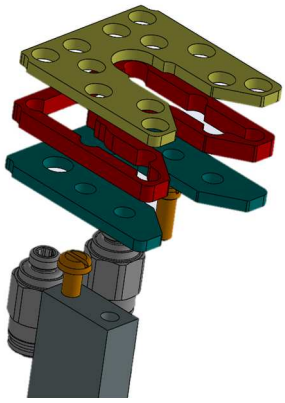

Figure 115 - Prototype 2 vacuum system

In order to be able to create this system significantly quickly, the suggestion is to produce these parts also by laser cutting and, due to the small dimensions and thicknesses of them, the connection would be performed using a glue.

4.6.3 Prototype 3

The last prototype uses an adjustable guide mechanism after the servo roll feeder that guides the metal sheet to a clamping mechanism (Figure 116).

This clamping mechanism is constituted by two parts, a lower one that is fixed to the laser machine and does not move and an upper part that performs the clamping that is actuated by two pneumatic cylinders that are also fixed to the lower part of the clamping mechanism (Figure 117).

In the top part there are also four pilot pins that in likeness to the previous prototypes actuates in the pilot holes immediately before and after the pilot holes associated to the zone where the laser will actuate. This mechanism also clamps the metal sheet around all the zone where the laser cut is going to be executed with a total force of 120 N.

This prototype also has some disadvantages being that these parts need to be made with a high level of accuracy and it is only possible to use to produce parts that have the pilot pins distanced equally length and width wise to this prototype. Another potential

problem is the fact that the movement of the top part of the mechanism is done with two independent cylinders which can end up in a jamming.

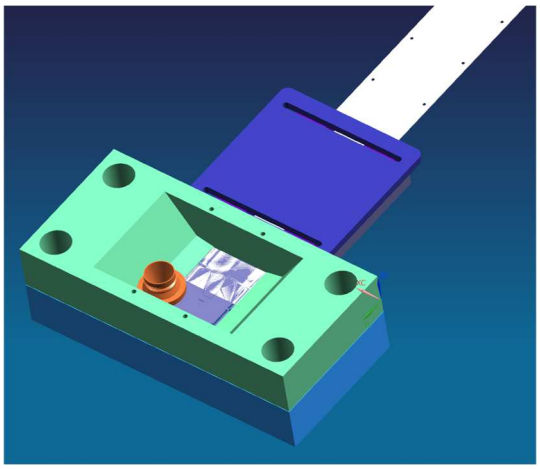

Figure 116 - Prototype 3

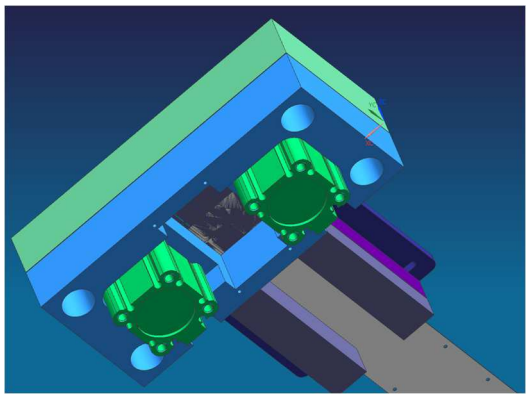

Figure 117 - Prototype 3 lower part

CONCLUSIONS

5 CONCLUSIONS

5.1 Conclusions

With the performed tests and achieved results, it is possible to conclude that:

- Even though most of the dimensions related to the outer geometry of the samples were within the required tolerances, it was observed in the analysis of the colormap that some specific zones did not achieved those tolerances;
- When analyzing the smaller features, none of the performed tests achieved the required tolerances or quality;
- Throughout the different performed samples and tests, the laser machine achieved a required repeatability;
- Regarding the burr, the test performed with the highest assist gas pressure achieved the best results on the outer contour, with a dimension of approximately 20 µm, which is also a burr dimension acceptable for punching (≈5% of the sheet thickness);
- The HAZ reached small dimensions, with the microhardness decreasing in that zone;
- The influence of the parameters also varies with the intended geometry to cut, being that some parameters that improved the quality in the outer geometry, presented the opposite influence in the smaller features;

Table 12- Study conclusions

Objective	Conclusions	State
Laser cutting parameters influence	The increase in cutting power decreased the HAZ; Increased gas pressure led to better dross.	✗ ✓
Precision and repeatability of laser cutting (20 µm)	The repeatability of the laser equipment is within the desired range; The outer geometry meets the requirements while the smaller geometries do not.	✗ ✓
Compare laser and stamping cut	Burr values were obtained similar to the values produced by stamping; Decreasing the laser cutting hardness can shorten the life of some components.	✓

Feasibility of producing Ultron Guard prototypes	It is feasible to produce prototypes, but it is advisable to refine the laser path.	

Having this into account, it is also possible to state that given the fact that all the deviations observed repeated in all samples, it is possible to improve those deviations with some fine tuning of the laser path in other to achieve the intended tolerances, which according to the laser machine manufacturer can achieve 5 µm. Highlight that he observed deviations were also within the tolerance provided by the laser manufacturer for a non-refined laser path. The fact that these deviations repeat also proves that the repeatability of the laser machine itself is within the required. On the other hand, some deviations such as the ovalization of the pilot holes were potentially caused by an incorrect fixation of the metal sheet.

Regarding the HAZ, the observed harness has some advantages and disadvantages, being this good for the punching tools, since they will not wear faster. However, the opposite happens to the produced parts that will wear faster and can be a problem for a production part, whereby it is more recommended to produce prototypes rather than production parts.

Regarding the cutting speed, it was not observed any accuracy difference between the tests performed at different cutting speeds, meaning that with the used laser cutting machine, there is still room to increase the cutting speed, in order to reduce production times. The same can be said about the burr dimension since the only test performed with the higher assist gas pressure translated in a significant decrease of burr.

One aspect that may have had a big impact on the cut quality, more specifically on the burr and on the HAZ was the insufficient fixation of the metal sheet that allowed the metal sheet to bend changing the focal point position less effective position.

Answering the main question which is if it is feasible to produce prototypes of the Ultron Guard by combining laser cutting with cold forming, it is possible to produce prototypes of the Ultron Guard, however, not with the performed samples but, as mentioned before, using an improved laser path.

5.2 Limitations and suggestions for future research

As previously mentioned, the present work was performed during the pandemic situation. This led to some limitations, especially related to the practical work being that most of it had to be carried out near the end of the internship.

In the beginning of the internship, it was pretended to do a design of experiments study to analyze and understand the influence of some cutting parameters in the cut quality. However, this was not possible to achieve since the number of performed tests had to be limited. The same happened in the analysis of the samples being that it was also limited due to the lack of time.

For these reasons it is suggested for future research:

- Perform a design of experiments study analyzing the influence of cutting parameters such as laser power, cutting speed and assist gas pressure on the cut quality;
- Perform new tests using an improved laser path and analyze its accuracy;
- Perform new tests with new parameters in order to improve the quality of the smaller features;
- Perform new tests using a fixation mechanism similar to a prototyped mechanism and analyze its repeatability.

BIBLIOGRAPHY

6 BIBLIOGRAPHY

Abbas, A. (2014). *Master's thesis: Optimization of parameters of laser non-linear inclined cutting on stainless steel metal.* Malaysia: Master of Mechanical Engineering at Faculty of Mechanical and Manufacturing Engineering. https://doi.org/10.13140/RG.2.2.13197.95209

Amaral, I., Silva, F. J. G., Pinto, G. F. L., Campilho, R. D. S., & Gouveia, R. M. (2019). Improving the Cut Surface Quality by Optimizing Parameters in the Fibre Laser Cutting Process. *Procedia Manufacturing, 38*, 1111-1120. https://doi.org/10.1016/j.promfg.2020.01.199

Amorim, J. P. (2016). *Dissertação de Mestrado: Soldadura laser do aço dual-phase 1000*. Aveiro: Departamento de Engenharia Mecânica da Universidade de Aveiro. Disponível em: http://hdl.handle.net/10773/17954.

Arunachalam, G. K. (2018). *Metal forming processes with analysis*. Disponível em: https://www.slideshare.net/GKArunachalam1/metal-forming-processes-with-analysis.

Bell Laser. (2020). *Laser cutting parameters*. Retrieved from: https://cdn.thomasnet.com/ccp/30498769/185895.pdf.

Bergström, D., Powell, J., & Kaplan, A. (2007). The absorptance of steels to Nd:YLF and Nd:YAG laser light at room temperature. *Applied Surface Science, 253*(11), 5017-5028. https://doi.org/10.1016/j.apsusc.2006.11.018

Berkmanns, I., & Faerber, I. (2008). *Laser cutting Laserline® Technical*. Retrieved from: https://www.boconline.co.uk/en/images/laser-cutting_tcm410-39553.pdf.

Bhatt, A. (2012). Insight – How Eletric Beard Trimmer Works. Retrieved from: https://www.engineersgarage.com/insight/insight-how-electric-beard-trimmer-works/.

Caristan, C. L. (2004). *Laser Cutting Guide for Manufacturing* (1st Edition). Dearborn, Michigan: Society of Manufacturing Engineers. ISBN: 0-87263-686-0.

Conrado, R. D. (2014). *Dissertação de Mestrado: Efeitos do corte por laser sobre a integridade superficial de um aço médio carbono.* Brasil: Programa de Pós-Graduação em Engenharia Mecânica da Universidade de Caxias do Sul. Disponível

em: https://repositorio.ucs.br/handle/11338/877.

Cordeiro, I. J. (2016). *Dissertação de Mestrado: Desgaste de ferramentas em operações de conformação plástica de chapas com aços de alta resistência*. Porto: Mestrado Integrado em Engenharia Mecânica na Faculdade de Engenharia da Universidade do Porto. Disponível em: https://repositorio-aberto.up.pt/handle/10216/85517.

Eltawahni, H. A., Hagino, M., Benyounis, K. Y., Inoue, T., & Olabi, A. G. (2012). Effect of CO_2 laser cutting process parameters on edge quality and operating cost of AISI316L. *Optics & Laser Technology, 44*(4), 1068-1082. https://doi.org/10.1016/j.optlastec.2011.10.008

Encerrabodes, A. M. (2018). *Master's thesis: Specification and Design of a Measuring System for Spring Systems in Cold Form Tooling*. Porto: Mechanical Engineering Department at the ISEP - School of Engineering. Retrieved from: http://hdl.handle.net/10400.22/13835

Faro, T. M. (2006). *Dissertação de Mestrado: Estudo e Optimização do Corte Laser de Alta Velocidade em Chapa Metálica Fina.* Porto: Mestrado em Engenharia Mecânica (Área de Especialização em Materiais e Processos de Fabrico) na Faculdade de Engenharia da Universidade do Porto. Disponível em: http://hdl.handle.net/10216/11467.

Ferreira, A. T. (2017). *Dissertação de Mestrado: Otimização de Planilhas de corte Laser Fibra 2kW com cabeçote 2D.* Aveiro: Departamento de Engenharia Mecânica na Universidade de Aveiro. Disponível em: http://hdl.handle.net/10773/23690.

Gerck, E., & Lima, J. (1997). O corte a laser: da teoria à máquina (tutorial). *'97 International Seminar "Láseres: usos y aplicaciones industriales*": Instituto Nacional de Investicaciones Nucleares, México.

Ghany, K. A., & Newishy, M. (2005). Cutting of 1.2 mm thick austenitic stainless steel sheet using pulsed and CW Nd:YAG laser. *Journal of Materials Processing Technology, 168*, 438-447. https://doi.org/10.1016/j.jmatprotec.2005.02.251

Gomes, T., Silva, F. J. G., Campilho, R. D. S. G. (2017). Reducing the simulation cost on dual-phase steel stamping process. *Procedia Manufacturing*, 11, 474-481. https://doi.org/1 0.1016/j.promfg.2017.07.138

Hashemzadeh, M. (2014). *PhD thesis: Investigations into fibre laser cutting*. Nottingham: Department of Mechanical, Materials and Manufacturing Engineering at University of Nottingham. Retrieved from: http://eprints.nottingham.ac.uk/id/eprint/14057.

Junior, D. F., Ventrella, V. A., & Gallego, J. (2016). Microfuração com laser pulsado Nd:YAG em chapas de aço inoxidável AISI 316L. *Congresso Brasileiro de Engenharia*

e Ciências dos Materiais, Brasil, 7259-7315. Disponível em: https://www.feis.unesp.br/Home/departamentos/engenhariamecanica/maprotec/cbecimat2016h.pdf.

Kellens, K., Rodrigues, G. C., Dewulf, W., & Duflou, J. R. (2014). Energy and Resource Efficiency of Laser Cutting Processes. *Physics Procedia, 56*, 854-864. https://doi.org/10.1016/j.phpro.2014.08.104

Kheloufi, K., & Amara, E. (2014). CFD Study on the Role of Gas Friction on the Molten Layer Shape and Melt Removal Mechanism in Laser Cutting Process of Steel. *Advanced Materials Research, 856,* 220-225. https://doi.org/10.4028/www.scientific.net/AMR.856.220

Kleine, K. F., Whitney, B., & Watkins, K. G. (2002). Use of fiber lasers for micro cutting applications in the medical device industry. *ICALEO, 70*. https://doi.org/10.2351/1.5065757

Kumar, V. S., & Jayaprakash, G. (2017). State of Art of Laser Cutting Process. *International Journal for Modern Trends in Science and Technology, 3(*4), 76-80. Retrieved from: https://ijmtst.com/vol3issue4/IJMTSTTRP1113.pdf.

Lazov, L., Deneva, H., & Narica, P. (2015). A task for laser cutting of lamellae with TruLaser 1030. *Environment Technology Resources Proceedings of the International Scientific and Practical Conference, 1*, 96-101. https://doi.org/10.17770/etr2015vol1.222

Li, J. (2018). *PhD Thesis: Advanced laser beam shaping using spatial light modulators for material surface processing*. Liverpool: Doctor of Philosopy at School of Engineering. https://doi.org/10.17638/03022554

Liu, Q., Duan, X., & Peng, C. (2014). *Novel Optical Technologies for Nanofabrication*. Berlin: Springer. https://doi.org/10.1007/978-3-642-40387-3

Lv, S. J., Wang, Y., & Ji, S. (2006). Quality Analysis of Pulsed Laser Cutting of Superalloy Sheet. *Key Engineering Materials*, *315-316*, 113-117. https://doi.org/10.4028/www.scientific.net/KEM.315-316.113

Madić, M., Mladenović, S., Gostimirović, M., Radovanović, M., & Janković, P. (2020). Laser cutting optimization model with constraints: Maximization of material removal rate in CO_2 laser cutting of mild steel. *Journal of Engineering Manufacture*, 1-10. https://doi.org/10.1177%2F0954405420911529

Madić, M., & Radovanović, M. (2012). Analysis of the heat affected zone in CO_2 laser cutting of stainless steel. *Thermal Science, 16*(2), 363-373. https://doi.org/10.2298/TSCI120424175M

Majumdar, J. D., & Manna, I. (2003). Laser processing of materials. *Sadhana, 28*(3), 495-562. https://doi.org/10.1007/BF02706446

Makich, H., Carpentier, L., Monteil, G., Roizard, X., Chambert, J., & Picart, P. (2008). Metrology of the burr amount - correlation with blanking operation parameters (blanked material – wear of the punch). *International Journal of Material Forming, 1*, 1243-1246. https://doi.org/10.1007/s12289-008-0167-0

Miraoui, I., Boujelbene, M., & Bayraktar, E. (2013). Effects of Laser Cutting Main Parameters on Microhardness and Microstructure Changes of Stainless Steel. *Advanced Materials Research, 664*, 881-816. https://doi.org/10.4028/www.scientific.net/AMR.664.811

Miraoui, I., Boujelbene, M., & Zaied, M. (2016). High-Power Laser Cutting of Steel Plates: Heat Affected Zone Analysis. *Advances in Materials Science and Engineering, 2016*. https://doi.org/10.1155/2016/1242565

Moreira, B. G. (2018). *Dissertação de Mestrado: Análise numérica de corte e estampagem em punçonadora.* Porto: Departamento de Engenharia Mecânica no Instituto Superior de Engenharia do Porto. Disponível em: http://hdl.handle.net/10400.22/13840.

Muhammad, N. (2012). *PhD thesis: Laser micromachining of coronary stents for medical applications.* Manchester: Doctor of Philosophy at Faculty of Engineering and Physical Sciences. Retrieved from: https://ethos.bl.uk/OrderDetails.do?uin=uk.bl.ethos.559334.

Patel, U. V., & Sanghavi, S. M. (2014). Parametric Analysis of Process Parameters of Laser Cutting Machine (Mazak Hyper Gear 510) By Using Anova Method On SS 304. *International Journal of Engineering Sciences & Research Technology, 3*(4), 3007-3011.

Patel, Y., Varsi, A., & Marathe, S. (2016). Experimental Investigation of Process Parameters of Fibre Laser on Cutting Quality of Stainless Steel 304 – A review. *International Journal of Advance Research in Engineering, Science & Technology, 3*(4), 550-555. ISSN: 2393-9877.

Pocorni, J. K., Powell, J., Ilar, T., Schwarz, A., & Kaplan, A. F. (2013). Measuring the state-of-the-art in laser cut quality. *14th Nordic Laser Materials Processing Conference*, 101-108.

Powell, J., & Kaplan, A. (2004). Laser cutting: From first principles to the state of the art. *1st Pacific International Conference on Application of Lasers and Optics 2004*. https://doi.org/10.2351/1.5056075

Rajaram, N., Sheikh-Ahmad, J., & Cheraghi, S. H. (2003). CO_2 laser cut quality of 4130 steel. *International Journal of Machine Tools & Manufacture, 43*(4), 351-358. https://doi.org/10.1016/S0890-6955(02)00270-5

Rodrigues, J., & Martins, P. (2010). *Tecnologia Mecânica – Tecnologia da Deformação Plástica – Vol. I Fundamentos Teóricos* (2ª Edição). Lisboa: Escolar Editora. ISBN: 9789725922798.

Selvan, C. P., Rammohan, N., & Sachidananda, H. K. (2015). Laser Beam Machining: A Literature Review on Heat affected Zones, Cut Quality and Comparative Study. *European Journal of Advances in Engineering and Technology, 2(*10), 70-76.

Sharp, T. (2019). *What Is an Atom?* Retrieved from: https://www.livescience.com/37206-atom-definition.html.

Sheng, P. S., & Joshi, V. S. (1995). Analysis of heat-affected zone formation for laser cutting of stainless steel. *Journal of Materials Processing Technology, 53*, 879-892. https://doi.org/10.1016/0924-0136(94)01761-O

Silva, C. R. M., Silva, F. J. G., Gouveia, R. M. (2018). Investigation on the edge crack defect in Dual-Phase steel stamping process. Procedia Manufacturing, 17, 737-745. https://doi.org/10 .1016/j.promfg.2018.10.124

Silva, M. E. (2008). *Relatório do Projeto Final: Instalação, teste e lançamento em exploração de equipamento de corte por laser.* Porto: Mestrado Integrado em Engenharia Mecânica na Faculdade de Engenharia da Universidade do Porto. Disponível em: http://hdl.handle.net/10216/58974.

Stelzer, S., Mahrle, A., Wetzig, A., & Beyer, E. (2013). Experimental investigations on fusion cutting stainless steel with fiber and CO_2 laser beams. *Physics Procedia, 41*, 399-404. https://doi.org/10.1016/j.phpro.2013.03.093

Tschaetsch, H. (2005). *Metal Forming Practise: Processes – Machines – Tools*. Berlin: Springer. ISBN: 3-540-33216-2.

Wandera, C. (2006). *Master's thesis: Laser Cutting of Austenitic Steel with a High Quality Laser Beam.* Finland: Department of Mechanical Engineering at Lappeenranta University of Technology. Retrieved from: http://urn.fi/URN:NBN:fi-fe20061326.

Wardhana, B. S., Anam, K., Ogana, R. M., & Kurniawan, A. (2019). Laser Cutting Parameters Effect on 316L Stainless Steel Surface. *International Conference on Mechanical Engineering Research and Application, 494*(1). https://doi.org/10.1088/1757-899X/494/1/012041

ANNEXES

7 ANNEXES

7.1 Annex 1- Sample 1 test 1 report

Control View

Control View Name	control view 1
Units	Millimeters
Coordinate Systems	world
Data Alignments	best-fit to ref 3
All Statistics	Total: 58, Measured: 58 (100.0000%), Pass: 42 (72.4138%), Fail: 16 (27.5862%), Warning: 0 (0.0000%)

Char No.	Object Name	Control	Nom	Meas	Tol	Dev	Test	Out Tol
	circle 5	Diameter	2.0000	1.9809	±0.0200	-0.0191	Pass	
	circle 5	X	18.5000	18.5011	±0.0200	0.0011	Pass	
	circle 5	Y	55.4000	55.4015	±0.0200	0.0015	Pass	
	circle 5	Z	0.0000	0.0000	±1.0000	0.0000	Pass	
	circle 6	Diameter	2.0000	1.9789	±0.0200	-0.0211	Fail	-0.0011
	circle 6	X	18.5000	18.4859	±0.0200	-0.0141	Pass	
	circle 6	Y	18.4000	18.4158	±0.0200	0.0158	Pass	
	circle 6	Z	0.0000	0.0000	±1.0000	0.0000	Pass	
	distance 1	3D Distance	37.0000	36.9857	±0.0200	-0.0143	Pass	
	circle 7	Diameter	2.0000	1.9694	±0.0200	-0.0306	Fail	-0.0106
	circle 7	X	-18.5000	-18.5027	±0.0200	-0.0027	Pass	
	circle 7	Y	18.4000	18.3940	±0.0200	-0.0060	Pass	
	circle 7	Z	0.0000	0.0000	±1.0000	0.0000	Pass	
	circle 8	Diameter	2.0000	1.9694	±0.0200	-0.0306	Fail	-0.0106
	circle 8	X	-18.5000	-18.4821	±0.0200	0.0179	Pass	
	circle 8	Y	55.4000	55.3873	±0.0200	-0.0127	Pass	
	circle 8	Z	0.0000	0.0000	±1.0000	0.0000	Pass	
	distance 2	3D Distance	37.0000	36.9932	±0.0200	-0.0068	Pass	
	distance 3	3D Distance	37.0000	36.9886	±0.0200	-0.0114	Pass	
	distance 4	3D Distance	37.0000	36.9833	±0.0200	-0.0167	Pass	
	distance 5	3D Distance	35.2000	35.2357	±0.0200	0.0357	Fail	0.0157
	distance 6	3D Distance	32.6000	32.5895	±0.0200	-0.0105	Pass	
	distance 7	3D Distance	32.6000	32.5914	±0.0200	-0.0086	Pass	
	distance 8	3D Distance	32.6000	32.5989	±0.0200	-0.0011	Pass	
	distance 9	3D Distance	32.6000	32.5932	±0.0200	-0.0068	Pass	
	circle 11	Diameter	0.2000	0.1704	±0.0200	-0.0296	Fail	-0.0096
	circle 11	X	0.0000	0.0236	±0.0200	0.0236	Fail	0.0036
	circle 11	Y	55.8500	55.8430	±0.0200	-0.0070	Pass	
	circle 11	Z	0.0000	0.0000	±1.0000	0.0000	Pass	
	circle 13	Diameter	0.2000	0.1690	±0.0200	-0.0310	Fail	-0.0110
	circle 13	X	0.0000	0.0121	±0.0200	0.0121	Pass	
	circle 13	Y	18.8500	18.8460	±0.0200	-0.0040	Pass	
	circle 13	Z	0.0000	0.0000	±1.0000	0.0000	Pass	
	circle 15	Diameter	0.4000	0.3935	±0.0200	-0.0065	Pass	

Organization:	Part name:
Operator:	Part number:
E-mail:	Piece: piece 1

circle 15	X	0.0000	0.0022	±0.0200	0.0022	Pass	
circle 15	Y	23.1500	23.1562	±0.0200	0.0062	Pass	
circle 15	Z	0.0000	0.0000	±1.0000	0.0000	Pass	
circle 17	Diameter	0.4000	0.3927	±0.0200	-0.0073	Pass	
circle 17	X	0.0000	0.0192	±0.0200	0.0192	Pass	
circle 17	Y	60.1500	60.1463	±0.0200	-0.0037	Pass	
circle 17	Z	0.0000	0.0000	±1.0000	0.0000	Pass	
distance 10	3D Distance	72.2000	72.2166	±0.0200	0.0166	Pass	
distance 11	3D Distance	16.3000	16.3143	±0.0200	0.0143	Pass	
distance 12	3D Distance	16.3000	16.3256	±0.0200	0.0256	Fail	0.0056
distance 13	3D Distance	18.9500	18.9911	±0.0200	0.0411	Fail	0.0211
distance 14	3D Distance	23.2500	23.3011	±0.0200	0.0511	Fail	0.0311
distance 15	3D Distance	23.2500	23.2444	±0.0200	-0.0056	Pass	
distance 16	3D Distance	18.9500	18.9411	±0.0200	-0.0089	Pass	
distance 17	3D Distance	16.3000	16.3124	±0.0200	0.0124	Pass	
distance 18	3D Distance	16.3000	16.3221	±0.0200	0.0221	Fail	0.0021
distance 19	3D Distance	32.6000	32.5932	±0.0200	-0.0068	Pass	
distance 20	3D Distance	35.2000	35.1996	±0.0200	-0.0004	Pass	
distance 21	3D Distance	32.6000	32.5895	±0.0200	-0.0105	Pass	
distance 22	3D Distance	35.2000	35.2351	±0.0200	0.0351	Fail	0.0151
distance 23	3D Distance	0.3000	0.2685	±0.0200	-0.0315	Fail	-0.0115
distance 24	3D Distance	0.3000	0.2688	±0.0200	-0.0312	Fail	-0.0112
distance 25	3D Distance	21.1000	21.1511	±0.0200	0.0511	Fail	0.0311
distance 26	3D Distance	58.1000	58.1433	±0.0200	0.0433	Fail	0.0233

Organization:	Part name:
Operator:	Part number:
E-mail:	Piece: piece 1

7.2 Annex 2- Sample 2 test 1 report

Control View

Control View Name	control view 1
Units	Millimeters
Coordinate Systems	world
Data Alignments	best-fit to ref 3
All Statistics	Total: 58, Measured: 58 (100.0000%), Pass: 43 (74.1379%), Fail: 15 (25.8621%), Warning: 0 (0.0000%)

Char No.	Object Name	Control	Nom	Meas	Tol	Dev	Test	Out Tol
	circle 5	Diameter	2.0000	1.9782	±0.0200	-0.0218	Fail	-0.0018
	circle 5	X	18.5000	18.4957	±0.0200	-0.0043	Pass	
	circle 5	Y	55.4000	55.3946	±0.0200	-0.0054	Pass	
	circle 5	Z	0.0000	0.0000	±1.0000	0.0000	Pass	
	circle 6	Diameter	2.0000	1.9785	±0.0200	-0.0215	Fail	-0.0015
	circle 6	X	18.5000	18.4912	±0.0200	-0.0088	Pass	
	circle 6	Y	18.4000	18.4134	±0.0200	0.0134	Pass	
	circle 6	Z	0.0000	0.0000	±1.0000	0.0000	Pass	
	distance 1	3D Distance	37.0000	36.9813	±0.0200	-0.0187	Pass	
	circle 7	Diameter	2.0000	1.9650	±0.0200	-0.0350	Fail	-0.0150
	circle 7	X	-18.5000	-18.4962	±0.0200	0.0038	Pass	
	circle 7	Y	18.4000	18.4065	±0.0200	0.0065	Pass	
	circle 7	Z	0.0000	0.0000	±1.0000	0.0000	Pass	
	circle 8	Diameter	2.0000	1.9686	±0.0200	-0.0314	Fail	-0.0114
	circle 8	X	-18.5000	-18.4839	±0.0200	0.0161	Pass	
	circle 8	Y	55.4000	55.3885	±0.0200	-0.0115	Pass	
	circle 8	Z	0.0000	0.0000	±1.0000	0.0000	Pass	
	distance 2	3D Distance	37.0000	36.9820	±0.0200	-0.0180	Pass	
	distance 3	3D Distance	37.0000	36.9874	±0.0200	-0.0126	Pass	
	distance 4	3D Distance	37.0000	36.9796	±0.0200	-0.0204	Fail	-0.0004
	distance 5	3D Distance	35.2000	35.2087	±0.0200	0.0087	Pass	
	distance 6	3D Distance	32.6000	32.5933	±0.0200	-0.0067	Pass	
	distance 7	3D Distance	32.6000	32.5912	±0.0200	-0.0088	Pass	
	distance 8	3D Distance	32.6000	32.5971	±0.0200	-0.0029	Pass	
	distance 9	3D Distance	32.6000	32.5968	±0.0200	-0.0032	Pass	
	circle 11	Diameter	0.2000	0.1682	±0.0200	-0.0318	Fail	-0.0118
	circle 11	X	0.0000	0.0181	±0.0200	0.0181	Pass	
	circle 11	Y	55.8500	55.8382	±0.0200	-0.0118	Pass	
	circle 11	Z	0.0000	0.0000	±1.0000	0.0000	Pass	
	circle 13	Diameter	0.2000	0.1649	±0.0200	-0.0351	Fail	-0.0151
	circle 13	X	0.0000	0.0129	±0.0200	0.0129	Pass	
	circle 13	Y	18.8500	18.8499	±0.0200	-0.0001	Pass	
	circle 13	Z	0.0000	0.0000	±1.0000	0.0000	Pass	
	circle 15	Diameter	0.4000	0.3844	±0.0200	-0.0156	Pass	

Organization:	Part name:
Operator:	Part number:
E-mail:	Piece: piece 1

circle 15	X	0.0000	0.0106	±0.0200	0.0106	Pass	
circle 15	Y	23.1500	23.1593	±0.0200	0.0093	Pass	
circle 15	Z	0.0000	0.0000	±1.0000	0.0000	Pass	
circle 17	Diameter	0.4000	0.3913	±0.0200	-0.0087	Pass	
circle 17	X	0.0000	0.0173	±0.0200	0.0173	Pass	
circle 17	Y	60.1500	60.1430	±0.0200	-0.0070	Pass	
circle 17	Z	0.0000	0.0000	±1.0000	0.0000	Pass	
distance 10	3D Distance	72.2000	72.1938	±0.0200	-0.0062	Pass	
distance 11	3D Distance	16.3000	16.3149	±0.0200	0.0149	Pass	
distance 12	3D Distance	16.3000	16.3201	±0.0200	0.0201	Fail	0.0001
distance 13	3D Distance	18.9500	19.0023	±0.0200	0.0523	Fail	0.0323
distance 14	3D Distance	23.2500	23.3116	±0.0200	0.0616	Fail	0.0416
distance 15	3D Distance	23.2500	23.2743	±0.0200	0.0243	Fail	0.0043
distance 16	3D Distance	18.9500	18.9696	±0.0200	0.0196	Pass	
distance 17	3D Distance	16.3000	16.3129	±0.0200	0.0129	Pass	
distance 18	3D Distance	16.3000	16.3152	±0.0200	0.0152	Pass	
distance 19	3D Distance	32.6000	32.5973	±0.0200	-0.0027	Pass	
distance 20	3D Distance	35.2000	35.2009	±0.0200	0.0009	Pass	
distance 21	3D Distance	32.6000	32.5934	±0.0200	-0.0066	Pass	
distance 22	3D Distance	35.2000	35.2081	±0.0200	0.0081	Pass	
distance 23	3D Distance	0.3000	0.2679	±0.0200	-0.0321	Fail	-0.0121
distance 24	3D Distance	0.3000	0.2691	±0.0200	-0.0309	Fail	-0.0109
distance 25	3D Distance	21.1000	21.1574	±0.0200	0.0574	Fail	0.0374
distance 26	3D Distance	58.1000	58.1440	±0.0200	0.0440	Fail	0.0240

Organization:	Part name:
Operator:	Part number:
E-mail:	Piece: piece 1

7.3 Annex 3- Sample 3 test 1 report

Control View

Control View Name	control view 1
Units	Millimeters
Coordinate Systems	world
Data Alignments	best-fit to ref 3
All Statistics	Total: 58, Measured: 58 (100.0000%), Pass: 47 (81.0345%), Fail: 11 (18.9655%), Warning: 0 (0.0000%)

Char No.	Object Name	Control	Nom	Meas	Tol	Dev	Test	Out Tol
	circle 5	Diameter	2.0000	1.9783	±0.0200	-0.0217	Fail	-0.0017
	circle 5	X	18.5000	18.5015	±0.0200	0.0015	Pass	
	circle 5	Y	55.4000	55.3965	±0.0200	-0.0035	Pass	
	circle 5	Z	0.0000	0.0000	±1.0000	0.0000	Pass	
	circle 6	Diameter	2.0000	1.9780	±0.0200	-0.0220	Fail	-0.0020
	circle 6	X	18.5000	18.4820	±0.0200	-0.0180	Pass	
	circle 6	Y	18.4000	18.4189	±0.0200	0.0189	Pass	
	circle 6	Z	0.0000	0.0000	±1.0000	0.0000	Pass	
	distance 1	3D Distance	37.0000	36.9776	±0.0200	-0.0224	Fail	-0.0024
	circle 7	Diameter	2.0000	1.9652	±0.0200	-0.0348	Fail	-0.0148
	circle 7	X	-18.5000	-18.5011	±0.0200	-0.0011	Pass	
	circle 7	Y	18.4000	18.4040	±0.0200	0.0040	Pass	
	circle 7	Z	0.0000	0.0000	±1.0000	0.0000	Pass	
	circle 8	Diameter	2.0000	1.9694	±0.0200	-0.0306	Fail	-0.0106
	circle 8	X	-18.5000	-18.4903	±0.0200	0.0097	Pass	
	circle 8	Y	55.4000	55.3848	±0.0200	-0.0152	Pass	
	circle 8	Z	0.0000	0.0000	±1.0000	0.0000	Pass	
	distance 2	3D Distance	37.0000	36.9808	±0.0200	-0.0192	Pass	
	distance 3	3D Distance	37.0000	36.9832	±0.0200	-0.0168	Pass	
	distance 4	3D Distance	37.0000	36.9917	±0.0200	-0.0083	Pass	
	distance 5	3D Distance	35.2000	35.2150	±0.0200	0.0150	Pass	
	distance 6	3D Distance	32.6000	32.6000	±0.0200	0.0000	Pass	
	distance 7	3D Distance	32.6000	32.5928	±0.0200	-0.0072	Pass	
	distance 8	3D Distance	32.6000	32.5974	±0.0200	-0.0026	Pass	
	distance 9	3D Distance	32.6000	32.5974	±0.0200	-0.0026	Pass	
	circle 11	Diameter	0.2000	0.1671	±0.0200	-0.0329	Fail	-0.0129
	circle 11	X	0.0000	0.0143	±0.0200	0.0143	Pass	
	circle 11	Y	55.8500	55.8390	±0.0200	-0.0110	Pass	
	circle 11	Z	0.0000	0.0000	±1.0000	0.0000	Pass	
	circle 13	Diameter	0.2000	0.1695	±0.0200	-0.0305	Fail	-0.0105
	circle 13	X	0.0000	0.0060	±0.0200	0.0060	Pass	
	circle 13	Y	18.8500	18.8480	±0.0200	-0.0020	Pass	
	circle 13	Z	0.0000	0.0000	±1.0000	0.0000	Pass	
	circle 15	Diameter	0.4000	0.3927	±0.0200	-0.0073	Pass	

Organization:	Part name:
Operator:	Part number:
E-mail:	Piece: piece 1

circle 15	X	0.0000	-0.0036	±0.0200	-0.0036	Pass	
circle 15	Y	23.1500	23.1605	±0.0200	0.0105	Pass	
circle 15	Z	0.0000	0.0000	±1.0000	0.0000	Pass	
circle 17	Diameter	0.4000	0.3912	±0.0200	-0.0088	Pass	
circle 17	X	0.0000	0.0125	±0.0200	0.0125	Pass	
circle 17	Y	60.1500	60.1387	±0.0200	-0.0113	Pass	
circle 17	Z	0.0000	0.0000	±1.0000	0.0000	Pass	
distance 10	3D Distance	72.2000	72.1910	±0.0200	-0.0090	Pass	
distance 11	3D Distance	16.3000	16.3106	±0.0200	0.0106	Pass	
distance 12	3D Distance	16.3000	16.3219	±0.0200	0.0219	Fail	0.0019
distance 13	3D Distance	18.9500	18.9392	±0.0200	-0.0108	Pass	
distance 14	3D Distance	23.2500	23.2516	±0.0200	0.0016	Pass	
distance 15	3D Distance	23.2500	23.2575	±0.0200	0.0075	Pass	
distance 16	3D Distance	18.9500	18.9577	±0.0200	0.0077	Pass	
distance 17	3D Distance	16.3000	16.3082	±0.0200	0.0082	Pass	
distance 18	3D Distance	16.3000	16.3145	±0.0200	0.0145	Pass	
distance 19	3D Distance	32.6000	32.5976	±0.0200	-0.0024	Pass	
distance 20	3D Distance	35.2000	35.1988	±0.0200	-0.0012	Pass	
distance 21	3D Distance	32.6000	32.6004	±0.0200	0.0004	Pass	
distance 22	3D Distance	35.2000	35.2149	±0.0200	0.0149	Pass	
distance 23	3D Distance	0.3000	0.2669	±0.0200	-0.0331	Fail	-0.0131
distance 24	3D Distance	0.3000	0.2671	±0.0200	-0.0329	Fail	-0.0129
distance 25	3D Distance	21.1000	21.1514	±0.0200	0.0514	Fail	0.0314
distance 26	3D Distance	58.1000	58.0840	±0.0200	-0.0160	Pass	

Organization:	Part name:
Operator:	Part number:
E-mail:	Piece: piece 1

circle 15	X	0.0000	-0.0036	±0.0200	-0.0036	Pass	
circle 15	Y	23.1500	23.1605	±0.0200	0.0105	Pass	
circle 15	Z	0.0000	0.0000	±1.0000	0.0000	Pass	
circle 17	Diameter	0.4000	0.3912	±0.0200	-0.0088	Pass	
circle 17	X	0.0000	0.0125	±0.0200	0.0125	Pass	
circle 17	Y	60.1500	60.1387	±0.0200	-0.0113	Pass	
circle 17	Z	0.0000	0.0000	±1.0000	0.0000	Pass	
distance 10	3D Distance	72.2000	72.1910	±0.0200	-0.0090	Pass	
distance 11	3D Distance	16.3000	16.3106	±0.0200	0.0106	Pass	
distance 12	3D Distance	16.3000	16.3219	±0.0200	0.0219	Fail	0.0019
distance 13	3D Distance	18.9500	18.9392	±0.0200	-0.0108	Pass	
distance 14	3D Distance	23.2500	23.2516	±0.0200	0.0016	Pass	
distance 15	3D Distance	23.2500	23.2575	±0.0200	0.0075	Pass	
distance 16	3D Distance	18.9500	18.9577	±0.0200	0.0077	Pass	
distance 17	3D Distance	16.3000	16.3082	±0.0200	0.0082	Pass	
distance 18	3D Distance	16.3000	16.3145	±0.0200	0.0145	Pass	
distance 19	3D Distance	32.6000	32.5976	±0.0200	-0.0024	Pass	
distance 20	3D Distance	35.2000	35.1988	±0.0200	-0.0012	Pass	
distance 21	3D Distance	32.6000	32.6004	±0.0200	0.0004	Pass	
distance 22	3D Distance	35.2000	35.2149	±0.0200	0.0149	Pass	
distance 23	3D Distance	0.3000	0.2669	±0.0200	-0.0331	Fail	-0.0131
distance 24	3D Distance	0.3000	0.2671	±0.0200	-0.0329	Fail	-0.0129
distance 25	3D Distance	21.1000	21.1514	±0.0200	0.0514	Fail	0.0314
distance 26	3D Distance	58.1000	58.0840	±0.0200	-0.0160	Pass	

Organization:	Part name:
Operator:	Part number:
E-mail:	Piece: piece 1

7.4 Annex 4- Sample 1 test 2 report

Control View

Control View Name	control view 1
Units	Millimeters
Coordinate Systems	world
Data Alignments	best-fit to ref 3
All Statistics	Total: 58, Measured: 58 (100.0000%), Pass: 47 (81.0345%), Fail: 11 (18.9655%), Warning: 0 (0.0000%)

Char No.	Object Name	Control	Nom	Meas	Tol	Dev	Test	Out Tol
	circle 5	Diameter	2.0000	1.9814	±0.0200	-0.0186	Pass	
	circle 5	X	18.5000	18.4947	±0.0200	-0.0053	Pass	
	circle 5	Y	55.4000	55.3915	±0.0200	-0.0085	Pass	
	circle 5	Z	0.0000	0.0000	±1.0000	0.0000	Pass	
	circle 6	Diameter	2.0000	1.9765	±0.0200	-0.0235	Fail	-0.0035
	circle 6	X	18.5000	18.4890	±0.0200	-0.0110	Pass	
	circle 6	Y	18.4000	18.4113	±0.0200	0.0113	Pass	
	circle 6	Z	0.0000	0.0000	±1.0000	0.0000	Pass	
	distance 1	3D Distance	37.0000	36.9801	±0.0200	-0.0199	Pass	
	circle 7	Diameter	2.0000	1.9698	±0.0200	-0.0302	Fail	-0.0102
	circle 7	X	-18.5000	-18.4982	±0.0200	0.0018	Pass	
	circle 7	Y	18.4000	18.4059	±0.0200	0.0059	Pass	
	circle 7	Z	0.0000	0.0000	±1.0000	0.0000	Pass	
	circle 8	Diameter	2.0000	1.9666	±0.0200	-0.0334	Fail	-0.0134
	circle 8	X	-18.5000	-18.4901	±0.0200	0.0099	Pass	
	circle 8	Y	55.4000	55.3900	±0.0200	-0.0100	Pass	
	circle 8	Z	0.0000	0.0000	±1.0000	0.0000	Pass	
	distance 2	3D Distance	37.0000	36.9841	±0.0200	-0.0159	Pass	
	distance 3	3D Distance	37.0000	36.9871	±0.0200	-0.0129	Pass	
	distance 4	3D Distance	37.0000	36.9847	±0.0200	-0.0153	Pass	
	distance 5	3D Distance	35.2000	35.2107	±0.0200	0.0107	Pass	
	distance 6	3D Distance	32.6000	32.5967	±0.0200	-0.0033	Pass	
	distance 7	3D Distance	32.6000	32.5929	±0.0200	-0.0071	Pass	
	distance 8	3D Distance	32.6000	32.5953	±0.0200	-0.0047	Pass	
	distance 9	3D Distance	32.6000	32.5944	±0.0200	-0.0056	Pass	
	circle 11	Diameter	0.2000	0.1738	±0.0200	-0.0262	Fail	-0.0062
	circle 11	X	0.0000	0.0191	±0.0200	0.0191	Pass	
	circle 11	Y	55.8500	55.8360	±0.0200	-0.0140	Pass	
	circle 11	Z	0.0000	0.0000	±1.0000	0.0000	Pass	
	circle 13	Diameter	0.2000	0.1708	±0.0200	-0.0292	Fail	-0.0092
	circle 13	X	0.0000	0.0134	±0.0200	0.0134	Pass	
	circle 13	Y	18.8500	18.8455	±0.0200	-0.0045	Pass	
	circle 13	Z	0.0000	0.0000	±1.0000	0.0000	Pass	
	circle 15	Diameter	0.4000	0.3939	±0.0200	-0.0061	Pass	

Organization:	Part name:
Operator:	Part number:
E-mail:	Piece: piece 1

circle 15	X	0.0000	0.0045	±0.0200	0.0045	Pass	
circle 15	Y	23.1500	23.1556	±0.0200	0.0056	Pass	
circle 15	Z	0.0000	0.0000	±1.0000	0.0000	Pass	
circle 17	Diameter	0.4000	0.3985	±0.0200	-0.0015	Pass	
circle 17	X	0.0000	0.0114	±0.0200	0.0114	Pass	
circle 17	Y	60.1500	60.1419	±0.0200	-0.0081	Pass	
circle 17	Z	0.0000	0.0000	±1.0000	0.0000	Pass	
distance 10	3D Distance	72.2000	72.1995	±0.0200	-0.0005	Pass	
distance 11	3D Distance	16.3000	16.3119	±0.0200	0.0119	Pass	
distance 12	3D Distance	16.3000	16.3253	±0.0200	0.0253	Fail	0.0053
distance 13	3D Distance	18.9500	18.9572	±0.0200	0.0072	Pass	
distance 14	3D Distance	23.2500	23.2673	±0.0200	0.0173	Pass	
distance 15	3D Distance	23.2500	23.1850	±0.0200	-0.0650	Fail	-0.0450
distance 16	3D Distance	18.9500	18.8791	±0.0200	-0.0709	Fail	-0.0509
distance 17	3D Distance	16.3000	16.3072	±0.0200	0.0072	Pass	
distance 18	3D Distance	16.3000	16.3221	±0.0200	0.0221	Fail	0.0021
distance 19	3D Distance	32.6000	32.5946	±0.0200	-0.0054	Pass	
distance 20	3D Distance	35.2000	35.2042	±0.0200	0.0042	Pass	
distance 21	3D Distance	32.6000	32.5972	±0.0200	-0.0028	Pass	
distance 22	3D Distance	35.2000	35.2097	±0.0200	0.0097	Pass	
distance 23	3D Distance	0.3000	0.2706	±0.0200	-0.0294	Fail	-0.0094
distance 24	3D Distance	0.3000	0.2698	±0.0200	-0.0302	Fail	-0.0102
distance 25	3D Distance	21.1000	21.1184	±0.0200	0.0184	Pass	
distance 26	3D Distance	58.1000	58.1026	±0.0200	0.0026	Pass	

Organization:	Part name:
Operator:	Part number:
E-mail:	Piece: piece 1

7.5 Annex 5- Sample 2 test 2 report

Control View

Control View Name	control view 1
Units	Millimeters
Coordinate Systems	world
Data Alignments	best-fit to ref 3
All Statistics	Total: 58, Measured: 58 (100.0000%), Pass: 47 (81.0345%), Fail: 11 (18.9655%), Warning: 0 (0.0000%)

Char No.	Object Name	Control	Nom	Meas	Tol	Dev	Test	Out Tol
	circle 5	Diameter	2.0000	1.9813	±0.0200	-0.0187	Pass	
	circle 5	X	18.5000	18.4928	±0.0200	-0.0072	Pass	
	circle 5	Y	55.4000	55.3975	±0.0200	-0.0025	Pass	
	circle 5	Z	0.0000	0.0000	±1.0000	0.0000	Pass	
	circle 6	Diameter	2.0000	1.9797	±0.0200	-0.0203	Fail	-0.0003
	circle 6	X	18.5000	18.4889	±0.0200	-0.0111	Pass	
	circle 6	Y	18.4000	18.4069	±0.0200	0.0069	Pass	
	circle 6	Z	0.0000	0.0000	±1.0000	0.0000	Pass	
	distance 1	3D Distance	37.0000	36.9907	±0.0200	-0.0093	Pass	
	circle 7	Diameter	2.0000	1.9723	±0.0200	-0.0277	Fail	-0.0077
	circle 7	X	-18.5000	-18.4994	±0.0200	0.0006	Pass	
	circle 7	Y	18.4000	18.4014	±0.0200	0.0014	Pass	
	circle 7	Z	0.0000	0.0000	±1.0000	0.0000	Pass	
	circle 8	Diameter	2.0000	1.9698	±0.0200	-0.0302	Fail	-0.0102
	circle 8	X	-18.5000	-18.4904	±0.0200	0.0096	Pass	
	circle 8	Y	55.4000	55.3945	±0.0200	-0.0055	Pass	
	circle 8	Z	0.0000	0.0000	±1.0000	0.0000	Pass	
	distance 2	3D Distance	37.0000	36.9931	±0.0200	-0.0069	Pass	
	distance 3	3D Distance	37.0000	36.9883	±0.0200	-0.0117	Pass	
	distance 4	3D Distance	37.0000	36.9832	±0.0200	-0.0168	Pass	
	distance 5	3D Distance	35.2000	35.2122	±0.0200	0.0122	Pass	
	distance 6	3D Distance	32.6000	32.5979	±0.0200	-0.0021	Pass	
	distance 7	3D Distance	32.6000	32.5942	±0.0200	-0.0058	Pass	
	distance 8	3D Distance	32.6000	32.5943	±0.0200	-0.0057	Pass	
	distance 9	3D Distance	32.6000	32.5940	±0.0200	-0.0060	Pass	
	circle 11	Diameter	0.2000	0.1621	±0.0200	-0.0379	Fail	-0.0179
	circle 11	X	0.0000	0.0101	±0.0200	0.0101	Pass	
	circle 11	Y	55.8500	55.8269	±0.0200	-0.0231	Fail	-0.0031
	circle 11	Z	0.0000	0.0000	±1.0000	0.0000	Pass	
	circle 13	Diameter	0.2000	0.1745	±0.0200	-0.0255	Fail	-0.0055
	circle 13	X	0.0000	0.0095	±0.0200	0.0095	Pass	
	circle 13	Y	18.8500	18.8411	±0.0200	-0.0089	Pass	
	circle 13	Z	0.0000	0.0000	±1.0000	0.0000	Pass	
	circle 15	Diameter	0.4000	0.3958	±0.0200	-0.0032	Pass	

Organization:	Part name:
Operator:	Part number:
E-mail:	Piece: piece 1

circle 15	X	0.0000	0.0033	±0.0200	0.0033	Pass	
circle 15	Y	23.1500	23.1550	±0.0200	0.0050	Pass	
circle 15	Z	0.0000	0.0000	±1.0000	0.0000	Pass	
circle 17	Diameter	0.4000	0.3962	±0.0200	-0.0038	Pass	
circle 17	X	0.0000	0.0087	±0.0200	0.0087	Pass	
circle 17	Y	60.1500	60.1441	±0.0200	-0.0059	Pass	
circle 17	Z	0.0000	0.0000	±1.0000	0.0000	Pass	
distance 10	3D Distance	72.2000	72.2066	±0.0200	0.0066	Pass	
distance 11	3D Distance	16.3000	16.3091	±0.0200	0.0091	Pass	
distance 12	3D Distance	16.3000	16.3179	±0.0200	0.0179	Pass	
distance 13	3D Distance	18.9500	18.9603	±0.0200	0.0103	Pass	
distance 14	3D Distance	23.2500	23.2741	±0.0200	0.0241	Fail	0.0041
distance 15	3D Distance	23.2500	23.2856	±0.0200	0.0356	Fail	0.0156
distance 16	3D Distance	18.9500	18.9685	±0.0200	0.0185	Pass	
distance 17	3D Distance	16.3000	16.3074	±0.0200	0.0074	Pass	
distance 18	3D Distance	16.3000	16.3106	±0.0200	0.0106	Pass	
distance 19	3D Distance	32.6000	32.5939	±0.0200	-0.0061	Pass	
distance 20	3D Distance	35.2000	35.2052	±0.0200	0.0052	Pass	
distance 21	3D Distance	32.6000	32.5979	±0.0200	-0.0021	Pass	
distance 22	3D Distance	35.2000	35.2118	±0.0200	0.0118	Pass	
distance 23	3D Distance	0.3000	0.2708	±0.0200	-0.0292	Fail	-0.0092
distance 24	3D Distance	0.3000	0.2711	±0.0200	-0.0289	Fail	-0.0089
distance 25	3D Distance	21.1000	21.1256	±0.0200	0.0256	Fail	0.0056
distance 26	3D Distance	58.1000	58.1142	±0.0200	0.0142	Pass	

Organization:	Part name:
Operator:	Part number:
E-mail:	Piece: piece 1

7.6 Annex 6- Sample 3 test 2 report

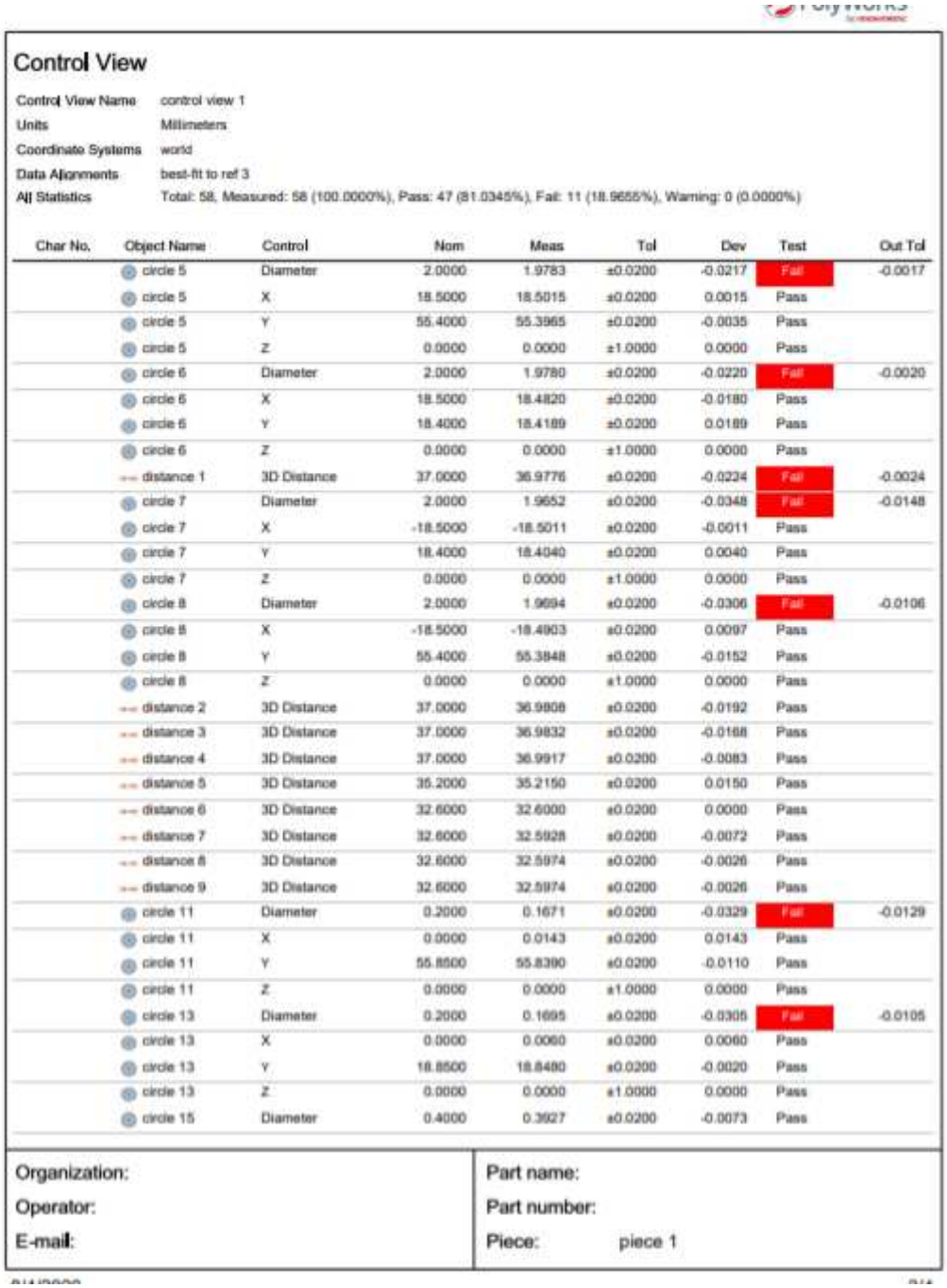

Control View

Control View Name	control view 1
Units	Millimeters
Coordinate Systems	world
Data Alignments	best-fit to ref 3
All Statistics	Total: 58, Measured: 58 (100.0000%), Pass: 47 (81.0345%), Fail: 11 (18.9655%), Warning: 0 (0.0000%)

Char No.	Object Name	Control	Nom	Meas	Tol	Dev	Test	Out Tol
	circle 5	Diameter	2.0000	1.9783	±0.0200	-0.0217	Fail	-0.0017
	circle 5	X	18.5000	18.5015	±0.0200	0.0015	Pass	
	circle 5	Y	55.4000	55.3965	±0.0200	-0.0035	Pass	
	circle 5	Z	0.0000	0.0000	±1.0000	0.0000	Pass	
	circle 6	Diameter	2.0000	1.9780	±0.0200	-0.0220	Fail	-0.0020
	circle 6	X	18.5000	18.4820	±0.0200	-0.0180	Pass	
	circle 6	Y	18.4000	18.4189	±0.0200	0.0189	Pass	
	circle 6	Z	0.0000	0.0000	±1.0000	0.0000	Pass	
	distance 1	3D Distance	37.0000	36.9776	±0.0200	-0.0224	Fail	-0.0024
	circle 7	Diameter	2.0000	1.9652	±0.0200	-0.0348	Fail	-0.0148
	circle 7	X	-18.5000	-18.5011	±0.0200	-0.0011	Pass	
	circle 7	Y	18.4000	18.4040	±0.0200	0.0040	Pass	
	circle 7	Z	0.0000	0.0000	±1.0000	0.0000	Pass	
	circle 8	Diameter	2.0000	1.9694	±0.0200	-0.0306	Fail	-0.0106
	circle 8	X	-18.5000	-18.4903	±0.0200	0.0097	Pass	
	circle 8	Y	55.4000	55.3848	±0.0200	-0.0152	Pass	
	circle 8	Z	0.0000	0.0000	±1.0000	0.0000	Pass	
	distance 2	3D Distance	37.0000	36.9808	±0.0200	-0.0192	Pass	
	distance 3	3D Distance	37.0000	36.9832	±0.0200	-0.0168	Pass	
	distance 4	3D Distance	37.0000	36.9917	±0.0200	-0.0083	Pass	
	distance 5	3D Distance	35.2000	35.2150	±0.0200	0.0150	Pass	
	distance 6	3D Distance	32.6000	32.6000	±0.0200	0.0000	Pass	
	distance 7	3D Distance	32.6000	32.5928	±0.0200	-0.0072	Pass	
	distance 8	3D Distance	32.6000	32.5974	±0.0200	-0.0026	Pass	
	distance 9	3D Distance	32.6000	32.5974	±0.0200	-0.0026	Pass	
	circle 11	Diameter	0.2000	0.1671	±0.0200	-0.0329	Fail	-0.0129
	circle 11	X	0.0000	0.0143	±0.0200	0.0143	Pass	
	circle 11	Y	55.8500	55.8390	±0.0200	-0.0110	Pass	
	circle 11	Z	0.0000	0.0000	±1.0000	0.0000	Pass	
	circle 13	Diameter	0.2000	0.1695	±0.0200	-0.0305	Fail	-0.0105
	circle 13	X	0.0000	0.0060	±0.0200	0.0060	Pass	
	circle 13	Y	18.8500	18.8480	±0.0200	-0.0020	Pass	
	circle 13	Z	0.0000	0.0000	±1.0000	0.0000	Pass	
	circle 15	Diameter	0.4000	0.3927	±0.0200	-0.0073	Pass	

Organization:	Part name:
Operator:	Part number:
E-mail:	Piece: piece 1

circle 15	X	0.0000	-0.0036	±0.0200	-0.0036	Pass	
circle 15	Y	23.1500	23.1605	±0.0200	0.0105	Pass	
circle 15	Z	0.0000	0.0000	±1.0000	0.0000	Pass	
circle 17	Diameter	0.4000	0.3912	±0.0200	-0.0088	Pass	
circle 17	X	0.0000	0.0125	±0.0200	0.0125	Pass	
circle 17	Y	60.1500	60.1387	±0.0200	-0.0113	Pass	
circle 17	Z	0.0000	0.0000	±1.0000	0.0000	Pass	
distance 10	3D Distance	72.2000	72.1910	±0.0200	-0.0090	Pass	
distance 11	3D Distance	16.3000	16.3106	±0.0200	0.0106	Pass	
distance 12	3D Distance	16.3000	16.3219	±0.0200	0.0219	Fail	0.0019
distance 13	3D Distance	18.9500	18.9392	±0.0200	-0.0108	Pass	
distance 14	3D Distance	23.2500	23.2516	±0.0200	0.0016	Pass	
distance 15	3D Distance	23.2500	23.2575	±0.0200	0.0075	Pass	
distance 16	3D Distance	18.9500	18.9577	±0.0200	0.0077	Pass	
distance 17	3D Distance	16.3000	16.3082	±0.0200	0.0082	Pass	
distance 18	3D Distance	16.3000	16.3145	±0.0200	0.0145	Pass	
distance 19	3D Distance	32.6000	32.5976	±0.0200	-0.0024	Pass	
distance 20	3D Distance	35.2000	35.1988	±0.0200	-0.0012	Pass	
distance 21	3D Distance	32.6000	32.6004	±0.0200	0.0004	Pass	
distance 22	3D Distance	35.2000	35.2149	±0.0200	0.0149	Pass	
distance 23	3D Distance	0.3000	0.2669	±0.0200	-0.0331	Fail	-0.0131
distance 24	3D Distance	0.3000	0.2671	±0.0200	-0.0329	Fail	-0.0129
distance 25	3D Distance	21.1000	21.1514	±0.0200	0.0514	Fail	0.0314
distance 26	3D Distance	58.1000	58.0840	±0.0200	-0.0160	Pass	

Organization:	Part name:
Operator:	Part number:
E-mail:	Piece: piece 1

7.7 Annex 7- Sample 1 test 3 report

Control View

Control View Name	control view 1
Units	Millimeters
Coordinate Systems	world
Data Alignments	best-fit to ref 3
All Statistics	Total: 58, Measured: 58 (100.0000%), Pass: 46 (79.3103%), Fail: 12 (20.6897%), Warning: 0 (0.0000%)

Char No.	Object Name	Control	Nom	Meas	Tol	Dev	Test	Out Tol
	circle 5	Diameter	2.0000	1.9800	±0.0200	-0.0200	Pass	
	circle 5	X	18.5000	18.5006	±0.0200	0.0006	Pass	
	circle 5	Y	55.4000	55.3918	±0.0200	-0.0082	Pass	
	circle 5	Z	0.0000	0.0000	±1.0000	0.0000	Pass	
	circle 6	Diameter	2.0000	1.9798	±0.0200	-0.0202	Fail	-0.0002
	circle 6	X	18.5000	18.4895	±0.0200	-0.0105	Pass	
	circle 6	Y	18.4000	18.4174	±0.0200	0.0174	Pass	
	circle 6	Z	0.0000	0.0000	±1.0000	0.0000	Pass	
	distance 1	3D Distance	37.0000	36.9744	±0.0200	-0.0256	Fail	-0.0056
	circle 7	Diameter	2.0000	1.9691	±0.0200	-0.0309	Fail	-0.0109
	circle 7	X	-18.5000	-18.4983	±0.0200	0.0017	Pass	
	circle 7	Y	18.4000	18.4017	±0.0200	0.0017	Pass	
	circle 7	Z	0.0000	0.0000	±1.0000	0.0000	Pass	
	circle 8	Diameter	2.0000	1.9702	±0.0200	-0.0298	Fail	-0.0098
	circle 8	X	-18.5000	-18.4923	±0.0200	0.0077	Pass	
	circle 8	Y	55.4000	55.3860	±0.0200	-0.0140	Pass	
	circle 8	Z	0.0000	0.0000	±1.0000	0.0000	Pass	
	distance 2	3D Distance	37.0000	36.9842	±0.0200	-0.0158	Pass	
	distance 3	3D Distance	37.0000	36.9878	±0.0200	-0.0122	Pass	
	distance 4	3D Distance	37.0000	36.9929	±0.0200	-0.0071	Pass	
	distance 5	3D Distance	35.2000	35.2256	±0.0200	0.0256	Fail	0.0056
	distance 6	3D Distance	32.6000	32.5948	±0.0200	-0.0052	Pass	
	distance 7	3D Distance	32.6000	32.5869	±0.0200	-0.0131	Pass	
	distance 8	3D Distance	32.6000	32.5990	±0.0200	-0.0010	Pass	
	distance 9	3D Distance	32.6000	32.5954	±0.0200	-0.0046	Pass	
	circle 11	Diameter	0.2000	0.1661	±0.0200	-0.0339	Fail	-0.0139
	circle 11	X	0.0000	0.0147	±0.0200	0.0147	Pass	
	circle 11	Y	55.8500	55.8360	±0.0200	-0.0140	Pass	
	circle 11	Z	0.0000	0.0000	±1.0000	0.0000	Pass	
	circle 13	Diameter	0.2000	0.1532	±0.0200	-0.0468	Fail	-0.0268
	circle 13	X	0.0000	0.0066	±0.0200	0.0066	Pass	
	circle 13	Y	18.8500	18.8430	±0.0200	-0.0070	Pass	
	circle 13	Z	0.0000	0.0000	±1.0000	0.0000	Pass	
	circle 15	Diameter	0.4000	0.3891	±0.0200	-0.0109	Pass	

Organization:	Part name:
Operator:	Part number:
E-mail:	Piece: piece 1

circle 15	X	0.0000	0.0068	±0.0200	0.0068	Pass	
circle 15	Y	23.1500	23.1572	±0.0200	0.0072	Pass	
circle 15	Z	0.0000	0.0000	±1.0000	0.0000	Pass	
circle 17	Diameter	0.4000	0.3914	±0.0200	-0.0086	Pass	
circle 17	X	0.0000	0.0104	±0.0200	0.0104	Pass	
circle 17	Y	60.1500	60.1394	±0.0200	-0.0106	Pass	
circle 17	Z	0.0000	0.0000	±1.0000	0.0000	Pass	
distance 10	3D Distance	72.2000	72.1984	±0.0200	-0.0016	Pass	
distance 11	3D Distance	16.3000	16.3122	±0.0200	0.0122	Pass	
distance 12	3D Distance	16.3000	16.3151	±0.0200	0.0151	Pass	
distance 13	3D Distance	18.9500	18.9451	±0.0200	-0.0049	Pass	
distance 14	3D Distance	23.2500	23.2593	±0.0200	0.0093	Pass	
distance 15	3D Distance	23.2500	23.2777	±0.0200	0.0277	Fail	0.0077
distance 16	3D Distance	18.9500	18.9743	±0.0200	0.0243	Fail	0.0043
distance 17	3D Distance	16.3000	16.3020	±0.0200	0.0020	Pass	
distance 18	3D Distance	16.3000	16.3120	±0.0200	0.0120	Pass	
distance 19	3D Distance	32.6000	32.5963	±0.0200	-0.0037	Pass	
distance 20	3D Distance	35.2000	35.1986	±0.0200	-0.0014	Pass	
distance 21	3D Distance	32.6000	32.5949	±0.0200	-0.0051	Pass	
distance 22	3D Distance	35.2000	35.2255	±0.0200	0.0255	Fail	0.0055
distance 23	3D Distance	0.3000	0.2732	±0.0200	-0.0268	Fail	-0.0068
distance 24	3D Distance	0.3000	0.2717	±0.0200	-0.0283	Fail	-0.0083
distance 25	3D Distance	21.1000	21.1143	±0.0200	0.0143	Pass	
distance 26	3D Distance	58.1000	58.0939	±0.0200	-0.0061	Pass	

Organization:	Part name:
Operator:	Part number:
E-mail:	Piece: piece 1

7.8 Annex 7- Sample 2 test 3 report

Control View

Control View Name	control view 1
Units	Millimeters
Coordinate Systems	world
Data Alignments	best-fit to ref 3
All Statistics	Total: 58, Measured: 58 (100.0000%), Pass: 41 (70.6897%), Fail: 17 (29.3103%), Warning: 0 (0.0000%)

Char No.	Object Name	Control	Nom	Meas	Tol	Dev	Test	Out Tol
	circle 5	Diameter	2.0000	1.9800	±0.0200	-0.0200	Pass	
	circle 5	X	18.5000	18.4852	±0.0200	-0.0148	Pass	
	circle 5	Y	55.4000	55.3891	±0.0200	-0.0109	Pass	
	circle 5	Z	0.0000	0.0000	±1.0000	0.0000	Pass	
	circle 6	Diameter	2.0000	1.9789	±0.0200	-0.0211	Fail	-0.0011
	circle 6	X	18.5000	18.4971	±0.0200	-0.0029	Pass	
	circle 6	Y	18.4000	18.3966	±0.0200	-0.0034	Pass	
	circle 6	Z	0.0000	0.0000	±1.0000	0.0000	Pass	
	distance 1	3D Distance	37.0000	36.9926	±0.0200	-0.0074	Pass	
	circle 7	Diameter	2.0000	1.9708	±0.0200	-0.0292	Fail	-0.0092
	circle 7	X	-18.5000	-18.4908	±0.0200	0.0092	Pass	
	circle 7	Y	18.4000	18.4161	±0.0200	0.0161	Pass	
	circle 7	Z	0.0000	0.0000	±1.0000	0.0000	Pass	
	circle 8	Diameter	2.0000	1.9696	±0.0200	-0.0304	Fail	-0.0104
	circle 8	X	-18.5000	-18.5011	±0.0200	-0.0011	Pass	
	circle 8	Y	55.4000	55.3987	±0.0200	-0.0013	Pass	
	circle 8	Z	0.0000	0.0000	±1.0000	0.0000	Pass	
	distance 2	3D Distance	37.0000	36.9825	±0.0200	-0.0175	Pass	
	distance 3	3D Distance	37.0000	36.9879	±0.0200	-0.0121	Pass	
	distance 4	3D Distance	37.0000	36.9864	±0.0200	-0.0136	Pass	
	distance 5	3D Distance	35.2000	35.2148	±0.0200	0.0148	Pass	
	distance 6	3D Distance	32.6000	32.5938	±0.0200	-0.0062	Pass	
	distance 7	3D Distance	32.6000	32.5910	±0.0200	-0.0090	Pass	
	distance 8	3D Distance	32.6000	32.5978	±0.0200	-0.0022	Pass	
	distance 9	3D Distance	32.6000	32.5936	±0.0200	-0.0064	Pass	
	circle 11	Diameter	0.2000	0.1704	±0.0200	-0.0296	Fail	-0.0096
	circle 11	X	0.0000	0.0521	±0.0200	0.0521	Fail	0.0321
	circle 11	Y	55.8500	55.8361	±0.0200	-0.0139	Pass	
	circle 11	Z	0.0000	0.0000	±1.0000	0.0000	Pass	
	circle 13	Diameter	0.2000	0.1661	±0.0200	-0.0339	Fail	-0.0139
	circle 13	X	0.0000	0.0181	±0.0200	0.0181	Pass	
	circle 13	Y	18.8500	18.8454	±0.0200	-0.0046	Pass	
	circle 13	Z	0.0000	0.0000	±1.0000	0.0000	Pass	
	circle 15	Diameter	0.4000	0.3915	±0.0200	-0.0085	Pass	

Organization:	Part name:
Operator:	Part number:
E-mail:	Piece: piece 1

circle 15	X	0.0000	0.0154	±0.0200	0.0154	Pass	
circle 15	Y	23.1500	23.1552	±0.0200	0.0052	Pass	
circle 15	Z	0.0000	0.0000	±1.0000	0.0000	Pass	
circle 17	Diameter	0.4000	0.3113	±0.0200	-0.0887	Fail	-0.0687
circle 17	X	0.0000	0.0272	±0.0200	0.0272	Fail	0.0072
circle 17	Y	60.1500	60.1752	±0.0200	0.0252	Fail	0.0052
circle 17	Z	0.0000	0.0000	±1.0000	0.0000	Pass	
distance 10	3D Distance	72.2000	72.2031	±0.0200	0.0031	Pass	
distance 11	3D Distance	16.3000	16.3097	±0.0200	0.0097	Pass	
distance 12	3D Distance	16.3000	16.3190	±0.0200	0.0190	Pass	
distance 13	3D Distance	18.9500	18.9744	±0.0200	0.0244	Fail	0.0044
distance 14	3D Distance	23.2500	23.2842	±0.0200	0.0342	Fail	0.0142
distance 15	3D Distance	23.2500	23.2993	±0.0200	0.0493	Fail	0.0293
distance 16	3D Distance	18.9500	18.9603	±0.0200	0.0103	Pass	
distance 17	3D Distance	16.3000	16.3324	±0.0200	0.0324	Fail	0.0124
distance 18	3D Distance	16.3000	16.3628	±0.0200	0.0628	Fail	0.0428
distance 19	3D Distance	32.6000	32.5936	±0.0200	-0.0064	Pass	
distance 20	3D Distance	35.2000	35.2100	±0.0200	0.0100	Pass	
distance 21	3D Distance	32.6000	32.5938	±0.0200	-0.0062	Pass	
distance 22	3D Distance	35.2000	35.2147	±0.0200	0.0147	Pass	
distance 23	3D Distance	0.3000	0.2739	±0.0200	-0.0261	Fail	-0.0061
distance 24	3D Distance	0.3000	0.2748	±0.0200	-0.0252	Fail	-0.0052
distance 25	3D Distance	21.1000	21.1370	±0.0200	0.0370	Fail	0.0170
distance 26	3D Distance	58.1000	58.1068	±0.0200	0.0068	Pass	

Organization:	Part name:
Operator:	Part number:
E-mail:	Piece: piece 1

7.9 Annex 7- Sample 3 test 3 report

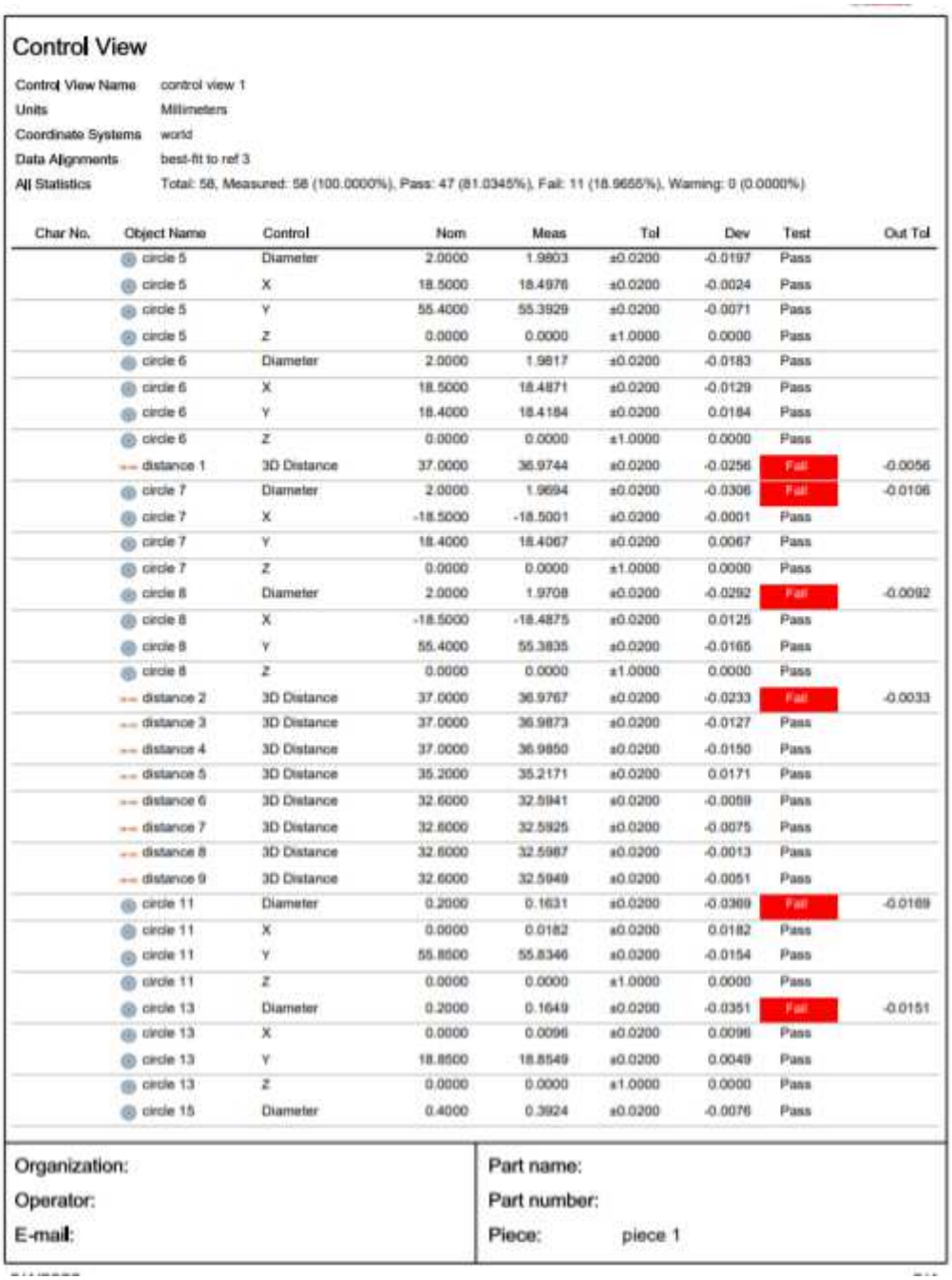

Control View

Control View Name	control view 1
Units	Millimeters
Coordinate Systems	world
Data Alignments	best-fit to ref 3
All Statistics	Total: 58, Measured: 58 (100.0000%), Pass: 47 (81.0345%), Fail: 11 (18.9655%), Warning: 0 (0.0000%)

Char No.	Object Name	Control	Nom	Meas	Tol	Dev	Test	Out Tol
	circle 5	Diameter	2.0000	1.9803	±0.0200	-0.0197	Pass	
	circle 5	X	18.5000	18.4976	±0.0200	-0.0024	Pass	
	circle 5	Y	55.4000	55.3929	±0.0200	-0.0071	Pass	
	circle 5	Z	0.0000	0.0000	±1.0000	0.0000	Pass	
	circle 6	Diameter	2.0000	1.9817	±0.0200	-0.0183	Pass	
	circle 6	X	18.5000	18.4871	±0.0200	-0.0129	Pass	
	circle 6	Y	18.4000	18.4184	±0.0200	0.0184	Pass	
	circle 6	Z	0.0000	0.0000	±1.0000	0.0000	Pass	
	distance 1	3D Distance	37.0000	36.9744	±0.0200	-0.0256	Fail	-0.0056
	circle 7	Diameter	2.0000	1.9694	±0.0200	-0.0306	Fail	-0.0106
	circle 7	X	-18.5000	-18.5001	±0.0200	-0.0001	Pass	
	circle 7	Y	18.4000	18.4067	±0.0200	0.0067	Pass	
	circle 7	Z	0.0000	0.0000	±1.0000	0.0000	Pass	
	circle 8	Diameter	2.0000	1.9708	±0.0200	-0.0292	Fail	-0.0092
	circle 8	X	-18.5000	-18.4875	±0.0200	0.0125	Pass	
	circle 8	Y	55.4000	55.3835	±0.0200	-0.0165	Pass	
	circle 8	Z	0.0000	0.0000	±1.0000	0.0000	Pass	
	distance 2	3D Distance	37.0000	36.9767	±0.0200	-0.0233	Fail	-0.0033
	distance 3	3D Distance	37.0000	36.9873	±0.0200	-0.0127	Pass	
	distance 4	3D Distance	37.0000	36.9850	±0.0200	-0.0150	Pass	
	distance 5	3D Distance	35.2000	35.2171	±0.0200	0.0171	Pass	
	distance 6	3D Distance	32.6000	32.5941	±0.0200	-0.0059	Pass	
	distance 7	3D Distance	32.6000	32.5925	±0.0200	-0.0075	Pass	
	distance 8	3D Distance	32.6000	32.5987	±0.0200	-0.0013	Pass	
	distance 9	3D Distance	32.6000	32.5949	±0.0200	-0.0051	Pass	
	circle 11	Diameter	0.2000	0.1631	±0.0200	-0.0369	Fail	-0.0169
	circle 11	X	0.0000	0.0182	±0.0200	0.0182	Pass	
	circle 11	Y	55.8000	55.8346	±0.0200	-0.0154	Pass	
	circle 11	Z	0.0000	0.0000	±1.0000	0.0000	Pass	
	circle 13	Diameter	0.2000	0.1649	±0.0200	-0.0351	Fail	-0.0151
	circle 13	X	0.0000	0.0096	±0.0200	0.0096	Pass	
	circle 13	Y	18.8500	18.8549	±0.0200	0.0049	Pass	
	circle 13	Z	0.0000	0.0000	±1.0000	0.0000	Pass	
	circle 15	Diameter	0.4000	0.3924	±0.0200	-0.0076	Pass	

Organization:	Part name:
Operator:	Part number:
E-mail:	Piece: piece 1

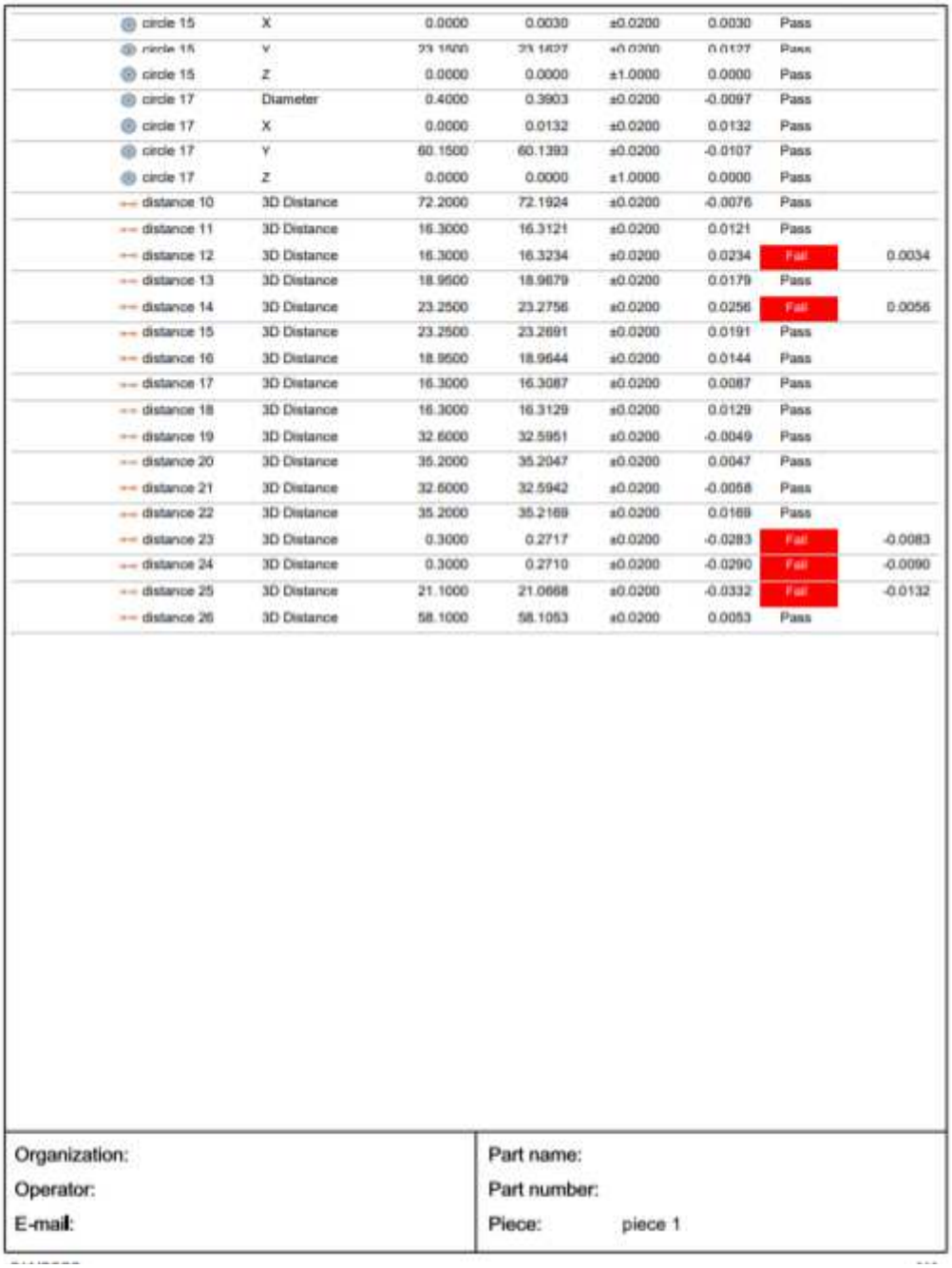

circle 15	X	0.0000	0.0030	±0.0200	0.0030	Pass	
circle 15	Y	23.1600	23.1627	±0.0200	0.0127	Pass	
circle 15	Z	0.0000	0.0000	±1.0000	0.0000	Pass	
circle 17	Diameter	0.4000	0.3903	±0.0200	-0.0097	Pass	
circle 17	X	0.0000	0.0132	±0.0200	0.0132	Pass	
circle 17	Y	60.1500	60.1393	±0.0200	-0.0107	Pass	
circle 17	Z	0.0000	0.0000	±1.0000	0.0000	Pass	
distance 10	3D Distance	72.2000	72.1924	±0.0200	-0.0076	Pass	
distance 11	3D Distance	16.3000	16.3121	±0.0200	0.0121	Pass	
distance 12	3D Distance	16.3000	16.3234	±0.0200	0.0234	Fail	0.0034
distance 13	3D Distance	18.9500	18.9679	±0.0200	0.0179	Pass	
distance 14	3D Distance	23.2500	23.2756	±0.0200	0.0256	Fail	0.0056
distance 15	3D Distance	23.2500	23.2691	±0.0200	0.0191	Pass	
distance 16	3D Distance	18.9500	18.9644	±0.0200	0.0144	Pass	
distance 17	3D Distance	16.3000	16.3087	±0.0200	0.0087	Pass	
distance 18	3D Distance	16.3000	16.3129	±0.0200	0.0129	Pass	
distance 19	3D Distance	32.6000	32.5951	±0.0200	-0.0049	Pass	
distance 20	3D Distance	35.2000	35.2047	±0.0200	0.0047	Pass	
distance 21	3D Distance	32.6000	32.5942	±0.0200	-0.0058	Pass	
distance 22	3D Distance	35.2000	35.2169	±0.0200	0.0169	Pass	
distance 23	3D Distance	0.3000	0.2717	±0.0200	-0.0283	Fail	-0.0083
distance 24	3D Distance	0.3000	0.2710	±0.0200	-0.0290	Fail	-0.0090
distance 25	3D Distance	21.1000	21.0668	±0.0200	-0.0332	Fail	-0.0132
distance 26	3D Distance	58.1000	58.1053	±0.0200	0.0053	Pass	

Organization:	Part name:
Operator:	Part number:
E-mail:	Piece: piece 1

7.10 Annex 8- Sample 1 test 4 report

Control View

Control View Name	control view 1
Units	Millimeters
Coordinate Systems	world
Data Alignments	best-fit to ref 3
All Statistics	Total: 58, Measured: 58 (100.0000%), Pass: 46 (79.3103%), Fail: 12 (20.6897%), Warning: 0 (0.0000%)

Char No.	Object Name	Control	Nom	Meas	Tol	Dev	Test	Out Tol
	circle 5	Diameter	2.0000	1.9789	±0.0200	-0.0211	Fail	-0.0011
	circle 5	X	18.5000	18.4972	±0.0200	-0.0028	Pass	
	circle 5	Y	55.4000	55.3936	±0.0200	-0.0064	Pass	
	circle 5	Z	0.0000	0.0000	±1.0000	0.0000	Pass	
	circle 6	Diameter	2.0000	1.9801	±0.0200	-0.0199	Pass	
	circle 6	X	18.5000	18.4906	±0.0200	-0.0094	Pass	
	circle 6	Y	18.4000	18.4149	±0.0200	0.0149	Pass	
	circle 6	Z	0.0000	0.0000	±1.0000	0.0000	Pass	
	distance 1	3D Distance	37.0000	36.9787	±0.0200	-0.0213	Fail	-0.0013
	circle 7	Diameter	2.0000	1.9699	±0.0200	-0.0301	Fail	-0.0101
	circle 7	X	-18.5000	-18.4963	±0.0200	0.0037	Pass	
	circle 7	Y	18.4000	18.4057	±0.0200	0.0057	Pass	
	circle 7	Z	0.0000	0.0000	±1.0000	0.0000	Pass	
	circle 8	Diameter	2.0000	1.9685	±0.0200	-0.0315	Fail	-0.0115
	circle 8	X	-18.5000	-18.4871	±0.0200	0.0129	Pass	
	circle 8	Y	55.4000	55.3876	±0.0200	-0.0124	Pass	
	circle 8	Z	0.0000	0.0000	±1.0000	0.0000	Pass	
	distance 2	3D Distance	37.0000	36.9820	±0.0200	-0.0180	Pass	
	distance 3	3D Distance	37.0000	36.9869	±0.0200	-0.0131	Pass	
	distance 4	3D Distance	37.0000	36.9843	±0.0200	-0.0157	Pass	
	distance 5	3D Distance	35.2000	35.2172	±0.0200	0.0172	Pass	
	distance 6	3D Distance	32.6000	32.5982	±0.0200	-0.0018	Pass	
	distance 7	3D Distance	32.6000	32.5949	±0.0200	-0.0051	Pass	
	distance 8	3D Distance	32.6000	32.5959	±0.0200	-0.0041	Pass	
	distance 9	3D Distance	32.6000	32.5961	±0.0200	-0.0039	Pass	
	circle 11	Diameter	0.2000	0.1662	±0.0200	-0.0338	Fail	-0.0138
	circle 11	X	0.0000	0.0163	±0.0200	0.0163	Pass	
	circle 11	Y	55.8500	55.8374	±0.0200	-0.0126	Pass	
	circle 11	Z	0.0000	0.0000	±1.0000	0.0000	Pass	
	circle 13	Diameter	0.2000	0.1696	±0.0200	-0.0304	Fail	-0.0104
	circle 13	X	0.0000	0.0161	±0.0200	0.0161	Pass	
	circle 13	Y	18.8500	18.8486	±0.0200	-0.0014	Pass	
	circle 13	Z	0.0000	0.0000	±1.0000	0.0000	Pass	
	circle 15	Diameter	0.4000	0.3919	±0.0200	-0.0081	Pass	

Organization:	Part name:
Operator:	Part number:
E-mail:	Piece: piece 1

circle 15	X	0.0000	0.0072	±0.0200	0.0072	Pass	
circle 15	Y	23.1500	23.1598	±0.0200	0.0098	Pass	
circle 15	Z	0.0000	0.0000	±1.0000	0.0000	Pass	
circle 17	Diameter	0.4000	0.3933	±0.0200	-0.0067	Pass	
circle 17	X	0.0000	0.0120	±0.0200	0.0120	Pass	
circle 17	Y	60.1500	60.1390	±0.0200	-0.0110	Pass	
circle 17	Z	0.0000	0.0000	±1.0000	0.0000	Pass	
distance 10	3D Distance	72.2000	72.1952	±0.0200	-0.0048	Pass	
distance 11	3D Distance	16.3000	16.3105	±0.0200	0.0105	Pass	
distance 12	3D Distance	16.3000	16.3238	±0.0200	0.0238	Fail	0.0038
distance 13	3D Distance	18.9500	18.9593	±0.0200	0.0093	Pass	
distance 14	3D Distance	23.2500	23.2705	±0.0200	0.0205	Fail	0.0005
distance 15	3D Distance	23.2500	23.2731	±0.0200	0.0231	Fail	0.0031
distance 16	3D Distance	18.9500	18.9715	±0.0200	0.0215	Fail	0.0015
distance 17	3D Distance	16.3000	16.3096	±0.0200	0.0096	Pass	
distance 18	3D Distance	16.3000	16.3141	±0.0200	0.0141	Pass	
distance 19	3D Distance	32.6000	32.5961	±0.0200	-0.0039	Pass	
distance 20	3D Distance	35.2000	35.2055	±0.0200	0.0055	Pass	
distance 21	3D Distance	32.6000	32.5993	±0.0200	-0.0007	Pass	
distance 22	3D Distance	35.2000	35.2158	±0.0200	0.0158	Pass	
distance 23	3D Distance	0.3000	0.2685	±0.0200	-0.0315	Fail	-0.0115
distance 24	3D Distance	0.3000	0.2693	±0.0200	-0.0307	Fail	-0.0107
distance 25	3D Distance	21.1000	21.1167	±0.0200	0.0167	Pass	
distance 26	3D Distance	58.1000	58.1017	±0.0200	0.0017	Pass	

Organization:	Part name:
Operator:	Part number:
E-mail:	Piece: piece 1

7.11 Annex 9- Sample 2 test 4 report

Control View

Control View Name	control view 1
Units	Millimeters
Coordinate Systems	world
Data Alignments	best-fit to ref 3
All Statistics	Total: 58, Measured: 58 (100.0000%), Pass: 47 (81.0345%), Fail: 11 (18.9655%), Warning: 0 (0.0000%)

Char No.	Object Name	Control	Nom	Meas	Tol	Dev	Test	Out Tol
	circle 5	Diameter	2.0000	1.9793	±0.0200	-0.0207	Fail	-0.0007
	circle 5	X	18.5000	18.5048	±0.0200	0.0048	Pass	
	circle 5	Y	55.4000	55.3982	±0.0200	-0.0018	Pass	
	circle 5	Z	0.0000	0.0000	±1.0000	0.0000	Pass	
	circle 6	Diameter	2.0000	1.9797	±0.0200	-0.0203	Fail	-0.0003
	circle 6	X	18.5000	18.4837	±0.0200	-0.0163	Pass	
	circle 6	Y	18.4000	18.4210	±0.0200	0.0210	Fail	0.0010
	circle 6	Z	0.0000	0.0000	±1.0000	0.0000	Pass	
	distance 1	3D Distance	37.0000	36.9772	±0.0200	-0.0228	Fail	-0.0028
	circle 7	Diameter	2.0000	1.9683	±0.0200	-0.0317	Fail	-0.0117
	circle 7	X	-18.5000	-18.5026	±0.0200	-0.0026	Pass	
	circle 7	Y	18.4000	18.3994	±0.0200	-0.0006	Pass	
	circle 7	Z	0.0000	0.0000	±1.0000	0.0000	Pass	
	circle 8	Diameter	2.0000	1.9702	±0.0200	-0.0298	Fail	-0.0098
	circle 8	X	-18.5000	-18.4875	±0.0200	0.0125	Pass	
	circle 8	Y	55.4000	55.3827	±0.0200	-0.0173	Pass	
	circle 8	Z	0.0000	0.0000	±1.0000	0.0000	Pass	
	distance 2	3D Distance	37.0000	36.9833	±0.0200	-0.0167	Pass	
	distance 3	3D Distance	37.0000	36.9863	±0.0200	-0.0137	Pass	
	distance 4	3D Distance	37.0000	36.9923	±0.0200	-0.0077	Pass	
	distance 5	3D Distance	35.2000	35.2157	±0.0200	0.0157	Pass	
	distance 6	3D Distance	32.6000	32.6012	±0.0200	0.0012	Pass	
	distance 7	3D Distance	32.6000	32.5970	±0.0200	-0.0030	Pass	
	distance 8	3D Distance	32.6000	32.6021	±0.0200	0.0021	Pass	

Organization:	Part name:
Operator:	Part number:
E-mail:	Piece: piece 1

distance 9	3D Distance	32.6000	32.5995	±0.0200	-0.0005	Pass	
circle 11	Diameter	0.2000	0.1661	±0.0200	-0.0339	Fail	-0.0139
circle 11	X	0.0000	0.0173	±0.0200	0.0173	Pass	
circle 11	Y	55.8500	55.8339	±0.0200	-0.0161	Pass	
circle 11	Z	0.0000	0.0000	±1.0000	0.0000	Pass	
circle 13	Diameter	0.2000	0.1653	±0.0200	-0.0347	Fail	-0.0147
circle 13	X	0.0000	0.0089	±0.0200	0.0089	Pass	
circle 13	Y	18.8500	18.8497	±0.0200	-0.0003	Pass	
circle 13	Z	0.0000	0.0000	±1.0000	0.0000	Pass	
circle 15	Diameter	0.4000	0.3857	±0.0200	-0.0143	Pass	
circle 15	X	0.0000	-0.0024	±0.0200	-0.0024	Pass	
circle 15	Y	23.1500	23.1570	±0.0200	0.0070	Pass	
circle 15	Z	0.0000	0.0000	±1.0000	0.0000	Pass	
circle 17	Diameter	0.4000	0.3876	±0.0200	-0.0124	Pass	
circle 17	X	0.0000	0.0167	±0.0200	0.0167	Pass	
circle 17	Y	60.1500	60.1401	±0.0200	-0.0099	Pass	
circle 17	Z	0.0000	0.0000	±1.0000	0.0000	Pass	
distance 10	3D Distance	72.2000	72.1921	±0.0200	-0.0079	Pass	
distance 11	3D Distance	16.3000	16.3119	±0.0200	0.0119	Pass	
distance 12	3D Distance	16.3000	16.3236	±0.0200	0.0236	Fail	0.0036
distance 13	3D Distance	18.9500	18.9533	±0.0200	0.0033	Pass	
distance 14	3D Distance	23.2500	23.2605	±0.0200	0.0105	Pass	
distance 15	3D Distance	23.2500	23.2564	±0.0200	0.0064	Pass	
distance 16	3D Distance	18.9500	18.9502	±0.0200	0.0002	Pass	
distance 17	3D Distance	16.3000	16.3110	±0.0200	0.0110	Pass	
distance 18	3D Distance	16.3000	16.3130	±0.0200	0.0130	Pass	
distance 19	3D Distance	32.6000	32.6000	±0.0200	0.0000	Pass	
distance 20	3D Distance	35.2000	35.1971	±0.0200	-0.0029	Pass	
distance 21	3D Distance	32.6000	32.6014	±0.0200	0.0014	Pass	
distance 22	3D Distance	35.2000	35.2154	±0.0200	0.0154	Pass	
distance 23	3D Distance	0.3000	0.2681	±0.0200	-0.0319	Fail	-0.0119
distance 24	3D Distance	0.3000	0.2674	±0.0200	-0.0326	Fail	-0.0126
distance 25	3D Distance	21.1000	21.1115	±0.0200	0.0115	Pass	
distance 26	3D Distance	58.1000	58.0943	±0.0200	-0.0057	Pass	

Organization:	Part name:
Operator:	Part number:
E-mail:	Piece: piece 1

7.12 Annex 10- Sample 3 test 4 report

Control View

Control View Name	control view 1
Units	Millimeters
Coordinate Systems	world
Data Alignments	best-fit to ref 3
All Statistics	Total: 58, Measured: 58 (100.0000%), Pass: 45 (77.5862%), Fail: 13 (22.4138%), Warning: 0 (0.0000%)

Char No.	Object Name	Control	Nom	Meas	Tol	Dev	Test	Out Tol
	circle 5	Diameter	2.0000	1.9789	±0.0200	-0.0211	Fail	-0.0011
	circle 5	X	18.5000	18.5012	±0.0200	0.0012	Pass	
	circle 5	Y	55.4000	55.3981	±0.0200	-0.0019	Pass	
	circle 5	Z	0.0000	0.0000	±1.0000	0.0000	Pass	
	circle 6	Diameter	2.0000	1.9800	±0.0200	-0.0200	Pass	
	circle 6	X	18.5000	18.4884	±0.0200	-0.0116	Pass	
	circle 6	Y	18.4000	18.4212	±0.0200	0.0212	Fail	0.0012
	circle 6	Z	0.0000	0.0000	±1.0000	0.0000	Pass	
	distance 1	3D Distance	37.0000	36.9769	±0.0200	-0.0231	Fail	-0.0031
	circle 7	Diameter	2.0000	1.9706	±0.0200	-0.0294	Fail	-0.0094
	circle 7	X	-18.5000	-18.4991	±0.0200	0.0009	Pass	
	circle 7	Y	18.4000	18.3995	±0.0200	-0.0005	Pass	
	circle 7	Z	0.0000	0.0000	±1.0000	0.0000	Pass	
	circle 8	Diameter	2.0000	1.9710	±0.0200	-0.0290	Fail	-0.0090
	circle 8	X	-18.5000	-18.4879	±0.0200	0.0121	Pass	
	circle 8	Y	55.4000	55.3820	±0.0200	-0.0180	Pass	
	circle 8	Z	0.0000	0.0000	±1.0000	0.0000	Pass	
	distance 2	3D Distance	37.0000	36.9825	±0.0200	-0.0175	Pass	
	distance 3	3D Distance	37.0000	36.9875	±0.0200	-0.0125	Pass	
	distance 4	3D Distance	37.0000	36.9891	±0.0200	-0.0109	Pass	
	distance 5	3D Distance	35.2000	35.2174	±0.0200	0.0174	Pass	
	distance 6	3D Distance	32.6000	32.5969	±0.0200	-0.0031	Pass	
	distance 7	3D Distance	32.6000	32.5958	±0.0200	-0.0042	Pass	
	distance 8	3D Distance	32.6000	32.5997	±0.0200	-0.0003	Pass	
	distance 9	3D Distance	32.6000	32.5992	±0.0200	-0.0008	Pass	
	circle 11	Diameter	0.2000	0.1662	±0.0200	-0.0338	Fail	-0.0138
	circle 11	X	0.0000	0.0155	±0.0200	0.0155	Pass	
	circle 11	Y	55.8500	55.8349	±0.0200	-0.0151	Pass	
	circle 11	Z	0.0000	0.0000	±1.0000	0.0000	Pass	
	circle 13	Diameter	0.2000	0.1721	±0.0200	-0.0279	Fail	-0.0079
	circle 13	X	0.0000	0.0088	±0.0200	0.0088	Pass	
	circle 13	Y	18.8500	18.8525	±0.0200	0.0025	Pass	
	circle 13	Z	0.0000	0.0000	±1.0000	0.0000	Pass	
	circle 15	Diameter	0.4000	0.3930	±0.0200	-0.0070	Pass	

Organization:	Part name:
Operator:	Part number:
E-mail:	Piece: piece 1

circle 15	X	0.0000	0.0026	±0.0200	0.0026	Pass	
circle 15	Y	23.1500	23.1596	±0.0200	0.0096	Pass	
circle 15	Z	0.0000	0.0000	±1.0000	0.0000	Pass	
circle 17	Diameter	0.4000	0.3893	±0.0200	-0.0107	Pass	
circle 17	X	0.0000	0.0114	±0.0200	0.0114	Pass	
circle 17	Y	60.1500	60.1403	±0.0200	-0.0097	Pass	
circle 17	Z	0.0000	0.0000	±1.0000	0.0000	Pass	
distance 10	3D Distance	72.2000	72.1906	±0.0200	-0.0094	Pass	
distance 11	3D Distance	16.3000	16.3123	±0.0200	0.0123	Pass	
distance 12	3D Distance	16.3000	16.3186	±0.0200	0.0186	Pass	
distance 13	3D Distance	18.9500	18.9671	±0.0200	0.0171	Pass	
distance 14	3D Distance	23.2500	23.2742	±0.0200	0.0242	Fail	0.0042
distance 15	3D Distance	23.2500	23.2753	±0.0200	0.0253	Fail	0.0053
distance 16	3D Distance	18.9500	18.9700	±0.0200	0.0200	Pass	
distance 17	3D Distance	16.3000	16.3082	±0.0200	0.0082	Pass	
distance 18	3D Distance	16.3000	16.3121	±0.0200	0.0121	Pass	
distance 19	3D Distance	32.6000	32.5993	±0.0200	-0.0007	Pass	
distance 20	3D Distance	35.2000	35.2000	±0.0200	0.0000	Pass	
distance 21	3D Distance	32.6000	32.5970	±0.0200	-0.0030	Pass	
distance 22	3D Distance	35.2000	35.2162	±0.0200	0.0162	Pass	
distance 23	3D Distance	0.3000	0.2677	±0.0200	-0.0323	Fail	-0.0123
distance 24	3D Distance	0.3000	0.2664	±0.0200	-0.0336	Fail	-0.0136
distance 25	3D Distance	21.1000	21.1280	±0.0200	0.0280	Fail	0.0080
distance 26	3D Distance	58.1000	58.0772	±0.0200	-0.0228	Fail	-0.0028

Organization:	Part name:
Operator:	Part number:
E-mail:	Piece: piece 1

7.13 Annex 11- Sample 1 test 5 report

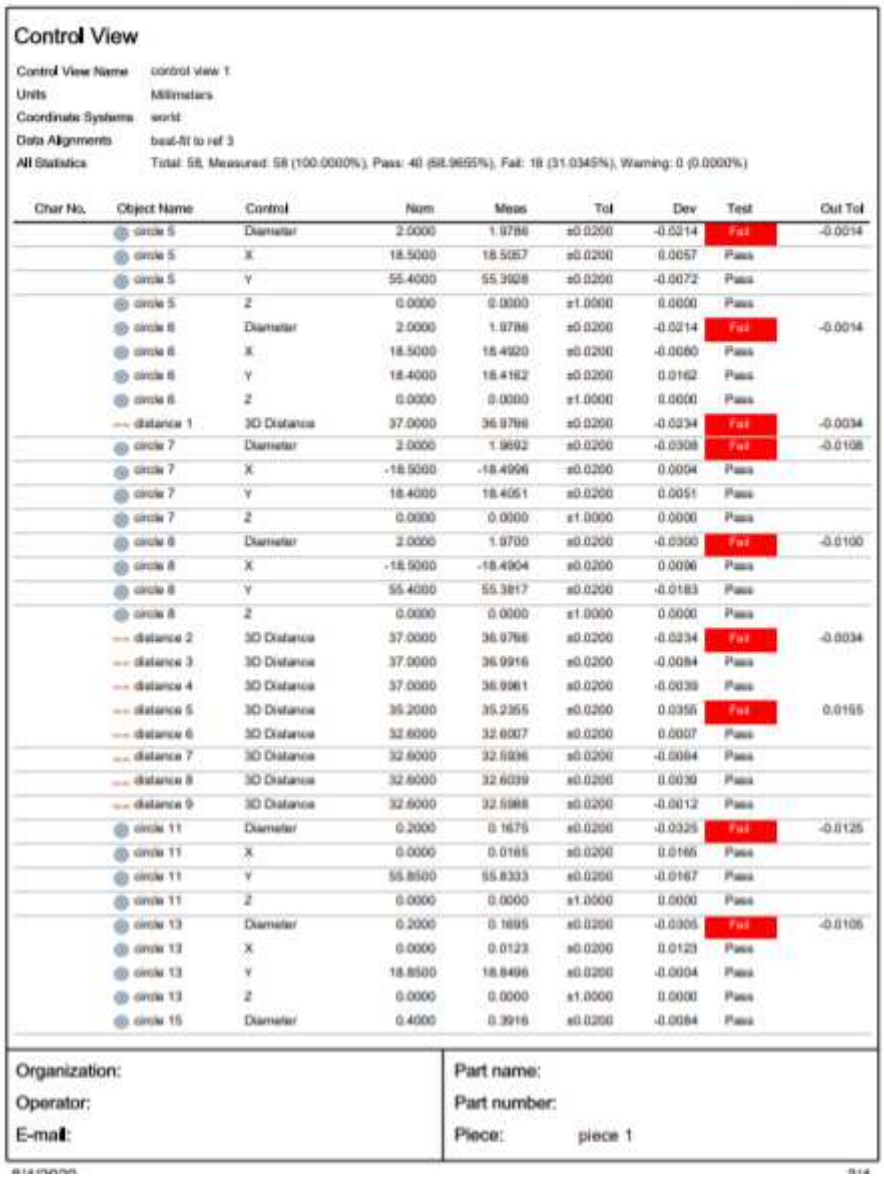

Control View

Control View Name	control view 1
Units	Millimeters
Coordinate Systems	world
Data Alignments	best-fit to ref 3
All Statistics	Total: 58, Measured: 58 (100.0000%), Pass: 40 (68.9655%), Fail: 18 (31.0345%), Warning: 0 (0.0000%)

Char No.	Object Name	Control	Nom	Meas	Tol	Dev	Test	Out Tol
	circle 5	Diameter	2.0000	1.9786	±0.0200	-0.0214	Fail	-0.0014
	circle 5	X	18.5000	18.5057	±0.0200	0.0057	Pass	
	circle 5	Y	55.4000	55.3928	±0.0200	-0.0072	Pass	
	circle 5	Z	0.0000	0.0000	±1.0000	0.0000	Pass	
	circle 6	Diameter	2.0000	1.9786	±0.0200	-0.0214	Fail	-0.0014
	circle 6	X	18.5000	18.4920	±0.0200	-0.0080	Pass	
	circle 6	Y	18.4000	18.4162	±0.0200	0.0162	Pass	
	circle 6	Z	0.0000	0.0000	±1.0000	0.0000	Pass	
	distance 1	3D Distance	37.0000	36.9766	±0.0200	-0.0234	Fail	-0.0034
	circle 7	Diameter	2.0000	1.9692	±0.0200	-0.0308	Fail	-0.0108
	circle 7	X	-18.5000	-18.4996	±0.0200	0.0004	Pass	
	circle 7	Y	18.4000	18.4051	±0.0200	0.0051	Pass	
	circle 7	Z	0.0000	0.0000	±1.0000	0.0000	Pass	
	circle 8	Diameter	2.0000	1.9700	±0.0200	-0.0300	Fail	-0.0100
	circle 8	X	-18.5000	-18.4904	±0.0200	0.0096	Pass	
	circle 8	Y	55.4000	55.3817	±0.0200	-0.0183	Pass	
	circle 8	Z	0.0000	0.0000	±1.0000	0.0000	Pass	
	distance 2	3D Distance	37.0000	36.9766	±0.0200	-0.0234	Fail	-0.0034
	distance 3	3D Distance	37.0000	36.9916	±0.0200	-0.0084	Pass	
	distance 4	3D Distance	37.0000	36.9961	±0.0200	-0.0039	Pass	
	distance 5	3D Distance	35.2000	35.2355	±0.0200	0.0355	Fail	0.0155
	distance 6	3D Distance	32.6000	32.6007	±0.0200	0.0007	Pass	
	distance 7	3D Distance	32.6000	32.5936	±0.0200	-0.0064	Pass	
	distance 8	3D Distance	32.6000	32.6039	±0.0200	0.0039	Pass	
	distance 9	3D Distance	32.6000	32.5988	±0.0200	-0.0012	Pass	
	circle 11	Diameter	0.2000	0.1675	±0.0200	-0.0325	Fail	-0.0125
	circle 11	X	0.0000	0.0165	±0.0200	0.0165	Pass	
	circle 11	Y	55.8500	55.8333	±0.0200	-0.0167	Pass	
	circle 11	Z	0.0000	0.0000	±1.0000	0.0000	Pass	
	circle 13	Diameter	0.2000	0.1695	±0.0200	-0.0305	Fail	-0.0105
	circle 13	X	0.0000	0.0123	±0.0200	0.0123	Pass	
	circle 13	Y	18.8500	18.8496	±0.0200	-0.0004	Pass	
	circle 13	Z	0.0000	0.0000	±1.0000	0.0000	Pass	
	circle 15	Diameter	0.4000	0.3916	±0.0200	-0.0084	Pass	

Organization:	Part name:
Operator:	Part number:
E-mail:	Piece: piece 1

circle 15	X	0.0000	0.0060	±0.0200	0.0060	Pass	
circle 15	Y	23.1500	23.1591	±0.0200	0.0091	Pass	
circle 15	Z	0.0000	0.0000	±1.0000	0.0000	Pass	
circle 17	Diameter	0.4000	0.3840	±0.0200	-0.0160	Pass	
circle 17	X	0.0000	0.0181	±0.0200	0.0181	Pass	
circle 17	Y	60.1500	60.1318	±0.0200	-0.0182	Pass	
circle 17	Z	0.0000	0.0000	±1.0000	0.0000	Pass	
distance 10	3D Distance	72.2000	72.2046	±0.0200	0.0046	Pass	
distance 11	3D Distance	16.3000	16.3140	±0.0200	0.0140	Pass	
distance 12	3D Distance	16.3000	16.3222	±0.0200	0.0222	Fail	0.0022
distance 13	3D Distance	18.9500	18.9773	±0.0200	0.0273	Fail	0.0073
distance 14	3D Distance	23.2500	23.2668	±0.0200	0.0368	Fail	0.0168
distance 15	3D Distance	23.2500	23.2658	±0.0200	0.0358	Fail	0.0158
distance 16	3D Distance	18.9500	18.9673	±0.0200	0.0373	Fail	0.0173
distance 17	3D Distance	16.3000	16.3078	±0.0200	0.0078	Pass	
distance 18	3D Distance	16.3000	16.3104	±0.0200	0.0104	Pass	
distance 19	3D Distance	32.6000	32.5994	±0.0200	-0.0006	Pass	
distance 20	3D Distance	35.2000	35.2004	±0.0200	0.0004	Pass	
distance 21	3D Distance	32.6000	32.6015	±0.0200	0.0015	Pass	
distance 22	3D Distance	35.2000	35.2343	±0.0200	0.0343	Fail	0.0143
distance 23	3D Distance	0.3000	0.2891	±0.0200	-0.0309	Fail	-0.0109
distance 24	3D Distance	0.3000	0.2653	±0.0200	-0.0347	Fail	-0.0147
distance 25	3D Distance	21.1000	21.1402	±0.0200	0.0402	Fail	0.0202
distance 26	3D Distance	58.1000	58.1166	±0.0200	0.0166	Pass	

Organization:	Part name:
Operator:	Part number:
E-mail:	Piece: piece 1

7.14 Annex 12- Sample 2 test 5 report

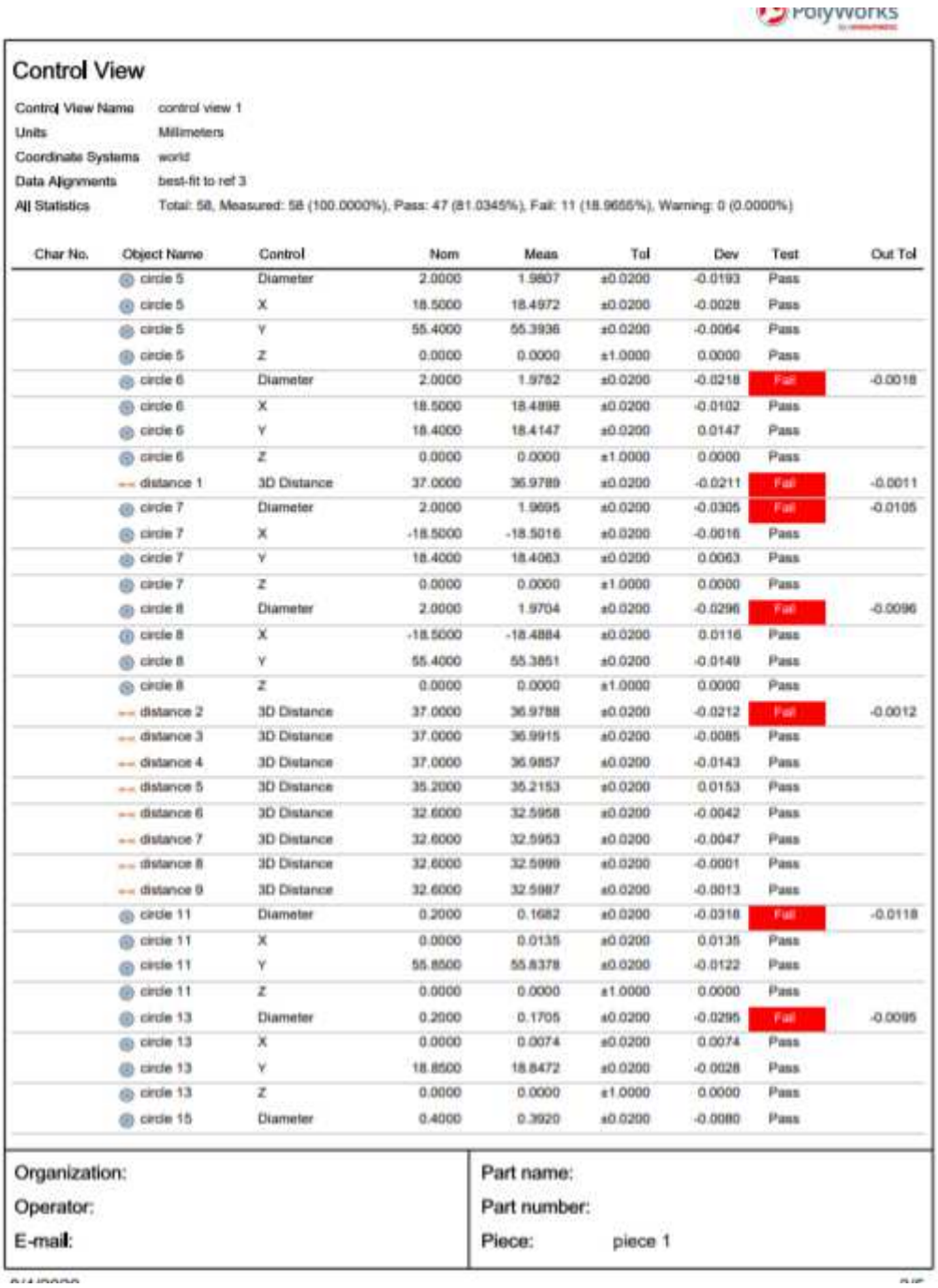

Control View

Control View Name	control view 1
Units	Millimeters
Coordinate Systems	world
Data Alignments	best-fit to ref 3
All Statistics	Total: 58, Measured: 58 (100.0000%), Pass: 47 (81.0345%), Fail: 11 (18.9655%), Warning: 0 (0.0000%)

Char No.	Object Name	Control	Nom	Meas	Tol	Dev	Test	Out Tol
	circle 5	Diameter	2.0000	1.9807	±0.0200	-0.0193	Pass	
	circle 5	X	18.5000	18.4972	±0.0200	-0.0028	Pass	
	circle 5	Y	55.4000	55.3936	±0.0200	-0.0064	Pass	
	circle 5	Z	0.0000	0.0000	±1.0000	0.0000	Pass	
	circle 6	Diameter	2.0000	1.9782	±0.0200	-0.0218	Fail	-0.0018
	circle 6	X	18.5000	18.4898	±0.0200	-0.0102	Pass	
	circle 6	Y	18.4000	18.4147	±0.0200	0.0147	Pass	
	circle 6	Z	0.0000	0.0000	±1.0000	0.0000	Pass	
	distance 1	3D Distance	37.0000	36.9789	±0.0200	-0.0211	Fail	-0.0011
	circle 7	Diameter	2.0000	1.9695	±0.0200	-0.0305	Fail	-0.0105
	circle 7	X	-18.5000	-18.5016	±0.0200	-0.0016	Pass	
	circle 7	Y	18.4000	18.4063	±0.0200	0.0063	Pass	
	circle 7	Z	0.0000	0.0000	±1.0000	0.0000	Pass	
	circle 8	Diameter	2.0000	1.9704	±0.0200	-0.0296	Fail	-0.0096
	circle 8	X	-18.5000	-18.4884	±0.0200	0.0116	Pass	
	circle 8	Y	55.4000	55.3851	±0.0200	-0.0149	Pass	
	circle 8	Z	0.0000	0.0000	±1.0000	0.0000	Pass	
	distance 2	3D Distance	37.0000	36.9788	±0.0200	-0.0212	Fail	-0.0012
	distance 3	3D Distance	37.0000	36.9915	±0.0200	-0.0085	Pass	
	distance 4	3D Distance	37.0000	36.9857	±0.0200	-0.0143	Pass	
	distance 5	3D Distance	35.2000	35.2153	±0.0200	0.0153	Pass	
	distance 6	3D Distance	32.6000	32.5958	±0.0200	-0.0042	Pass	
	distance 7	3D Distance	32.6000	32.5953	±0.0200	-0.0047	Pass	
	distance 8	3D Distance	32.6000	32.5999	±0.0200	-0.0001	Pass	
	distance 9	3D Distance	32.6000	32.5987	±0.0200	-0.0013	Pass	
	circle 11	Diameter	0.2000	0.1682	±0.0200	-0.0318	Fail	-0.0118
	circle 11	X	0.0000	0.0135	±0.0200	0.0135	Pass	
	circle 11	Y	55.8500	55.8378	±0.0200	-0.0122	Pass	
	circle 11	Z	0.0000	0.0000	±1.0000	0.0000	Pass	
	circle 13	Diameter	0.2000	0.1705	±0.0200	-0.0295	Fail	-0.0095
	circle 13	X	0.0000	0.0074	±0.0200	0.0074	Pass	
	circle 13	Y	18.8500	18.8472	±0.0200	-0.0028	Pass	
	circle 13	Z	0.0000	0.0000	±1.0000	0.0000	Pass	
	circle 15	Diameter	0.4000	0.3920	±0.0200	-0.0080	Pass	

Organization:	Part name:
Operator:	Part number:
E-mail:	Piece: piece 1

circle 15	X	0.0000	0.0026	±0.0200	0.0026	Pass	
circle 15	Y	23.1500	23.1570	±0.0200	0.0070	Pass	
circle 15	Z	0.0000	0.0000	±1.0000	0.0000	Pass	
circle 17	Diameter	0.4000	0.3892	±0.0200	-0.0108	Pass	
circle 17	X	0.0000	0.0113	±0.0200	0.0113	Pass	
circle 17	Y	60.1500	60.1370	±0.0200	-0.0130	Pass	
circle 17	Z	0.0000	0.0000	±1.0000	0.0000	Pass	
distance 10	3D Distance	72.2000	72.1950	±0.0200	-0.0050	Pass	
distance 11	3D Distance	16.3000	16.3122	±0.0200	0.0122	Pass	
distance 12	3D Distance	16.3000	16.3188	±0.0200	0.0188	Pass	
distance 13	3D Distance	18.9500	18.9527	±0.0200	0.0027	Pass	
distance 14	3D Distance	23.2500	23.2626	±0.0200	0.0126	Pass	
distance 15	3D Distance	23.2500	23.3145	±0.0200	0.0645	Fail	0.0445
distance 16	3D Distance	18.9500	19.0154	±0.0200	0.0654	Fail	0.0454
distance 17	3D Distance	16.3000	16.3067	±0.0200	0.0067	Pass	
distance 18	3D Distance	16.3000	16.3115	±0.0200	0.0115	Pass	
distance 19	3D Distance	32.6000	32.5986	±0.0200	-0.0014	Pass	
distance 20	3D Distance	35.2000	35.2034	±0.0200	0.0034	Pass	
distance 21	3D Distance	32.6000	32.5959	±0.0200	-0.0041	Pass	
distance 22	3D Distance	35.2000	35.2143	±0.0200	0.0143	Pass	
distance 23	3D Distance	0.3000	0.2690	±0.0200	-0.0310	Fail	-0.0110
distance 24	3D Distance	0.3000	0.2687	±0.0200	-0.0313	Fail	-0.0113
distance 25	3D Distance	21.1000	21.1178	±0.0200	0.0178	Pass	
distance 26	3D Distance	58.1000	58.0937	±0.0200	-0.0063	Pass	

Organization:	Part name:
Operator:	Part number:
E-mail:	Piece: piece 1

7.15 Annex 13- Sample 3 test 5 report

Control View

Control View Name	control view 1
Units	Millimeters
Coordinate Systems	world
Data Alignments	best-fit to ref 3
All Statistics	Total: 58, Measured: 58 (100.0000%), Pass: 47 (81.0345%), Fail: 11 (18.9655%), Warning: 0 (0.0000%)

Char No.	Object Name	Control	Nom	Meas	Tol	Dev	Test	Out Tol
	circle 5	Diameter	2.0000	1.9783	±0.0200	-0.0217	Fail	-0.0017
	circle 5	X	18.5000	18.4997	±0.0200	-0.0003	Pass	
	circle 5	Y	55.4000	55.4016	±0.0200	0.0016	Pass	
	circle 5	Z	0.0000	0.0000	±1.0000	0.0000	Pass	
	circle 6	Diameter	2.0000	1.9793	±0.0200	-0.0207	Fail	-0.0007
	circle 6	X	18.5000	18.4843	±0.0200	-0.0157	Pass	
	circle 6	Y	18.4000	18.4161	±0.0200	0.0161	Pass	
	circle 6	Z	0.0000	0.0000	±1.0000	0.0000	Pass	
	distance 1	3D Distance	37.0000	36.9855	±0.0200	-0.0145	Pass	
	circle 7	Diameter	2.0000	1.9702	±0.0200	-0.0298	Fail	-0.0098
	circle 7	X	-18.5000	-18.5010	±0.0200	-0.0010	Pass	
	circle 7	Y	18.4000	18.3954	±0.0200	-0.0046	Pass	
	circle 7	Z	0.0000	0.0000	±1.0000	0.0000	Pass	
	circle 8	Diameter	2.0000	1.9683	±0.0200	-0.0317	Fail	-0.0117
	circle 8	X	-18.5000	-18.4832	±0.0200	0.0168	Pass	
	circle 8	Y	55.4000	55.3870	±0.0200	-0.0130	Pass	
	circle 8	Z	0.0000	0.0000	±1.0000	0.0000	Pass	
	distance 2	3D Distance	37.0000	36.9916	±0.0200	-0.0084	Pass	
	distance 3	3D Distance	37.0000	36.9853	±0.0200	-0.0147	Pass	
	distance 4	3D Distance	37.0000	36.9829	±0.0200	-0.0171	Pass	
	distance 5	3D Distance	35.2000	35.2124	±0.0200	0.0124	Pass	
	distance 6	3D Distance	32.6000	32.5987	±0.0200	-0.0013	Pass	
	distance 7	3D Distance	32.6000	32.5971	±0.0200	-0.0029	Pass	
	distance 8	3D Distance	32.6000	32.5980	±0.0200	-0.0020	Pass	
	distance 9	3D Distance	32.6000	32.5934	±0.0200	-0.0066	Pass	
	circle 11	Diameter	0.2000	0.1675	±0.0200	-0.0325	Fail	-0.0125
	circle 11	X	0.0000	0.0212	±0.0200	0.0212	Fail	0.0012
	circle 11	Y	55.8500	55.8376	±0.0200	-0.0124	Pass	
	circle 11	Z	0.0000	0.0000	±1.0000	0.0000	Pass	
	circle 13	Diameter	0.2000	0.1693	±0.0200	-0.0307	Fail	-0.0107
	circle 13	X	0.0000	0.0052	±0.0200	0.0052	Pass	
	circle 13	Y	18.8500	18.8480	±0.0200	-0.0020	Pass	
	circle 13	Z	0.0000	0.0000	±1.0000	0.0000	Pass	
	circle 15	Diameter	0.4000	0.3876	±0.0200	-0.0124	Pass	

Organization:	Part name:
Operator:	Part number:
E-mail:	Piece: piece 1

circle 15	X	0.0000	-0.0009	±0.0200	-0.0009	Pass	
circle 15	Y	23.1500	23.1537	±0.0200	0.0037	Pass	
circle 15	Z	0.0000	0.0000	±1.0000	0.0000	Pass	
circle 17	Diameter	0.4000	0.3908	±0.0200	-0.0092	Pass	
circle 17	X	0.0000	0.0172	±0.0200	0.0172	Pass	
circle 17	Y	60.1500	60.1436	±0.0200	-0.0064	Pass	
circle 17	Z	0.0000	0.0000	±1.0000	0.0000	Pass	
distance 10	3D Distance	72.2000	72.2010	±0.0200	0.0010	Pass	
distance 11	3D Distance	16.3000	16.3108	±0.0200	0.0108	Pass	
distance 12	3D Distance	16.3000	16.3177	±0.0200	0.0177	Pass	
distance 13	3D Distance	18.9500	18.9675	±0.0200	0.0175	Pass	
distance 14	3D Distance	23.2500	23.2731	±0.0200	0.0231	Fail	0.0031
distance 15	3D Distance	23.2500	23.2608	±0.0200	0.0108	Pass	
distance 16	3D Distance	18.9500	18.9548	±0.0200	0.0048	Pass	
distance 17	3D Distance	16.3000	16.3107	±0.0200	0.0107	Pass	
distance 18	3D Distance	16.3000	16.3186	±0.0200	0.0186	Pass	
distance 19	3D Distance	32.6000	32.5934	±0.0200	-0.0066	Pass	
distance 20	3D Distance	35.2000	35.2025	±0.0200	0.0025	Pass	
distance 21	3D Distance	32.6000	32.5993	±0.0200	-0.0007	Pass	
distance 22	3D Distance	35.2000	35.2123	±0.0200	0.0123	Pass	
distance 23	3D Distance	0.3000	0.2668	±0.0200	-0.0332	Fail	-0.0132
distance 24	3D Distance	0.3000	0.2669	±0.0200	-0.0331	Fail	-0.0131
distance 25	3D Distance	21.1000	21.1309	±0.0200	0.0309	Fail	0.0109
distance 26	3D Distance	58.1000	58.1145	±0.0200	0.0145	Pass	

Organization:	Part name:
Operator:	Part number:
E-mail:	Piece: piece 1

7.16 Annex 14- Sample 1 test 6 report

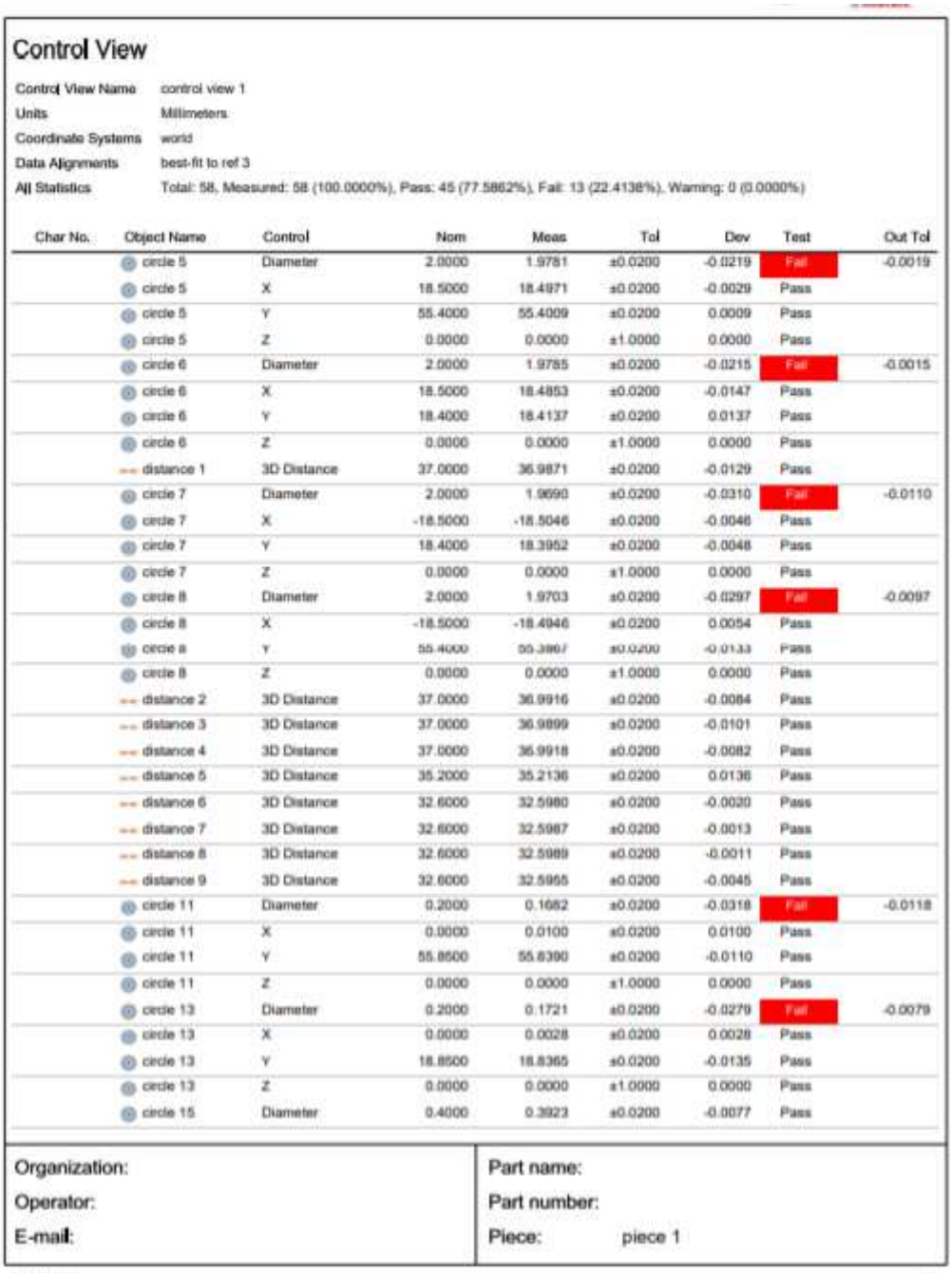

Control View

Control View Name	control view 1
Units	Millimeters
Coordinate Systems	world
Data Alignments	best-fit to ref 3
All Statistics	Total: 58, Measured: 58 (100.0000%), Pass: 45 (77.5862%), Fail: 13 (22.4138%), Warning: 0 (0.0000%)

Char No.	Object Name	Control	Nom	Meas	Tol	Dev	Test	Out Tol
	circle 5	Diameter	2.0000	1.9781	±0.0200	-0.0219	Fail	-0.0019
	circle 5	X	18.5000	18.4971	±0.0200	-0.0029	Pass	
	circle 5	Y	55.4000	55.4009	±0.0200	0.0009	Pass	
	circle 5	Z	0.0000	0.0000	±1.0000	0.0000	Pass	
	circle 6	Diameter	2.0000	1.9785	±0.0200	-0.0215	Fail	-0.0015
	circle 6	X	18.5000	18.4853	±0.0200	-0.0147	Pass	
	circle 6	Y	18.4000	18.4137	±0.0200	0.0137	Pass	
	circle 6	Z	0.0000	0.0000	±1.0000	0.0000	Pass	
	distance 1	3D Distance	37.0000	36.9871	±0.0200	-0.0129	Pass	
	circle 7	Diameter	2.0000	1.9690	±0.0200	-0.0310	Fail	-0.0110
	circle 7	X	-18.5000	-18.5046	±0.0200	-0.0046	Pass	
	circle 7	Y	18.4000	18.3952	±0.0200	-0.0048	Pass	
	circle 7	Z	0.0000	0.0000	±1.0000	0.0000	Pass	
	circle 8	Diameter	2.0000	1.9703	±0.0200	-0.0297	Fail	-0.0097
	circle 8	X	-18.5000	-18.4946	±0.0200	0.0054	Pass	
	circle 8	Y	55.4000	55.3867	±0.0200	-0.0133	Pass	
	circle 8	Z	0.0000	0.0000	±1.0000	0.0000	Pass	
	distance 2	3D Distance	37.0000	36.9916	±0.0200	-0.0084	Pass	
	distance 3	3D Distance	37.0000	36.9899	±0.0200	-0.0101	Pass	
	distance 4	3D Distance	37.0000	36.9918	±0.0200	-0.0082	Pass	
	distance 5	3D Distance	35.2000	35.2136	±0.0200	0.0136	Pass	
	distance 6	3D Distance	32.6000	32.5980	±0.0200	-0.0020	Pass	
	distance 7	3D Distance	32.6000	32.5987	±0.0200	-0.0013	Pass	
	distance 8	3D Distance	32.6000	32.5989	±0.0200	-0.0011	Pass	
	distance 9	3D Distance	32.6000	32.5955	±0.0200	-0.0045	Pass	
	circle 11	Diameter	0.2000	0.1682	±0.0200	-0.0318	Fail	-0.0118
	circle 11	X	0.0000	0.0100	±0.0200	0.0100	Pass	
	circle 11	Y	55.8500	55.8390	±0.0200	-0.0110	Pass	
	circle 11	Z	0.0000	0.0000	±1.0000	0.0000	Pass	
	circle 13	Diameter	0.2000	0.1721	±0.0200	-0.0279	Fail	-0.0079
	circle 13	X	0.0000	0.0028	±0.0200	0.0028	Pass	
	circle 13	Y	18.8500	18.8365	±0.0200	-0.0135	Pass	
	circle 13	Z	0.0000	0.0000	±1.0000	0.0000	Pass	
	circle 15	Diameter	0.4000	0.3923	±0.0200	-0.0077	Pass	

Organization:	Part name:
Operator:	Part number:
E-mail:	Piece: piece 1

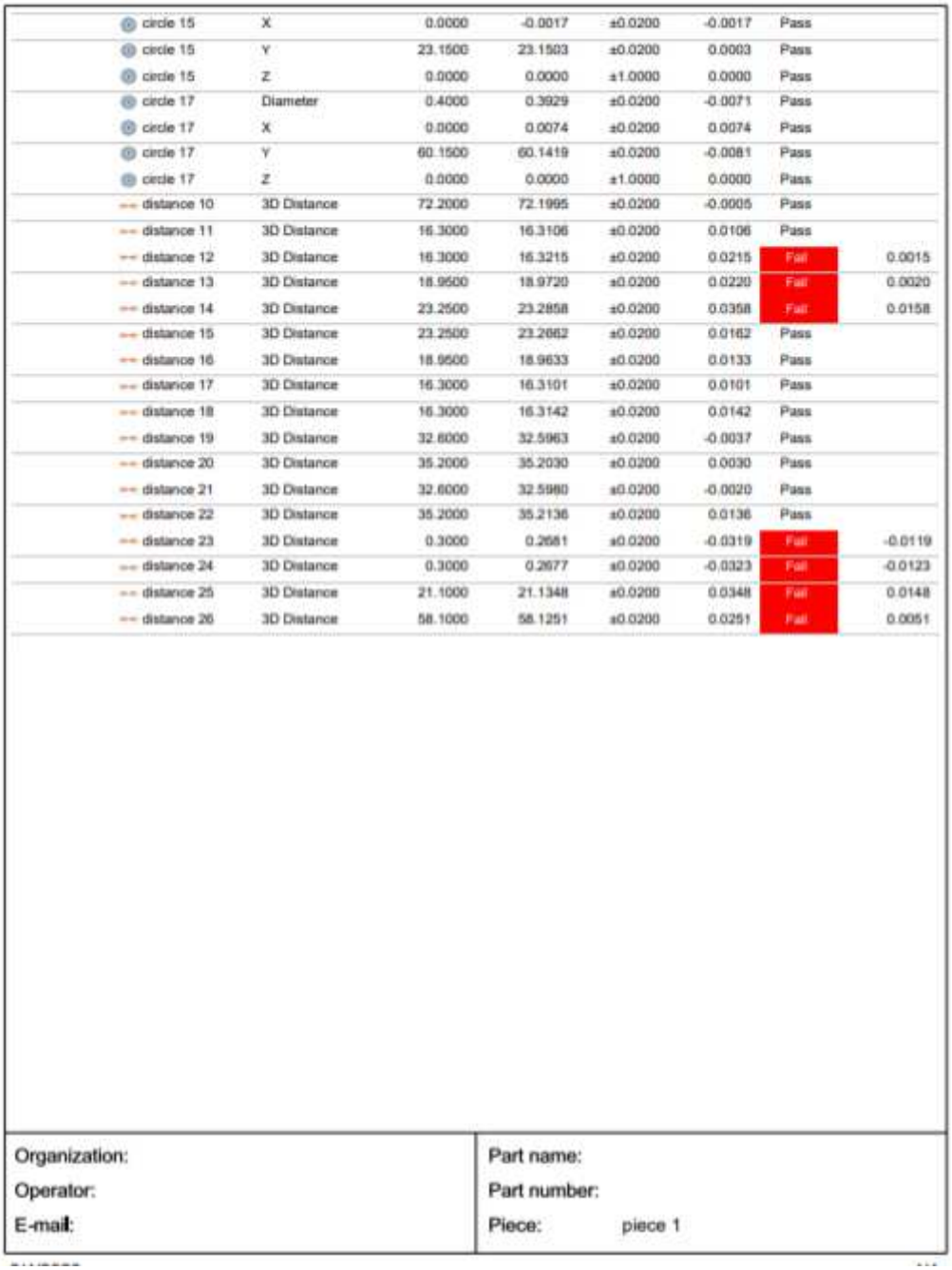

circle 15	X	0.0000	-0.0017	±0.0200	-0.0017	Pass	
circle 15	Y	23.1500	23.1503	±0.0200	0.0003	Pass	
circle 15	Z	0.0000	0.0000	±1.0000	0.0000	Pass	
circle 17	Diameter	0.4000	0.3929	±0.0200	-0.0071	Pass	
circle 17	X	0.0000	0.0074	±0.0200	0.0074	Pass	
circle 17	Y	60.1500	60.1419	±0.0200	-0.0081	Pass	
circle 17	Z	0.0000	0.0000	±1.0000	0.0000	Pass	
distance 10	3D Distance	72.2000	72.1995	±0.0200	-0.0005	Pass	
distance 11	3D Distance	16.3000	16.3106	±0.0200	0.0106	Pass	
distance 12	3D Distance	16.3000	16.3215	±0.0200	0.0215	Fail	0.0015
distance 13	3D Distance	18.9500	18.9720	±0.0200	0.0220	Fail	0.0020
distance 14	3D Distance	23.2500	23.2858	±0.0200	0.0358	Fail	0.0158
distance 15	3D Distance	23.2500	23.2662	±0.0200	0.0162	Pass	
distance 16	3D Distance	18.9500	18.9633	±0.0200	0.0133	Pass	
distance 17	3D Distance	16.3000	16.3101	±0.0200	0.0101	Pass	
distance 18	3D Distance	16.3000	16.3142	±0.0200	0.0142	Pass	
distance 19	3D Distance	32.6000	32.5963	±0.0200	-0.0037	Pass	
distance 20	3D Distance	35.2000	35.2030	±0.0200	0.0030	Pass	
distance 21	3D Distance	32.6000	32.5980	±0.0200	-0.0020	Pass	
distance 22	3D Distance	35.2000	35.2136	±0.0200	0.0136	Pass	
distance 23	3D Distance	0.3000	0.2681	±0.0200	-0.0319	Fail	-0.0119
distance 24	3D Distance	0.3000	0.2677	±0.0200	-0.0323	Fail	-0.0123
distance 25	3D Distance	21.1000	21.1348	±0.0200	0.0348	Fail	0.0148
distance 26	3D Distance	58.1000	58.1251	±0.0200	0.0251	Fail	0.0051

Organization:	Part name:
Operator:	Part number:
E-mail:	Piece: piece 1

7.17 Annex 15- Sample 2 test 6 report

Control View

Control View Name	control view 1
Units	Millimeters
Coordinate Systems	world
Data Alignments	best-fit to ref 3
All Statistics	Total: 58, Measured: 58 (100.0000%), Pass: 47 (81.0345%), Fail: 11 (18.9655%), Warning: 0 (0.0000%)

Char No.	Object Name	Control	Nom	Meas	Tol	Dev	Test	Out Tol
	circle 5	Diameter	2.0000	1.9803	±0.0200	-0.0197	Pass	
	circle 5	X	18.5000	18.5000	±0.0200	0.0000	Pass	
	circle 5	Y	55.4000	55.3948	±0.0200	-0.0052	Pass	
	circle 5	Z	0.0000	0.0000	±1.0000	0.0000	Pass	
	circle 6	Diameter	2.0000	1.9800	±0.0200	-0.0200	Pass	
	circle 6	X	18.5000	18.4899	±0.0200	-0.0101	Pass	
	circle 6	Y	18.4000	18.4121	±0.0200	0.0121	Pass	
	circle 6	Z	0.0000	0.0000	±1.0000	0.0000	Pass	
	distance 1	3D Distance	37.0000	36.9826	±0.0200	-0.0174	Pass	
	circle 7	Diameter	2.0000	1.9680	±0.0200	-0.0320	Fail	-0.0120
	circle 7	X	-18.5000	-18.5003	±0.0200	-0.0003	Pass	
	circle 7	Y	18.4000	18.4007	±0.0200	0.0007	Pass	
	circle 7	Z	0.0000	0.0000	±1.0000	0.0000	Pass	
	circle 8	Diameter	2.0000	1.9692	±0.0200	-0.0308	Fail	-0.0108
	circle 8	X	-18.5000	-18.4911	±0.0200	0.0089	Pass	
	circle 8	Y	55.4000	55.3901	±0.0200	-0.0099	Pass	
	circle 8	Z	0.0000	0.0000	±1.0000	0.0000	Pass	
	distance 2	3D Distance	37.0000	36.9894	±0.0200	-0.0106	Pass	
	distance 3	3D Distance	37.0000	36.9902	±0.0200	-0.0098	Pass	
	distance 4	3D Distance	37.0000	36.9911	±0.0200	-0.0089	Pass	
	distance 5	3D Distance	35.2000	35.2179	±0.0200	0.0179	Pass	
	distance 6	3D Distance	32.6000	32.5998	±0.0200	-0.0002	Pass	
	distance 7	3D Distance	32.6000	32.5937	±0.0200	-0.0063	Pass	
	distance 8	3D Distance	32.6000	32.6015	±0.0200	0.0015	Pass	
	distance 9	3D Distance	32.6000	32.6001	±0.0200	0.0001	Pass	
	circle 11	Diameter	0.2000	0.1635	±0.0200	-0.0365	Fail	-0.0165
	circle 11	X	0.0000	0.0096	±0.0200	0.0096	Pass	
	circle 11	Y	55.8500	55.8410	±0.0200	-0.0090	Pass	
	circle 11	Z	0.0000	0.0000	±1.0000	0.0000	Pass	
	circle 13	Diameter	0.2000	0.1648	±0.0200	-0.0352	Fail	-0.0152
	circle 13	X	0.0000	0.0104	±0.0200	0.0104	Pass	
	circle 13	Y	18.8500	18.8464	±0.0200	-0.0036	Pass	
	circle 13	Z	0.0000	0.0000	±1.0000	0.0000	Pass	
	circle 15	Diameter	0.4000	0.3912	±0.0200	-0.0088	Pass	

Organization:	Part name:
Operator:	Part number:
E-mail:	Piece: piece 1

circle 15	X	0.0000	0.0040	±0.0200	0.0040	Pass	
circle 15	Y	23.1500	23.1520	±0.0200	0.0020	Pass	
circle 15	Z	0.0000	0.0000	±1.0000	0.0000	Pass	
circle 17	Diameter	0.4000	0.3910	±0.0200	-0.0090	Pass	
circle 17	X	0.0000	0.0125	±0.0200	0.0125	Pass	
circle 17	Y	60.1500	60.1420	±0.0200	-0.0080	Pass	
circle 17	Z	0.0000	0.0000	±1.0000	0.0000	Pass	
distance 10	3D Distance	72.2000	72.2020	±0.0200	0.0020	Pass	
distance 11	3D Distance	16.3000	16.3135	±0.0200	0.0135	Pass	
distance 12	3D Distance	16.3000	16.3212	±0.0200	0.0212	Fail	0.0012
distance 13	3D Distance	18.9500	18.9805	±0.0200	0.0305	Fail	0.0105
distance 14	3D Distance	23.2500	23.2860	±0.0200	0.0360	Fail	0.0160
distance 15	3D Distance	23.2500	23.2385	±0.0200	-0.0115	Pass	
distance 16	3D Distance	18.9500	18.9375	±0.0200	-0.0125	Pass	
distance 17	3D Distance	16.3000	16.3057	±0.0200	0.0057	Pass	
distance 18	3D Distance	16.3000	16.3049	±0.0200	0.0049	Pass	
distance 19	3D Distance	32.6000	32.5999	±0.0200	-0.0001	Pass	
distance 20	3D Distance	35.2000	35.2016	±0.0200	0.0016	Pass	
distance 21	3D Distance	32.6000	32.5998	±0.0200	-0.0002	Pass	
distance 22	3D Distance	35.2000	35.2177	±0.0200	0.0177	Pass	
distance 23	3D Distance	0.3000	0.2678	±0.0200	-0.0322	Fail	-0.0122
distance 24	3D Distance	0.3000	0.2656	±0.0200	-0.0344	Fail	-0.0144
distance 25	3D Distance	21.1000	21.1347	±0.0200	0.0347	Fail	0.0147
distance 26	3D Distance	58.1000	58.1263	±0.0200	0.0263	Fail	0.0063

Organization:	Part name:
Operator:	Part number:
E-mail:	Piece: piece 1

7.18 Annex 16- Sample 3 test 6 report

Control View

Control View Name	control view 1
Units	Millimeters
Coordinate Systems	world
Data Alignments	best-fit to ref 3
All Statistics	Total: 58, Measured: 58 (100.0000%), Pass: 48 (82.7586%), Fail: 10 (17.2414%), Warning: 0 (0.0000%)

Char No.	Object Name	Control	Nom	Meas	Tol	Dev	Test	Out Tol
	circle 5	Diameter	2.0000	1.9794	±0.0200	-0.0206	Fail	-0.0006
	circle 5	X	18.5000	18.5010	±0.0200	0.0010	Pass	
	circle 5	Y	55.4000	55.3960	±0.0200	-0.0040	Pass	
	circle 5	Z	0.0000	0.0000	±1.0000	0.0000	Pass	
	circle 6	Diameter	2.0000	1.9779	±0.0200	-0.0221	Fail	-0.0021
	circle 6	X	18.5000	18.4860	±0.0200	-0.0140	Pass	
	circle 6	Y	18.4000	18.4174	±0.0200	0.0174	Pass	
	circle 6	Z	0.0000	0.0000	±1.0000	0.0000	Pass	
	distance 1	3D Distance	37.0000	36.9785	±0.0200	-0.0215	Fail	-0.0015
	circle 7	Diameter	2.0000	1.9672	±0.0200	-0.0328	Fail	-0.0128
	circle 7	X	-18.5000	-18.4982	±0.0200	0.0018	Pass	
	circle 7	Y	18.4000	18.4021	±0.0200	0.0021	Pass	
	circle 7	Z	0.0000	0.0000	±1.0000	0.0000	Pass	
	circle 8	Diameter	2.0000	1.9684	±0.0200	-0.0316	Fail	-0.0116
	circle 8	X	-18.5000	-18.4897	±0.0200	0.0103	Pass	
	circle 8	Y	55.4000	55.3855	±0.0200	-0.0145	Pass	
	circle 8	Z	0.0000	0.0000	±1.0000	0.0000	Pass	
	distance 2	3D Distance	37.0000	36.9834	±0.0200	-0.0166	Pass	
	distance 3	3D Distance	37.0000	36.9843	±0.0200	-0.0157	Pass	
	distance 4	3D Distance	37.0000	36.9907	±0.0200	-0.0093	Pass	
	distance 5	3D Distance	35.2000	35.2113	±0.0200	0.0113	Pass	
	distance 6	3D Distance	32.6000	32.6004	±0.0200	0.0004	Pass	
	distance 7	3D Distance	32.6000	32.5991	±0.0200	-0.0009	Pass	
	distance 8	3D Distance	32.6000	32.6027	±0.0200	0.0027	Pass	
	distance 9	3D Distance	32.6000	32.6002	±0.0200	0.0002	Pass	
	circle 11	Diameter	0.2000	0.1672	±0.0200	-0.0328	Fail	-0.0128
	circle 11	X	0.0000	0.0156	±0.0200	0.0156	Pass	
	circle 11	Y	55.8500	55.8354	±0.0200	-0.0146	Pass	
	circle 11	Z	0.0000	0.0000	±1.0000	0.0000	Pass	
	circle 13	Diameter	0.2000	0.1671	±0.0200	-0.0329	Fail	-0.0129
	circle 13	X	0.0000	0.0125	±0.0200	0.0125	Pass	
	circle 13	Y	18.8500	18.8393	±0.0200	-0.0107	Pass	
	circle 13	Z	0.0000	0.0000	±1.0000	0.0000	Pass	
	circle 15	Diameter	0.4000	0.3889	±0.0200	-0.0111	Pass	

Organization:	Part name:
Operator:	Part number:
E-mail:	Piece: piece 1

circle 15	X	0.0000	0.0041	±0.0200	0.0041	Pass	
circle 15	Y	23.1500	23.1553	±0.0200	0.0053	Pass	
circle 15	Z	0.0000	0.0000	±1.0000	0.0000	Pass	
circle 17	Diameter	0.4000	0.3914	±0.0200	-0.0086	Pass	
circle 17	X	0.0000	0.0130	±0.0200	0.0130	Pass	
circle 17	Y	60.1500	60.1382	±0.0200	-0.0118	Pass	
circle 17	Z	0.0000	0.0000	±1.0000	0.0000	Pass	
distance 10	3D Distance	72.2000	72.1889	±0.0200	-0.0111	Pass	
distance 11	3D Distance	16.3000	16.3140	±0.0200	0.0140	Pass	
distance 12	3D Distance	16.3000	16.3262	±0.0200	0.0262	Fail	0.0062
distance 13	3D Distance	18.9500	18.9384	±0.0200	-0.0116	Pass	
distance 14	3D Distance	23.2500	23.2544	±0.0200	0.0044	Pass	
distance 15	3D Distance	23.2500	23.2436	±0.0200	-0.0064	Pass	
distance 16	3D Distance	18.9500	18.9409	±0.0200	-0.0091	Pass	
distance 17	3D Distance	16.3000	16.3078	±0.0200	0.0078	Pass	
distance 18	3D Distance	16.3000	16.3094	±0.0200	0.0094	Pass	
distance 19	3D Distance	32.6000	32.6004	±0.0200	0.0004	Pass	
distance 20	3D Distance	35.2000	35.1974	±0.0200	-0.0026	Pass	
distance 21	3D Distance	32.6000	32.6005	±0.0200	0.0005	Pass	
distance 22	3D Distance	35.2000	35.2112	±0.0200	0.0112	Pass	
distance 23	3D Distance	0.3000	0.2690	±0.0200	-0.0310	Fail	-0.0110
distance 24	3D Distance	0.3000	0.2692	±0.0200	-0.0308	Fail	-0.0108
distance 25	3D Distance	21.1000	21.1064	±0.0200	0.0064	Pass	
distance 26	3D Distance	58.1000	58.0921	±0.0200	-0.0079	Pass	

Organization:	Part name:
Operator:	Part number:
E-mail:	Piece: piece 1

7.19 Annex 17- Sample 1 test 7 report

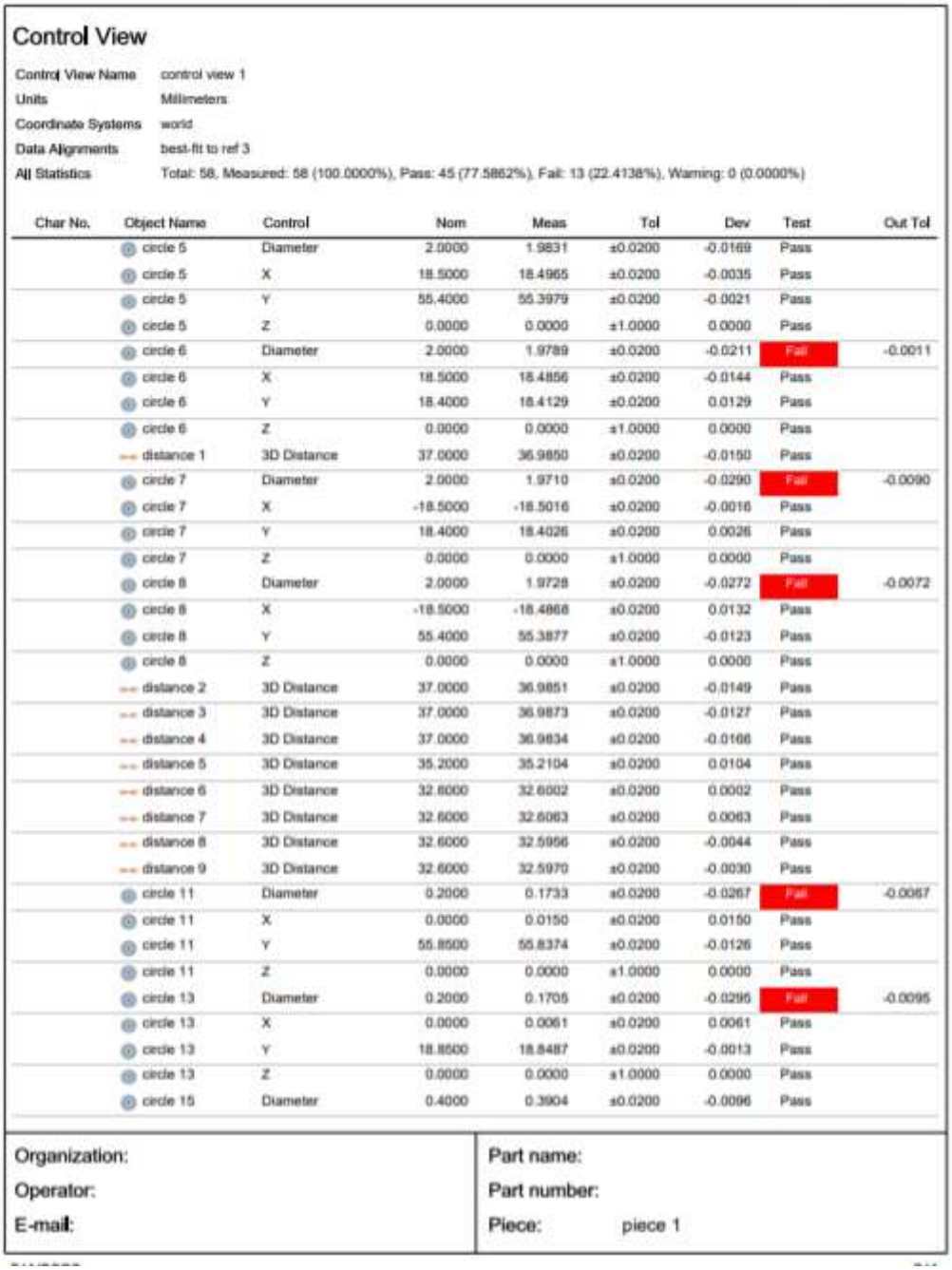

Control View

Control View Name	control view 1
Units	Millimeters
Coordinate Systems	world
Data Alignments	best-fit to ref 3
All Statistics	Total: 58, Measured: 58 (100.0000%), Pass: 45 (77.5862%), Fail: 13 (22.4138%), Warning: 0 (0.0000%)

Char No.	Object Name	Control	Nom	Meas	Tol	Dev	Test	Out Tol
	circle 5	Diameter	2.0000	1.9831	±0.0200	-0.0169	Pass	
	circle 5	X	18.5000	18.4965	±0.0200	-0.0035	Pass	
	circle 5	Y	55.4000	55.3979	±0.0200	-0.0021	Pass	
	circle 5	Z	0.0000	0.0000	±1.0000	0.0000	Pass	
	circle 6	Diameter	2.0000	1.9789	±0.0200	-0.0211	Fail	-0.0011
	circle 6	X	18.5000	18.4856	±0.0200	-0.0144	Pass	
	circle 6	Y	18.4000	18.4129	±0.0200	0.0129	Pass	
	circle 6	Z	0.0000	0.0000	±1.0000	0.0000	Pass	
	distance 1	3D Distance	37.0000	36.9850	±0.0200	-0.0150	Pass	
	circle 7	Diameter	2.0000	1.9710	±0.0200	-0.0290	Fail	-0.0090
	circle 7	X	-18.5000	-18.5016	±0.0200	-0.0016	Pass	
	circle 7	Y	18.4000	18.4026	±0.0200	0.0026	Pass	
	circle 7	Z	0.0000	0.0000	±1.0000	0.0000	Pass	
	circle 8	Diameter	2.0000	1.9728	±0.0200	-0.0272	Fail	-0.0072
	circle 8	X	-18.5000	-18.4868	±0.0200	0.0132	Pass	
	circle 8	Y	55.4000	55.3877	±0.0200	-0.0123	Pass	
	circle 8	Z	0.0000	0.0000	±1.0000	0.0000	Pass	
	distance 2	3D Distance	37.0000	36.9851	±0.0200	-0.0149	Pass	
	distance 3	3D Distance	37.0000	36.9873	±0.0200	-0.0127	Pass	
	distance 4	3D Distance	37.0000	36.9834	±0.0200	-0.0166	Pass	
	distance 5	3D Distance	35.2000	35.2104	±0.0200	0.0104	Pass	
	distance 6	3D Distance	32.6000	32.6002	±0.0200	0.0002	Pass	
	distance 7	3D Distance	32.6000	32.6063	±0.0200	0.0063	Pass	
	distance 8	3D Distance	32.6000	32.5956	±0.0200	-0.0044	Pass	
	distance 9	3D Distance	32.6000	32.5970	±0.0200	-0.0030	Pass	
	circle 11	Diameter	0.2000	0.1733	±0.0200	-0.0267	Fail	-0.0067
	circle 11	X	0.0000	0.0150	±0.0200	0.0150	Pass	
	circle 11	Y	55.8500	55.8374	±0.0200	-0.0126	Pass	
	circle 11	Z	0.0000	0.0000	±1.0000	0.0000	Pass	
	circle 13	Diameter	0.2000	0.1705	±0.0200	-0.0295	Fail	-0.0095
	circle 13	X	0.0000	0.0061	±0.0200	0.0061	Pass	
	circle 13	Y	18.8500	18.8487	±0.0200	-0.0013	Pass	
	circle 13	Z	0.0000	0.0000	±1.0000	0.0000	Pass	
	circle 15	Diameter	0.4000	0.3904	±0.0200	-0.0096	Pass	

Organization:	Part name:
Operator:	Part number:
E-mail:	Piece: piece 1

circle 15	X	0.0000	-0.0005	±0.0200	-0.0005	Pass	
circle 15	Y	23.1500	23.1560	±0.0200	0.0060	Pass	
circle 15	Z	0.0000	0.0000	±1.0000	0.0000	Pass	
circle 17	Diameter	0.4000	0.3897	±0.0200	-0.0103	Pass	
circle 17	X	0.0000	0.0118	±0.0200	0.0118	Pass	
circle 17	Y	60.1500	60.1422	±0.0200	-0.0078	Pass	
circle 17	Z	0.0000	0.0000	±1.0000	0.0000	Pass	
distance 10	3D Distance	72.2000	72.1994	±0.0200	-0.0006	Pass	
distance 11	3D Distance	16.3000	16.3065	±0.0200	0.0065	Pass	
distance 12	3D Distance	16.3000	16.3172	±0.0200	0.0172	Pass	
distance 13	3D Distance	18.9500	18.9772	±0.0200	0.0272	Fail	0.0072
distance 14	3D Distance	23.2500	23.2844	±0.0200	0.0344	Fail	0.0144
distance 15	3D Distance	23.2500	23.2805	±0.0200	0.0305	Fail	0.0105
distance 16	3D Distance	18.9500	18.9757	±0.0200	0.0257	Fail	0.0057
distance 17	3D Distance	16.3000	16.3060	±0.0200	0.0060	Pass	
distance 18	3D Distance	16.3000	16.3166	±0.0200	0.0166	Pass	
distance 19	3D Distance	32.6000	32.5973	±0.0200	-0.0027	Pass	
distance 20	3D Distance	35.2000	35.2007	±0.0200	0.0007	Pass	
distance 21	3D Distance	32.6000	32.6007	±0.0200	0.0007	Pass	
distance 22	3D Distance	35.2000	35.2097	±0.0200	0.0097	Pass	
distance 23	3D Distance	0.3000	0.2683	±0.0200	-0.0317	Fail	-0.0117
distance 24	3D Distance	0.3000	0.2679	±0.0200	-0.0321	Fail	-0.0121
distance 25	3D Distance	21.1000	21.1352	±0.0200	0.0352	Fail	0.0152
distance 26	3D Distance	58.1000	58.1267	±0.0200	0.0267	Fail	0.0067

Organization:	Part name:
Operator:	Part number:
E-mail:	Piece: piece 1

7.20 Annex 20- Sample 2 test 7 report

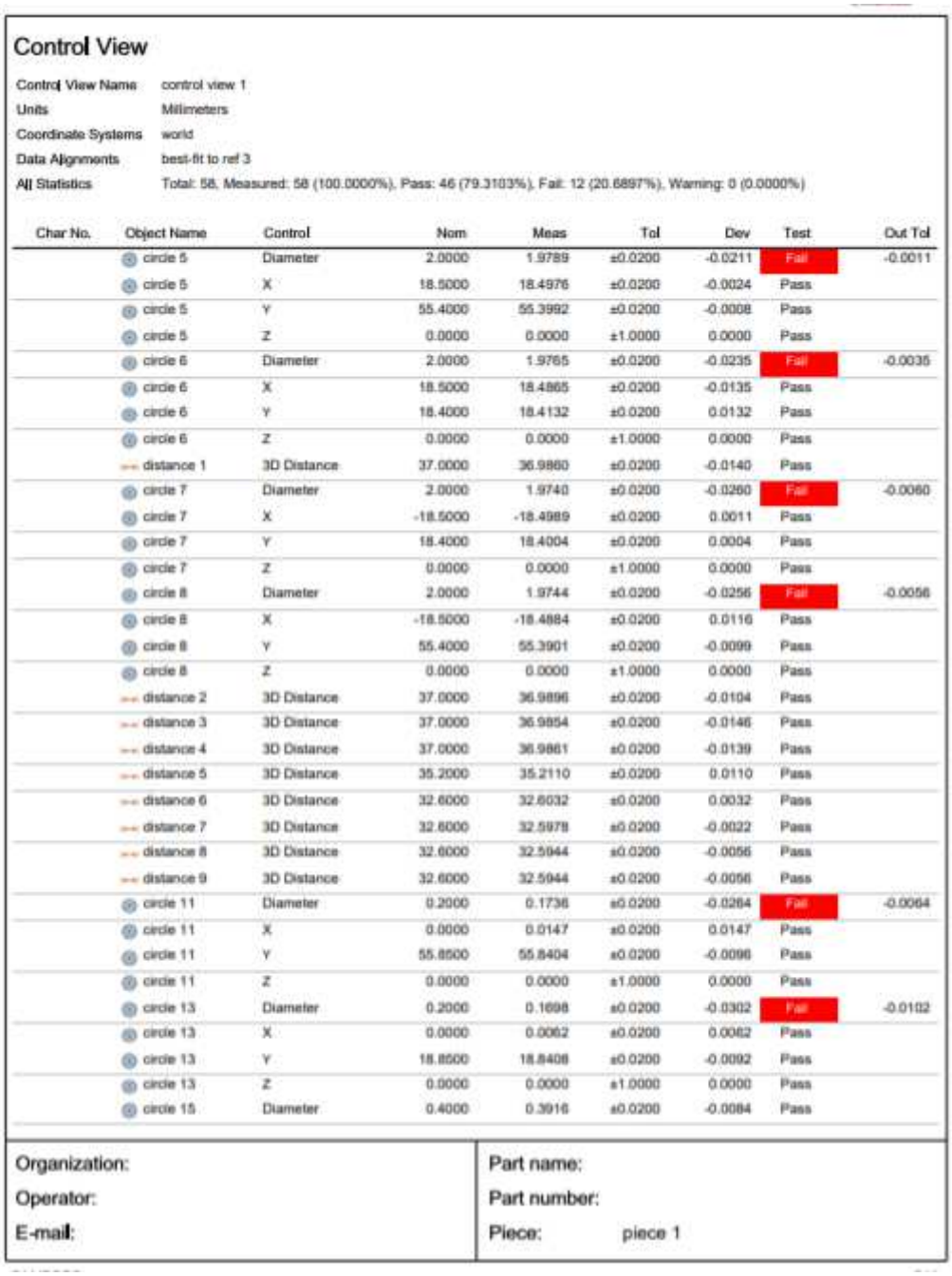

Control View

Control View Name	control view 1
Units	Millimeters
Coordinate Systems	world
Data Alignments	best-fit to ref 3
All Statistics	Total: 58, Measured: 58 (100.0000%), Pass: 46 (79.3103%), Fail: 12 (20.6897%), Warning: 0 (0.0000%)

Char No.	Object Name	Control	Nom	Meas	Tol	Dev	Test	Out Tol
	circle 5	Diameter	2.0000	1.9789	±0.0200	-0.0211	Fail	-0.0011
	circle 5	X	18.5000	18.4976	±0.0200	-0.0024	Pass	
	circle 5	Y	55.4000	55.3992	±0.0200	-0.0008	Pass	
	circle 5	Z	0.0000	0.0000	±1.0000	0.0000	Pass	
	circle 6	Diameter	2.0000	1.9765	±0.0200	-0.0235	Fail	-0.0035
	circle 6	X	18.5000	18.4865	±0.0200	-0.0135	Pass	
	circle 6	Y	18.4000	18.4132	±0.0200	0.0132	Pass	
	circle 6	Z	0.0000	0.0000	±1.0000	0.0000	Pass	
	distance 1	3D Distance	37.0000	36.9860	±0.0200	-0.0140	Pass	
	circle 7	Diameter	2.0000	1.9740	±0.0200	-0.0260	Fail	-0.0060
	circle 7	X	-18.5000	-18.4989	±0.0200	0.0011	Pass	
	circle 7	Y	18.4000	18.4004	±0.0200	0.0004	Pass	
	circle 7	Z	0.0000	0.0000	±1.0000	0.0000	Pass	
	circle 8	Diameter	2.0000	1.9744	±0.0200	-0.0256	Fail	-0.0056
	circle 8	X	-18.5000	-18.4884	±0.0200	0.0116	Pass	
	circle 8	Y	55.4000	55.3901	±0.0200	-0.0099	Pass	
	circle 8	Z	0.0000	0.0000	±1.0000	0.0000	Pass	
	distance 2	3D Distance	37.0000	36.9896	±0.0200	-0.0104	Pass	
	distance 3	3D Distance	37.0000	36.9854	±0.0200	-0.0146	Pass	
	distance 4	3D Distance	37.0000	36.9861	±0.0200	-0.0139	Pass	
	distance 5	3D Distance	35.2000	35.2110	±0.0200	0.0110	Pass	
	distance 6	3D Distance	32.6000	32.6032	±0.0200	0.0032	Pass	
	distance 7	3D Distance	32.6000	32.5978	±0.0200	-0.0022	Pass	
	distance 8	3D Distance	32.6000	32.5944	±0.0200	-0.0056	Pass	
	distance 9	3D Distance	32.6000	32.5944	±0.0200	-0.0056	Pass	
	circle 11	Diameter	0.2000	0.1736	±0.0200	-0.0264	Fail	-0.0064
	circle 11	X	0.0000	0.0147	±0.0200	0.0147	Pass	
	circle 11	Y	55.8500	55.8404	±0.0200	-0.0096	Pass	
	circle 11	Z	0.0000	0.0000	±1.0000	0.0000	Pass	
	circle 13	Diameter	0.2000	0.1698	±0.0200	-0.0302	Fail	-0.0102
	circle 13	X	0.0000	0.0062	±0.0200	0.0062	Pass	
	circle 13	Y	18.8500	18.8408	±0.0200	-0.0092	Pass	
	circle 13	Z	0.0000	0.0000	±1.0000	0.0000	Pass	
	circle 15	Diameter	0.4000	0.3916	±0.0200	-0.0084	Pass	

Organization:	Part name:
Operator:	Part number:
E-mail:	Piece: piece 1

circle 15	X	0.0000	-0.0016	±0.0200	-0.0016	Pass	
circle 15	Y	23.1500	23.1558	±0.0200	0.0058	Pass	
circle 15	Z	0.0000	0.0000	±1.0000	0.0000	Pass	
circle 17	Diameter	0.4000	0.3906	±0.0200	-0.0094	Pass	
circle 17	X	0.0000	0.0111	±0.0200	0.0111	Pass	
circle 17	Y	60.1500	60.1462	±0.0200	-0.0038	Pass	
circle 17	Z	0.0000	0.0000	±1.0000	0.0000	Pass	
distance 10	3D Distance	72.2000	72.1986	±0.0200	-0.0014	Pass	
distance 11	3D Distance	16.3000	16.3083	±0.0200	0.0083	Pass	
distance 12	3D Distance	16.3000	16.3189	±0.0200	0.0189	Pass	
distance 13	3D Distance	18.9500	18.9030	±0.0200	-0.0470	Fail	-0.0270
distance 14	3D Distance	23.2500	23.2179	±0.0200	-0.0321	Fail	-0.0121
distance 15	3D Distance	23.2500	23.2522	±0.0200	0.0022	Pass	
distance 16	3D Distance	18.9500	18.9464	±0.0200	-0.0036	Pass	
distance 17	3D Distance	16.3000	16.3070	±0.0200	0.0070	Pass	
distance 18	3D Distance	16.3000	16.3163	±0.0200	0.0163	Pass	
distance 19	3D Distance	32.6000	32.5946	±0.0200	-0.0054	Pass	
distance 20	3D Distance	35.2000	35.1964	±0.0200	-0.0036	Pass	
distance 21	3D Distance	32.6000	32.6031	±0.0200	0.0031	Pass	
distance 22	3D Distance	35.2000	35.2103	±0.0200	0.0103	Pass	
distance 23	3D Distance	0.3000	0.2676	±0.0200	-0.0324	Fail	-0.0124
distance 24	3D Distance	0.3000	0.2669	±0.0200	-0.0331	Fail	-0.0131
distance 25	3D Distance	21.1000	21.0652	±0.0200	-0.0348	Fail	-0.0148
distance 26	3D Distance	58.1000	58.0578	±0.0200	-0.0422	Fail	-0.0222

Organization:	Part name:
Operator:	Part number:
E-mail:	Piece: piece 1

7.21 Annex 21- Sample 3 test 7 report

Control View

Control View Name	control view 1
Units	Millimeters
Coordinate Systems	world
Data Alignments	best-fit to ref 3
All Statistics	Total: 58, Measured: 58 (100.0000%), Pass: 46 (79.3103%), Fail: 12 (20.6897%), Warning: 0 (0.0000%)

Char No.	Object Name	Control	Nom	Meas	Tol	Dev	Test	Out Tol
	circle 5	Diameter	2.0000	1.9801	±0.0200	-0.0199	Pass	
	circle 5	X	18.5000	18.4961	±0.0200	-0.0039	Pass	
	circle 5	Y	55.4000	55.4040	±0.0200	0.0040	Pass	
	circle 5	Z	0.0000	0.0000	±1.0000	0.0000	Pass	
	circle 6	Diameter	2.0000	1.9797	±0.0200	-0.0203	Fail	-0.0003
	circle 6	X	18.5000	18.4813	±0.0200	-0.0187	Pass	
	circle 6	Y	18.4000	18.4164	±0.0200	0.0164	Pass	
	circle 6	Z	0.0000	0.0000	±1.0000	0.0000	Pass	
	distance 1	3D Distance	37.0000	36.9876	±0.0200	-0.0124	Pass	
	circle 7	Diameter	2.0000	1.9734	±0.0200	-0.0266	Fail	-0.0066
	circle 7	X	-18.5000	-18.5030	±0.0200	-0.0030	Pass	
	circle 7	Y	18.4000	18.3930	±0.0200	-0.0070	Pass	
	circle 7	Z	0.0000	0.0000	±1.0000	0.0000	Pass	
	circle 8	Diameter	2.0000	1.9654	±0.0200	-0.0346	Fail	-0.0146
	circle 8	X	-18.5000	-18.4813	±0.0200	0.0187	Pass	
	circle 8	Y	55.4000	55.3885	±0.0200	-0.0115	Pass	
	circle 8	Z	0.0000	0.0000	±1.0000	0.0000	Pass	
	distance 2	3D Distance	37.0000	36.9955	±0.0200	-0.0045	Pass	
	distance 3	3D Distance	37.0000	36.9843	±0.0200	-0.0157	Pass	
	distance 4	3D Distance	37.0000	36.9775	±0.0200	-0.0225	Fail	-0.0025
	distance 5	3D Distance	35.2000	35.2102	±0.0200	0.0102	Pass	
	distance 6	3D Distance	32.6000	32.5984	±0.0200	-0.0016	Pass	
	distance 7	3D Distance	32.6000	32.5973	±0.0200	-0.0027	Pass	
	distance 8	3D Distance	32.6000	32.5967	±0.0200	-0.0033	Pass	
	distance 9	3D Distance	32.6000	32.5912	±0.0200	-0.0088	Pass	
	circle 11	Diameter	0.2000	0.1673	±0.0200	-0.0327	Fail	-0.0127
	circle 11	X	0.0000	0.0161	±0.0200	0.0161	Pass	
	circle 11	Y	55.8500	55.8393	±0.0200	-0.0107	Pass	
	circle 11	Z	0.0000	0.0000	±1.0000	0.0000	Pass	
	circle 13	Diameter	0.2000	0.1703	±0.0200	-0.0297	Fail	-0.0097
	circle 13	X	0.0000	0.0031	±0.0200	0.0031	Pass	
	circle 13	Y	18.8500	18.8413	±0.0200	-0.0087	Pass	
	circle 13	Z	0.0000	0.0000	±1.0000	0.0000	Pass	
	circle 15	Diameter	0.4000	0.3923	±0.0200	-0.0077	Pass	

Organization:	Part name:
Operator:	Part number:
E-mail:	Piece: piece 1

circle 15	X	0.0000	-0.0056	±0.0200	-0.0056	Pass	
circle 15	Y	23.1500	23.1544	±0.0200	0.0044	Pass	
circle 15	Z	0.0000	0.0000	±1.0000	0.0000	Pass	
circle 17	Diameter	0.4000	0.3898	±0.0200	-0.0102	Pass	
circle 17	X	0.0000	0.0129	±0.0200	0.0129	Pass	
circle 17	Y	60.1500	60.1464	±0.0200	-0.0036	Pass	
circle 17	Z	0.0000	0.0000	±1.0000	0.0000	Pass	
distance 10	3D Distance	72.2000	72.2000	±0.0200	0.0000	Pass	
distance 11	3D Distance	16.3000	16.3092	±0.0200	0.0092	Pass	
distance 12	3D Distance	16.3000	16.3194	±0.0200	0.0194	Pass	
distance 13	3D Distance	18.9500	18.8963	±0.0200	-0.0537	Fail	-0.0337
distance 14	3D Distance	23.2500	23.2094	±0.0200	-0.0406	Fail	-0.0206
distance 15	3D Distance	23.2500	23.2582	±0.0200	0.0082	Pass	
distance 16	3D Distance	18.9500	18.9511	±0.0200	0.0011	Pass	
distance 17	3D Distance	16.3000	16.3093	±0.0200	0.0093	Pass	
distance 18	3D Distance	16.3000	16.3167	±0.0200	0.0167	Pass	
distance 19	3D Distance	32.6000	32.5911	±0.0200	-0.0089	Pass	
distance 20	3D Distance	35.2000	35.1968	±0.0200	-0.0032	Pass	
distance 21	3D Distance	32.6000	32.5988	±0.0200	-0.0012	Pass	
distance 22	3D Distance	35.2000	35.2101	±0.0200	0.0101	Pass	
distance 23	3D Distance	0.3000	0.2673	±0.0200	-0.0327	Fail	-0.0127
distance 24	3D Distance	0.3000	0.2673	±0.0200	-0.0327	Fail	-0.0127
distance 25	3D Distance	21.1000	21.0583	±0.0200	-0.0417	Fail	-0.0217
distance 26	3D Distance	58.1000	58.0457	±0.0200	-0.0543	Fail	-0.0343

Organization:	Part name:
Operator:	Part number:
E-mail:	Piece: piece 1